The effects of a cigarette carcinogen on Glucocorticoid Receptor Methylation

by

Roxanne Jane Wheeler

B.Sc. (Hons) Biological Sciences

Submitted in fulfilment of the academic requirements for the degree of Master of Science in the School of Life Sciences, Department of Biological and Conservational Sciences, University of KwaZulu-Natal, Westville

February 2014

As the candidate's supervisors we have approved this thesis/dissertation for submission.

Signed: _____ Name: Dr Paula Sommer Date: _____

Signed: _____ Name: Dr Dalene Vosloo Date: _____

Abstract

Small cell lung cancer (SCLC) is an aggressive disease with an extremely poor prognosis. Lung cancer has been linked to cigarette smoking. SCLCs are glucocorticoid insensitive due to reduced levels of glucocorticoid receptor (GR) expression. Re-expression of the GR, both *in vitro* and *in vivo*, induces apoptosis. The loss of GR expression therefore provides a survival advantage in SCLC cells. The *GR* gene in SCLC cells may be epigenetically silenced by DNA hypermethylation of its promoter region. DNA methylation is carried out by DNA methyltransferase 1 (DNMT1), shown to be over-expressed in lung cancer patients who smoke.

The first aim of this study was to determine which GRα isoforms are re-expressed in SCLC cells after exposure to a demethylation agent. The SCLC cell line, DMS 79; the glucocorticoid-sensitive non-SCLC cell line, A549; and the glucocorticoid-resistant HEK 293 cell lines were treated with the DNMT1inhibitor, 5-Aza-2'-deoxycytidine (5-Aza), to determine which GRα isoforms are re-expressed in SCLC cells, compared to the control cell lines. Other studies have found certain GRα isoforms to be more effective at inducing apoptosis, such as GRα-C. DMS 79 cells and HEK cells showed GRα protein expression of isoform -A, -B and GRα-C, whilst only isoforms -A and -B were seen in the A549 cells.

A key carcinogen in cigarette smoke, nitrosamine 4-(methylnitrosamino)-1-(3-pyridyl)-1-butanone (NNK), has been linked to lung carcinoma development. NNK has been linked in the nuclear accumulation of DNMT1 and is thus responsible for the hypermethylation of multiple TSGs in lung cancers.

The second aim was to determine whether the NNK tobacco carcinogen induces DNMT1 accumulation and TSG hypermethylation at the *GR* gene. The MRC-5 normal lung fibroblast cell line was treated with NNK. There was a significant down-regulation of *GRα* mRNA expression after 2 hours of NNK treatment ($p < 0.05$). Long term treatment with NNK showed a further significant decrease in *GRα* mRNA expression in the MRC-5 cells ($p < 0.001$). GRα protein expression differed in the MRC-5 cell line between the vehicle (control) and the cells treated with NNK for 24, 48 and 72 hours ($p < 0.001$). These data indicated that long term treatment with NNK appeared to further decrease GRα protein expression. This is consistent with other studies which showed prolonged NNK or cigarette exposure inactivated tumour suppressor genes (TSGs). To determine whether down-regulation is due to NNK-induced recruitment of DNMT1 to the *GR* promoter, Chromatin Immunoprecipitation (ChIP) analysis

was performed. Preliminary ChIP analysis data showed possible recruitment of DNMT1 to promoter 1F and 1J of the *GR*, suggesting that NNK treatment resulted in the silencing of *GR* expression via promoter 1F and 1J. Recent data in our laboratory has indicated that when the *GR* is re-expressed the use of promoters 1F and 1J may be responsible for inducing apoptosis in SCLC cells. These preliminary data may provide insight into the mechanism of cigarette carcinogen induced SCLC carcinogenesis. *GRα* appears to be an important TSG in SCLC and may be fundamental in SCLC development. Elucidating the pathways involved in SCLC development and GRα expression could lead to a breakthrough in oncology and novel ways in which therapies can target this deadly disease.

Preface

The experimental work described in this dissertation was carried out in the School of Life Sciences, University of KwaZulu-Natal, Westville, from January 2012 to February 2014, under the supervision of Dr Paula Sommer and the co-supervision of Dr Dalene Vosloo.

These studies represent original work by the author and have not otherwise been submitted in any form for any degree or diploma to any tertiary institution.

Roxanne Wheeler

Plagiarism Declaration

I, Roxanne Wheeler, declare that

1. The research reported in this thesis, except where otherwise indicated, is my original research.

2. This thesis has not been submitted for any degree or examination at any other university.

3. This thesis does not contain other persons' data, pictures, graphs or other information, unless specifically acknowledged as being sourced from other persons.

4. This thesis does not contain other persons' writing, unless specifically acknowledged as being sourced from other researchers. Where other written sources have been quoted, then:

a. Their words have been re-written but the general information attributed to them has been referenced.

b. Where their exact words have been used, then their writing has been placed in italics and inside quotation marks, and referenced.

5. This thesis does not contain text, graphics or tables copied and pasted from the Internet, unless specifically acknowledged, and the source being detailed in the thesis and in the References sections.

Signed: …… Date: ……

Table of Contents

List of Tables

List of Figures

Abbreviations

11β-HSD	11β-hydroxysteroid dehydrogenase
5-Aza	5-Aza-2'-deoxycytidine
ACTH	Adrenocorticotrophin hormone
ANOVA	Analysis of variance
ATCC	American Type Culture Collection
BCA	Bicinchoninic Acid
BSA	Bovine serum albumin
CANSA	The Cancer Association of South Africa
CDK	Cyclin-dependent kinase inhibitor
ChIP	Chromatin Immunoprecipitation
CORT	Cortisol
CRH	Corticotrophin releasing hormone
DAPk	Death-associated protein kinase
DBD	DNA binding domain
DMEM	Dulbecco's Modified Eagle's Medium
DMSO	Dimethyl sulfoxide
DNMT	DNA methyltransferase
EDTA	Ethylenediaminetetraacetic acid
EGFR	Epidermal growth factor receptor
ERK	Extracellular signal-regulated kinase
FBS	Foetal bovine serum
FHIT	Fragile histidine triad protein
GAPDH	Glyceraldehyde-3-phosphate dehydrogenase
Gc	Glucocorticoid
GR	Glucocorticoid receptor
GRE	Glucocorticoid-response element
GZMA	Granzyme A
h	hour/s
HDAC	Histone deacetylase
HEK	Human embryonic kidney
HEPES	4-(2-Hydroxyethyl)-1-piperazineethane-sulfonic acid
HPA	Hypothalamic-pituitary-adrenal
HRP	Horse radish peroxidase

Hsp	Heat shock protein
IARC	International Agency for Research on Cancer
LBD	Ligand binding domain
MAPK	Mitogen-activated protein kinase
MIQE	Minimum Information for Publication of Quantitative Real-time PCR Experiments
MWM	Molecular weight marker
nGRE	negative glucocorticoid-response element
NF	Nuclear factor
NNK	Nitrosamine 4-(methylnitrosamino)-1-(3-pyridyl)-1-butanone
no-RT	No reverse transcriptase
NSCLC	Non-small cell lung cancer
NTC	No-template control
PBS	Phosphate-buffered saline
PCR	Polymerase chain reaction
POMC	Proopiomelanocortin
qPCR	Quantitative real-time polymerase chain reaction
RARB	Retinoic acid receptor β
RIPA	Radio-immunoprecipitation
RT	Reverse transcriptase
Runx	Runt-related transcription factor
SCLC	Small cell lung cancer
SEM	Standard error of the mean
TBE	Tris-base EDTA
TBS-T	Tris-buffered saline-tween
TF	Transcription factor
TNF	Tumour necrosis factor
TRAIL	TNF-related apoptosis-inducing ligand
TSG	Tumour suppressor gene
WHO	World Health Organisation
WR	Working reagent
UTR	Untranslated region

Acknowledgements

To my supervisor, Dr Paula Sommer; thank you for putting up with my singing and loud laughter in the lab. You always have such a concise and simple way of looking at things that I hope to gain someday. Thank you for all of your help and guidance over the last few years.

Thank you to my co-supervisor Dr Dalene Vosloo for your guidance and the use of your laboratory and equipment. I have been very lucky to have both you and Paula as my supervisors.

I would like to thank my lab mates Nimisha Singh, Kerryn Houston and Zenzele Silla for being great friends and helping me when I was in need. Nims, thank you for always lending a helping hand whenever I needed one, I could always count on you.

To my family and friends, thank you all of your support and understanding over the last two years.

A special thank you to all of my lovely ladies in my Postgrad office: Amanda, Jerusha, Benita, Sharon, Kim and Sylvana; thank you for being such amazing people and friends. You were my only motivation some days ;-).

Thank you to my lovely cocker spaniel, Martin, for giving me lots to love.

To my special husband, Ryan Wheeler, thank you for your support and understanding these past few years of studying. You have always been there when I've needed you.

To my funders, the National Research Foundation (NRF) and the University of KwaZulu-Natal, I would like to thank you for making this research possible.

1. Introduction and literature review

1.1 Lung Cancer

Cancer is a major cause for concern for public health services in both developing and industrialised countries. According to the World Health Organisation (WHO), lung cancer is the leading cause of all cancer-related deaths, accounting for 22% of cancer mortalities worldwide (Panani and Roussos, 2006; Vaissière *et al*., 2009). According to the Cancer Association of South Africa (CANSA), cancer is overtaking Tuberculosis and AIDS in developing countries. Furthermore, in South Africa, lung cancer is the third most prevalent cancer in men with 1 in 82 cases and is the ninth in women with 1 in 259 cases diagnosed as lung cancer. Although genetic, environmental and nutritional factors play a role in the development of the disease, over 80% of cases are caused by cigarette smoking (Maser, 2004; Akopyan and Bonavida, 2006; Panani and Roussos, 2006; Vaissière *et al*., 2009). Exposure to chemicals in cigarette smoke causes changes in the genetic expression of normal bronchial epithelial cells lining the lung (Jeong *et al*., 2010). Chemicals can cause structural damage to DNA by binding covalently to DNA and forming DNA-adducts which interfere with replication and can cause somatic mutations (Poirier, 2004). These alterations can ultimately cause changes in the expression of tumour suppressor genes (TSGs) and oncogene activation, which can cause cells to grow uncontrollably, forming a tumour (Poirier, 2004; Jeong *et al*., 2010).

The predicted survival rate of patients with lung cancer depends on the histological subtype of cancer presented and the stage at which the diagnosis is made (Jeong *et al*., 2010; Lin *et al*., 2010a). Tumours are usually classified using the TNM staging system where T-describes the size of the tumour and spread; N-describes the lymph nodes involved and M-describes whether the tumour has metastasized. Stage I tumours, if they are small and have not metastasized, are removed surgically, and the patients may undergo chemotherapy if necessary. Stage II and III tumours which have usually metastasized to the lymph nodes are treated with a combination of surgery and chemotherapy. Stage III (if spread throughout the chest) and IV (spread throughout the lungs and other organs) tumours are usually treated with chemotherapy alone. Patients with Stage I and II lung cancer have a survival rate of 60-70%, whereas only 2% of patients with Stage IV lung cancer survive five years after diagnosis (Jeong *et al*., 2010).

While there have been improvements in early stage diagnoses and chemo-targeted therapies to improve treatment responses, the survival rates remain low and the reoccurrence rate is high,

even in the earlier stages (Tessema and Belinsky, 2008; Lin *et al*., 2010a). Poor disease prognosis is due to late disease presentation and limited knowledge and understanding of tumour biology (Lin *et al*., 2010a). Lung cancer is divided into two major groups: non-small lung cancer (NSLC), comprising of adenocarcinoma, squamous cell and large cell carcinoma, occurring in ~80% of patients and small cell lung cancer (SCLC), accounting for the other 20% of the lung cancer cases diagnosed (Panani and Roussos, 2006; Tessema and Belinsky, 2008; Kay *et al*., 2011).

1.2 Small Cell Lung Cancer

SCLC is characterised as an aggressive tumour with a rapid growth rate and tends to metastasize early on in its development. Exposure to cigarette smoke and the frequency of smoking are linked to 90% of SCLC cases. Despite this correlation, when smoking is discontinued, disease prognosis is improved and there is a decreased chance of SCLC development when compared to individuals who continue to smoke (Micke *et al*., 2002; Jackman and Johnson, 2005; Lin *et al*., 2010b). The cancer spreads throughout the thoracic cavity and to the hilar and mediastinal nodes (Micke *et al*., 2002; Jackman and Johnson, 2005).

SCLC therapies consist of chemotherapy and at times radiation; radiation is beneficial for localised tumours (Micke *et al*., 2002). The surgical removal of SCLC is not typically possible because the tumours do not form solid masses and therefore the TNM staging system is not applicable for these tumours. Instead, a simpler system was introduced by the Veterans Administration Lung Group which categorises SCLC into limited and extensive disease lung cancer. Limited-stage disease refers to tumours that can be treated with one radiography portal, on one side of the chest which can encompass hilar and mediastinal nodes. The extensive-stage disease is beyond that of the limited-stage disease. Limited-stage disease can be treated with concurrent thoracic radiation and chemotherapy, whereas chemotherapy remains the standard therapy for extensive-stage disease (Micke *et al*., 2002; Jackman and Johnson, 2005; Zang and He, 2013).

Although most patients' tumours initially respond to chemotherapy, only 5% of SCLC patients survive 5 years post diagnosis (Jackman and Johnson, 2005). This poor prognosis is due to the ability of SCLC to develop resistance to therapies (Jackman and Johnson, 2005; Panani and Roussos, 2006; Tessema and Belinsky, 2008; Kay *et al*., 2011). SCLC tumours have also been associated with paraneoplastic syndromes such as Cushing's syndrome, which is a result of

tumour cell secretions. Neurological complications are also associated with SCLC, due to their ability to secrete neuropeptides ectopically which can cause antibody-mediated damage to the central nervous system (Jackman and Johnson, 2005).

1.2.1 ACTH production in small cell lung cancers

SCLCs are thought to arise from the transformation of the neuroendocrine cells of the lung and thus these neuroendocrine tumours are able to produce a variety of different neuropeptides such as gastrin releasing peptide and neuromedin B. Pertinent to this study, SCLC are able to secrete proopiomelanocortin (POMC), a precursor of adrenocorticotropin hormone (ACTH) (Parks *et al.*, 1998; Jackman and Johnson, 2005; Sommer *et al*., 2010). Approximately 45% of patients diagnosed with SCLC cancer display ectopic ACTH production or Cushing's syndrome (Ilias *et al*., 2005; Jackman and Johnson, 2005; Salgado *et al*., 2006). Normally, the gene encoding POMC is expressed at very low levels in the normal lung (Ray *et al*., 1994). The ectopic secretion of ACTH by the cancer cells is not affected by circulating glucocorticoids (Gcs) and is thus not controlled by the normal negative feedback of the hypothalamic-pituitary-adrenal (HPA) axis (Ray *et al.*, 1996; Ilias *et al.*, 2005; Sommer *et al*., 2007; 2010). This is evidence of Gc resistance in SCLC cells (Ray *et al*., 1994; 1996; Sommer *et al*., 2007; 2010).

1.2.2 The hypothalamic-pituitary-adrenal axis

The hypothalamic-pituitary-adrenal (HPA) axis is a complex system consisting of neuroendocrine interactions that control the stress response and regulate many other bodily processes. These interactions are between the hypothalamus, anterior pituitary and the adrenal glands, thereby connecting the central nervous system to the hormonal system. Normally, ACTH production is controlled by the HPA axis. Under stress, corticotrophin releasing hormone (CRH) is secreted by the hypothalamus, stimulating the production of ACTH in the anterior pituitary (Kudielka and Kirschbaum, 2005). ACTH then triggers the adrenal cortex, located above the kidneys, to synthesise and release Gcs into the bloodstream (Fig. 1.1) (Ray *et al.*, 1996; Parks *et al.*, 1998; Kudielka and Kirschbaum, 2005; Sommer and Ray, 2008). Normally, ACTH is produced by the anterior pituitary, stimulating Gc production (Ray *et al.*, 1996; Parks *et al.*, 1998; Kudielka and Kirschbaum, 2005). These Gcs then inhibit ACTH production via a negative feedback mechanism controlled by the HPA axis (Ray *et al.*, 1996; Sommer and Ray, 2008; Sommer *et al*., 2010).

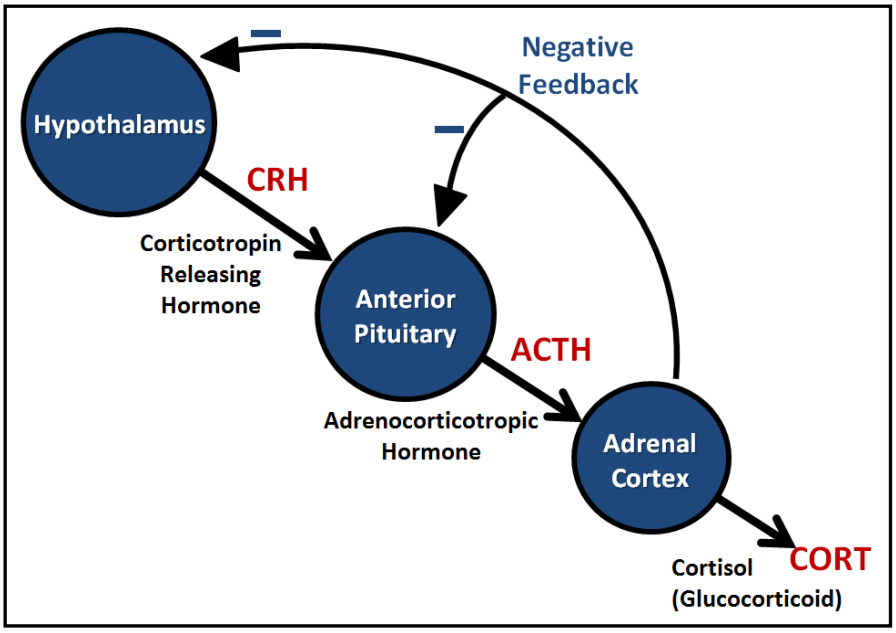

Figure 1.1. The hypothalamic-pituitary-adrenal (HPA) axis showing the negative feedback of cortisol on ACTH production. **CRH** – Corticotrophin releasing hormone, **ACTH** – Adrenocorticotropic hormone, **CORT** – Cortisol (Glucocorticoid). Image adapted from Pariante and Lightman (2008).

1.3 Glucocorticoids and the glucocorticoid receptor

Gcs are stress-induced hormones produced by the adrenal cortex; they play several vital roles in development, immunosuppression, metabolism, cell differentiation, proliferation and apoptosis (Kudielka and Kirschbaum, 2005; Zhou and Cidlowski, 2005; Duma *et al.*, 2006). Gcs are frequently used in the treatment of inflammatory conditions such as eczema, asthma, autoimmune disorders, as well as cancers such as acute lymphoblastic leukaemia and to relieve inflammation in the later stages of cancers (Wu *et al.*, 2013).

Due to their lipophilic structure, Gcs pass easily through the cell membrane into target cells, where they are cleaved by 11β-hydroxysteroid dehydrogenase type 1 (11β-HSD1) which converts inactive cortisone into the active form, cortisol (Fig. 1.2). In the kidney, colon, placenta and pancreas 11β-hydroxysteroid dehydrogenase type 2 (11β-HSD2) acts in the opposite manner, converting cortisol into cortisone, thereby preventing the unwanted activation of the glucocorticoid receptor (GR) by Gcs in these mineralocorticoid target tissues (Chrousos, 2004; Lu and Cidlowski, 2006; Sommer and Ray, 2008). The functional actions of Gcs are mediated by the GR, a transcription factor, capable of regulating various different genes (Sommer and Ray, 2008; Wu *et al.*, 2013).

1.3.1 Genomic actions mediated by the GR

The inactive GR complex, a 94 kDa protein, is found in the cytosol and has a high affinity for Gc binding. This GR complex contains several heat-shock proteins (Hsp), such as Hsp 90, 70, 56 and 40. There are also interactions with immunophilins such as FKBP51. When the Gc hormone binds to the GR, it causes a conformational change in the GR, resulting in the dissociation of chaperones and Hsps (Zhou and Cidlowski, 2005; Stahn *et al*., 2007). This GR-Gc complex is then translocated into the cell nucleus where it is responsible for transactivation or transrepression of target genes (Ray *et al.,* 1996; Stahn *et al*., 2007; Sommer and Ray, 2008).

The GR can directly initiate transcription of target genes by GR-GR dimers binding to glucocorticoid response elements (GREs) in the promoter regions of target genes; this is known as transactivation (Fig.1.2). The GR bound to the DNA recruits co-modulator proteins, which act to covalently modify histone proteins to remodel chromatin, or alter nucleosome phasing; thereby acting to expose the chromatin structure for gene transcription. GR monomers have been shown to bind to other DNA-bound transcription factors in a synergistic or composite manner, thereby increasing transcriptional activity (Chrousos, 2004; Zhou and Cidlowski, 2005; Stahn *et al*., 2007; Sommer and Ray, 2008; Oakley and Cidlowski, 2011).

Transrepression, or down-regulation, of genes by the GR can occur via different mechanisms (Fig. 1.2). The GR-GR dimers can bind to negative GREs (nGREs), thus preventing other transcription factors binding to target genes, thereby displacing them. Furthermore, GR monomers can act by attaching themselves to other transcription factors, rendering them unable to bind to target genes, and recruit co-repressors to inhibit gene transcription by remodelling chromatin (Chrousos, 2004; Stahn *et al*., 2007; Sommer and Ray, 2008; Oakley and Cidlowski, 2011). These pathways are thought to play a major role in the inflammatory effects of Gcs. Gc administration, mediated by the GR, causes apoptosis in some cancers and cell types. However these apoptotic pathways are tissue specific and cell-type dependent, and may be activated by non-genomic actions of the GR (Zhou and Cidlowski, 2005; Stahn *et al*., 2007; Sommer and Ray, 2008; Oakley and Cidlowski, 2011).

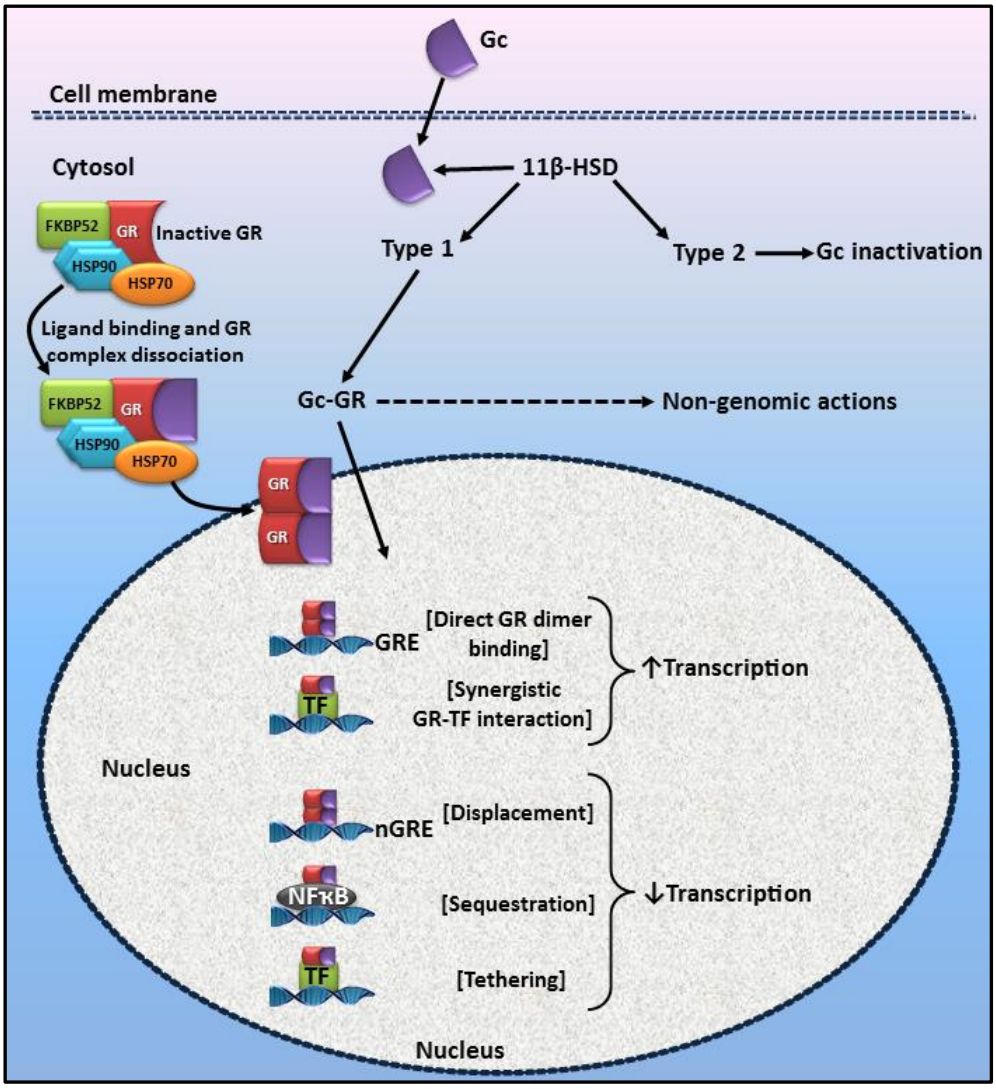

Figure 1.2. The glucocorticoid (**Gc**) and glucocorticoid receptor (**GR**) signalling pathway. The inactive GR complex resides in the cytosol. Gcs diffuse across the cell membrane, where they are cleaved by 11β-hydroxysteroid dehydrogenase type 1 (**11β-HSD1**) into the active form. Gcs bind to the GR with a high affinity, causing a conformational change in the GR rendering it active. The GR-Gc active complex is translocated into the nucleus, where it induces transactivation or transrepression of genes. Transactivation occurs either by direct GR dimer binding to the glucocorticoid response elements (**GREs**), or by interacting with other transcription factors (**TFs**) in a synergistic manner. Transrepression occurs either by displacing other factors bound to negative GREs (**nGREs**), or by sequestering other TFs (preventing them from binding to promoters of target genes), or by tethering the GR to other factors to prevent transcription. Image adapted from Sommer and Ray (2008).

1.3.2 The GR structure

The GR belongs to the nuclear receptor superfamily of transcription factors. The GR protein consists of three domains with numerous functions: the N-terminal domain, the DNA-binding domain and a ligand binding domain. The *GR* is a complex gene, located on chromosome 5q31–32, and is made up of 9 exons (Fig. 1.3) (Zhou and Cidlowski, 2005; Duma *et al.*, 2006; Stahn *et al*., 2007; Turner *et al*., 2010). Exon 1 contains the 5' untranslated region (UTR), whilst the translated region extends from exon 2 to 9 (Duma *et al.*, 2006; Turner *et al*., 2010). Exon 1 contains 9 untranslated alternative exons which are the promoter regions (Fig. 1.3) (Turner *et al*., 2010). Exon 1, containing the promoter regions, does not contain TATA, TATA-like boxes or CCAAT motifs. Instead, it contains many GC (guanine-cytosine) rich regions and transcription binding sites (Duma *et al.*, 2006; Turner *et al*., 2010).

The single *GR* gene can generate different isoforms via alternative splicing of exon 9, producing the GRα and β isoforms (Duma *et al.*, 2006; Wu *et al*., 2013). These two isoforms are identical up until amino acid 727, where they are spliced differently (Duma *et al.*, 2006; Lu and Cidlowski, 2006). GRα is expressed at higher levels compared to GRβ, in most tissues, and GRβ does not appear to be transcriptionally active in most tissues, being unable to bind glucocorticoids (Duma *et al.*, 2006; Lu and Cidlowski, 2006; Wu *et al*., 2013). However, GRβ appears to have an interaction with GRα by repressing the transactivation activity of endogenous GRα. Therefore, an increase in GRβ levels may coincide with Gc resistance (Lu and Cidlowski, 2006). The full length GRα isoform is 777 amino acids in length, whilst GRβ consists of 742 amino acids (Duma *et al.*, 2006; Lu and Cidlowski, 2006; Lu *et al.*, 2007; Turner *et al*., 2010).

Each *GRα* mRNA transcript can generate different isoforms via alternative translation initiation mechanisms such as ribosomal leaky scanning and ribosomal shunting (Fig. 1.3). The eight different GRα isoforms are namely hGRα-A, B, C1, C2, C3, D1, D2 and D3 (Duma *et al.*, 2006; Turner *et al*., 2010; Wu *et al*., 2013). GRα-A isoform is the full length receptor whilst the other GRα isoforms have shorter N-terminal domains (Duma *et al.*, 2006; Lu *et al.*, 2007; Turner *et al*., 2010).

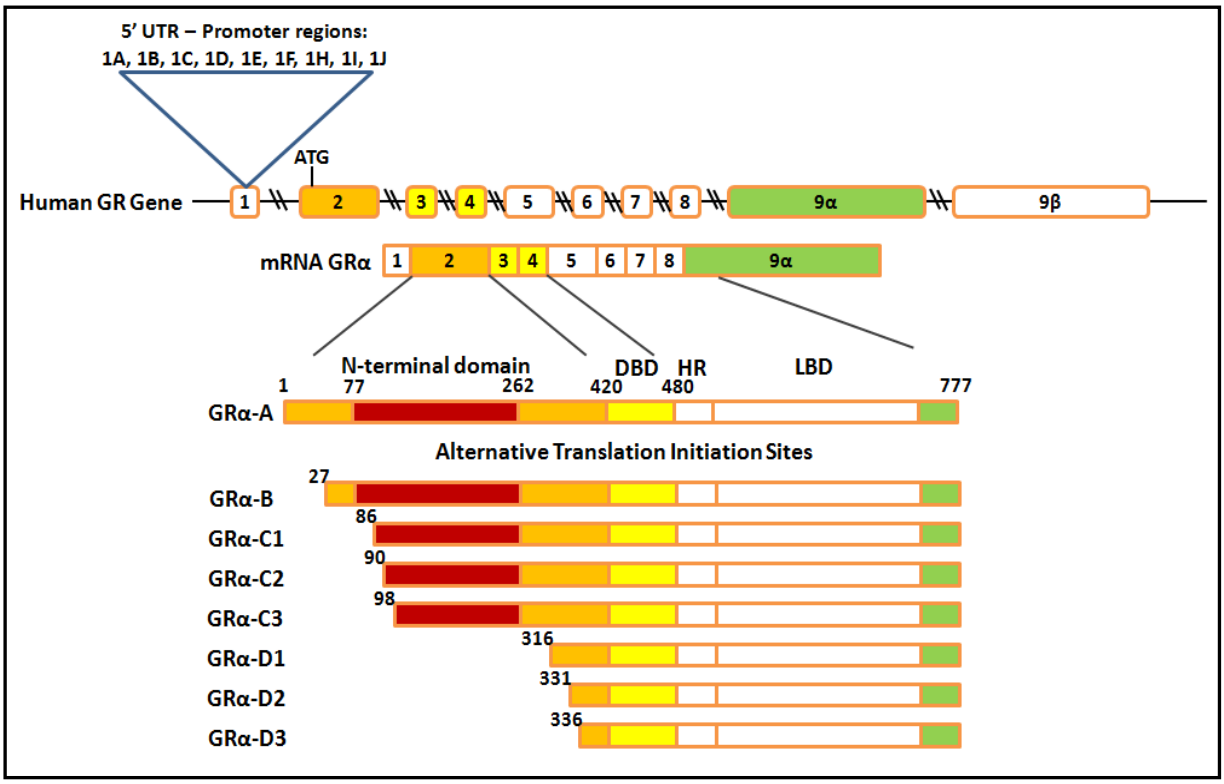

Figure 1.3. Genomic structure of the human glucocorticoid receptor alpha (**hGRα**). The 5' UTR (Exon 1) contains 9 alternative transcription initiation sites upstream of the *hGR* gene. Generation of multiple hGRα protein isoforms are as a result of alternative translation initiation sites. Translation can be initiated in each of the AUG start codons corresponding to the positions 1, 27, 86, 90, 98, 316, 331 and 336 of the GRα N-terminal domain, resulting in a set of hGRα isoforms with different lengths, sizes and functional domains. Abbreviations: (**UTR**) Untranslated region; (**DBD**) DNA binding domain; (**LBD**) ligand binding domain; (**HR**) hinge region (Duma *et al.*, 2006). Image adapted from Lu and Cidlowski (2006) and Turner *et al*. (2010).

It is not certain why all of these GR isoforms exist but it is apparent that GR isoform expression is tissue specific. The pancreas and colon have mostly GRα-C isoform expression, compared to the lung and spleen which display a higher GRα-D isoform presence (Wu *et al*., 2013). Lu *et al.* (2007) showed that, when the GR was over-expressed in U-2 OS cells, a bone cancer (osteosarcoma) cell line lacking endogenous GR expression, the cells underwent apoptosis. To determine which GR isoform is the most effective at inducing apoptosis, the U-2 OS cells were transfected with the different isoforms and it was shown that the GRα-C isoforms (C1-C3) were the most effective at inducing apoptosis. GRα-A and -B were less effective at inducing apoptosis compared to GRα-C; whilst the GRα-D (D1-D3) isoforms were the least effective at inducing apoptosis. GRα-C isoforms were able to recruit co-activators and induce chromatin modifications (acetylates histone H4) on proaopototic genes. Specifically, GRα-C isoforms

were able to induce the expression of proapoptotic molecules, such as granzyme A (GZMA) and to recruit activated RNA polymerase II to the GZMA promoter more efficiently (Lu *et al.*, 2007).

Wu *et al*. (2013) produced clones of Jurkat cells (T-lymphocytes) expressing individual GR isoforms in order to identify the functions of each GR isoform and examine the apoptosis inducing ability of each of the GR isoforms. These findings were similar to that of Lu *et al.* (2007), where the GRα-C isoforms were most effective at inducing apoptosis whilst GRα-D isoforms were less effective. They found that although the GRα-C isoforms were the most effective at inducing apoptosis, the apoptotic pathways and gene regulation by the GRα-C isoforms were carried out differently in the Jurkat cells, compared to the U-2 OS cells. The difference in the expression levels of the GR in these two cells lines could potentially contribute to some of the cell-specific gene profiles that mediate repression or expression of apoptotic genes. For example: T-cells (Jurkat cells) have selectively higher GRα-C isoform up-regulation which could make them more sensitive to Gcs (Lu *et al.*, 2007; Wu *et al*., 2013).

1.4 Apoptosis

Chemotherapy resistance is a problem in the treatment of SCLC. Radiation or chemotherapy used in cancer treatments results in DNA damage, which can lead to apoptotic cell death through a p53 dependent pathway (Elmore, 2007). SCLC cells are consistently resistant to the apoptotic effects of chemotherapy; this infers that apoptotic prevention is a survival advantage in tumour progression in SCLCs (Sethi *et al.*, 1999). Programmed cell death or apoptosis has two main signalling pathways: the extrinsic pathway and the intrinsic pathway. Apoptosis is carried out by a family known as caspases, which are activated by both pathways. When caspases are activated, they cause other caspases to be activated, resulting in a caspase cascade, which causes apoptosis via nuclear and cellular degradation (Schmidt *et al.*, 2004; Ghobrial *et al*., 2005; Schlossmacher *et al*., 2011).

The extrinsic pathway is triggered by ligand-mediated activation of membrane death receptors or the tumour necrosis factor (TNF) receptor cell surface superfamily, such as the Fas ligand/CD95 and the TNF-related apoptosis-inducing ligand (TRAIL). The Fas-associated death domain or TNF-associated death domain proteins bind to caspase 8 and 10, resulting in the catalytic activation of the caspase cascade, leading to apoptosis. The intrinsic pathway is more complex and controlled by members of the Bcl-2 family and mitochondria derived proteins

(Schmidt *et al.,* 2004; Ghobrial *et al*., 2005; Schlossmacher *et al*., 2011). The Bcl-2 family consists of pro- and anti-apoptotic proteins; these proteins control apoptotic cell death by controlling the balance of anti- and pro-apoptotic Bcl-2 family members. The pro-apoptotic members in the Bcl-2 family includes Bax, Bak, Bad, Bcl-Xs, Bid, Bik, Bim, and Hrk, and anti-apoptotic members such Bcl-2, Bcl-xL, Bcl-W, Bfl-1, and Mcl-1 (Ghobrial *et al*., 2005; Molitoris *et al.,* 2011; Schlossmacher *et al*., 2011). The anti-apoptotic Bcl-2 family members repress apoptosis by blocking the release of cytochrome *c*, whereas pro-apoptotic members act as promoters (Ghobrial *et al*., 2005; Schlossmacher *et al*., 2011). The balance of pro- and anti-apoptotic proteins is referred to as the 'Bcl-2 rheostat'. DNA damage, for example, can cause cellular stress which leads to an increase in pro-apoptotic Bcl-2 proteins which attach to the outer mitochondrial membrane, that cause cytochrome *c* to translocate into the cytoplasm. Cytochrome *c* then binds ATP, Apaf-1 and pro-caspase 9 which activates caspase 9 and subsequently caspase 3, causing the activation of the caspase cascade and finally apoptosis (Ghobrial *et al*., 2005; Schlossmacher *et al*., 2011).

1.4.1 Gc-GR mediated apoptosis in SCLC

There is a fair amount of evidence that suggests that in most cell types that have been studied, Gcs induce apoptosis via the intrinsic pathway. Gc-induced apoptosis has proven to be GR dependent (Molitoris *et al.,* 2011; Schlossmacher *et al*., 2011). SCLCs however, have reduced GR expression. Gc-GR interaction can activate cell death through the induction of pro-apoptotic members of the Bcl-2 family, such as Bim, Bid and Bad and/or repressing anti-apoptotic proteins such as Bcl-2 and Bcl-xL. Bad prevents the pro-survival activity of Bcl-2 and Bcl-xL, this stimulates Bax activation, committing the cell to apoptosis (Fig.1.4) (Molitoris *et al.,* 2011; Schlossmacher *et al*., 2011).

The overexpression of GR in SCLC *in vitro* induced apoptosis by up-regulating the pro-apoptotic genes; Bad and Bax (Sommer *et al.*, 2007). *In vivo*, DMS 79 xenografts were infected with GR-expressing adenovirus which resulted in apoptotic cell death by the up-regulation of Bad and down-regulation of anti-apoptotic/pro-survival genes Bcl-2, Bcl-xL and Mcl-1. Interestingly, the evidence in this study suggests that over-expression of the GR induced apoptosis in the absence of added ligand (Sommer *et al.,* 2010).

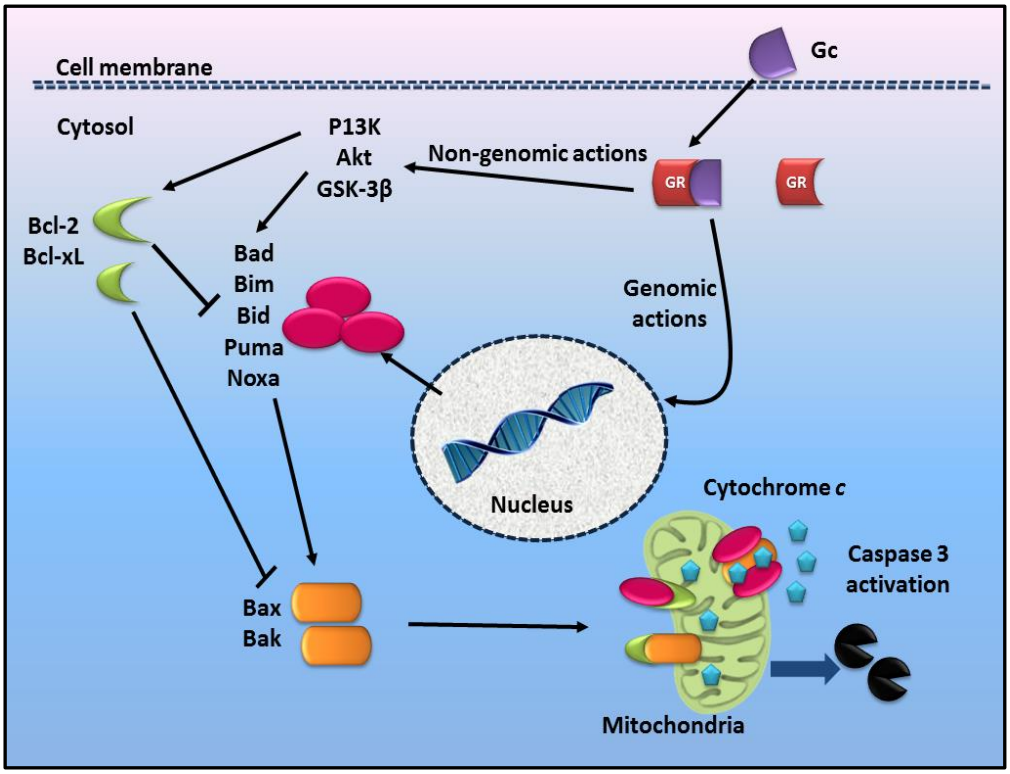

Figure 1.4. Glucocorticoid-mediated apoptosis pathways. Glucocorticoids act via genomic and non-genomic pathways. The pathways are cell-specific and it appears that there are canonical and non-canonical Gc-induced apoptotic pathways. It is thought that glucocorticoids act via the intrinsic pathway to result in apoptosis; however, there may be more than one pathway involved. Adapted from Schlossmacher *et al.* (2011).

1.5 Epigenetic modifications in cancer

SCLC cells have significantly reduced levels of the normally ubiquitously expressed GR, which accounts for their Gc resistance (Ray *et al.*, 1996; Sommer *et al.*, 2007; 2010). When the GR is re-expressed in SCLC cell lines and in xenograft, it results in tumour cell apoptosis. This suggests that GR expression is unfavourable for tumour development (Sommer *et al.*, 2007; 2010). Many tumours silence unwanted gene expression through a plethora of mechanisms; these genes are usually tumour suppressor genes (TSGs). Tumourigenesis is principally caused by fundamental DNA mutations in normal cells that subsequently result in cancer (Laird and Jaenisch, 1994; Baylin *et al.*, 2004; Baylin, 2005; Robertson, 2005; Weber *et al.*, 2005). Studies have found that TSGs, that would usually regulate cellular growth, are frequently silenced during tumourigenesis (Baylin, 2005; Robertson, 2005; Weber *et al.*, 2005). TSGs can be altered via genetic or epigenetic alterations. Genetic mutations that occur in oncogenes often

result in a gain in function; however, if there are deletions in tumour suppressor genes, it may result in a loss in function (Baylin, 2005; Robertson, 2005).

Epigenetics is defined as cellular modifications that can be heritable but are unrelated to DNA sequence changes and are able to be modified by environmental stimuli (Turner, 2000; Bell and Spector, 2011). Epigenetic alterations can give rise to many disorders including cancers, neuron diseases, psychosis, and cardiovascular diseases (Lin *et al*., 2010c). Epigenetic mechanisms comprise of DNA methylation, histone modifications, nucleosome positioning and may also include other mechanisms such as ATP-based chromatin remodelling complexes, non-coding RNA mediated gene silencing, Polycomb-Trithorax protein complexes, and many other mechanisms (Turner, 2000; Bell and Spector, 2011). During tumourgenesis many tumour suppressor and other genes are silenced via epigenetic factors.

Nucleosomes have an important function in the packaging of DNA, as well as a key role in genomic functioning (Fig. 1.5). The nucleosome is made up of a histone octamer, two copies of H2A, H2B, H3 and H4, which is wrapped around 146 base pairs of DNA. The structure is conserved in eukaryotes. There is a large amount of variability due to modifications that can be made via enzyme-catalysed reactions. Histones can be modified easily due to their exposed N-terminal tails on the nucleosome surface (Fig. 1.5); the most common modification is acetylation of the ε-amino group of lysine residues (Turner, 2000). Acetylation of the histones results in the relaxed state of the chromatin; therefore transcription factors can gain access to the DNA, indicative of an active transcription site (Turner, 2000; Deaton and Bird, 2011). DNA methylation at the promoter regions of genes is often accompanied by histone modifications, ultimately resulting in the loss of gene expression (Tessema and Belinsky, 2008).

1.5.1 DNA methylation

DNA methylation is a naturally occurring phenomenon in organisms, functioning to regulate many important genes. DNA methylation has been shown to play a role in differential gene silencing in normal development; X-chromosome inactivation and gene imprinting are methylation dependent and occur during the early stages of development. DNA methylation is not limited to imprinted regions and plays an important role in tissue specific gene expression and cell cycle regulation (Turner *et al*., 2008). DNA methylation is an epigenetic event that has been linked to the early onset of carcinogenesis because global methylation patterns are altered in many cancers. This can result in aberrant DNA methylation and TSG function due to hyper

and hypo-methylation (Baylin *et al*., 2004; Baylin, 2005; Weber *et al*., 2005; Vaissière *et al*., 2009; Lin *et al*., 2010c).

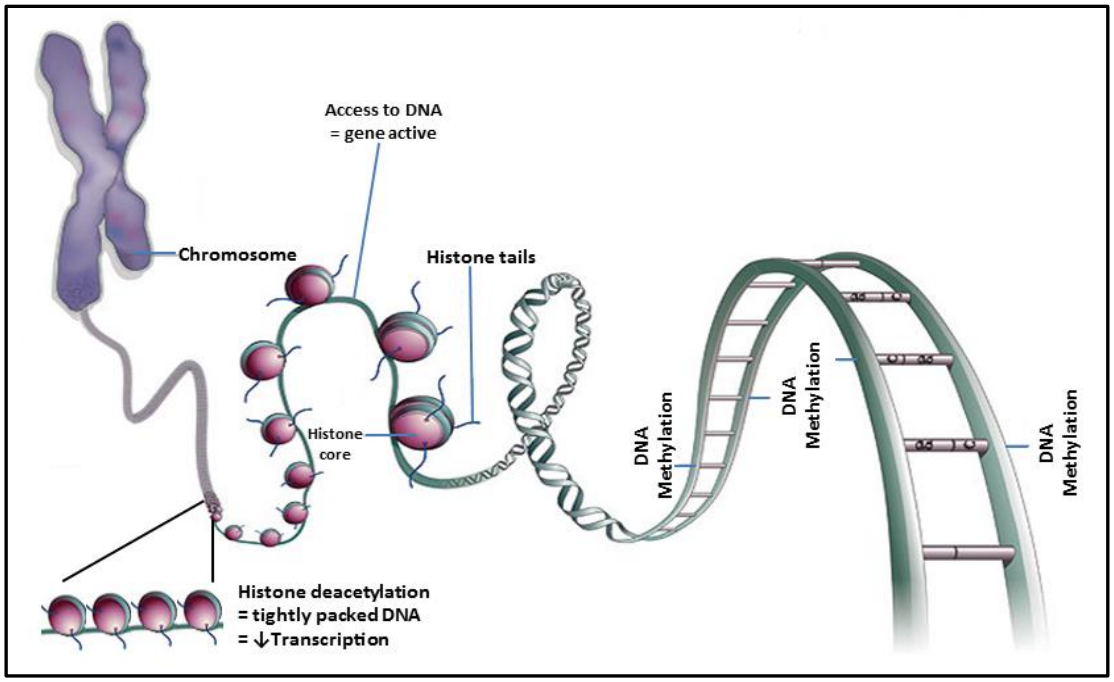

Figure 1.5. Methylation mechanisms. DNA methylation occurs on cytosine residues. Histone tails can be acetylated to "open" the DNA and allow gene transcription. Adapted from Qui (2006).

DNA methylation is considered an epigenetic event because although it is heritable, it does not involve a change in the nucleotide sequence (Baylin, 2005; Weber *et al*., 2005). DNA methylation involves the covalent addition of a methyl group on the 5' carbon on the cytosine ring (5-methylcytosine) (Baylin *et al.*, 2004; Baylin, 2005; Robertson, 2005; Weber *et al*., 2005). These methyl groups are found mainly at cytosine-guanosine dinucleotides (5'-CpG-3') and protrude into the major groove of DNA and prevent transcription (Fig. 1.5) (Baylin, 2005; Robertson, 2005; Weber *et al*., 2005).

1.5.1.1 CpG islands

Regions of high CpG content, known as CpG islands, occur at a relatively low frequency of ~4% throughout the genome but they are found at a much higher frequency in promoter regions of genes, where transcription begins (Momparler and Bovenzi, 2000; Baylin *et al.*, 2004; Baylin, 2005; Weber *et al*., 2007). In mammalian genomes, most of the CpGs (60-90%) are thought to be methylated, depending on their location within the genome (Turner *et al*., 2008).

However, CpG islands found in the promoters or first exons of genes (~70%) remain unmethylated (Turner *et al*., 2008; Deaton and Bird, 2011).

CpG islands generally lack promoter elements such as the TATA box. It has been proposed that CpG rich regions may function due to transcription factors recognising CpG rich regions specifically (Lin *et al*., 2010c). CpG islands can operate in the regulation of transcription in the promoter regions of genes; thus CpG islands that lack methylation are indicative of an active transcription site (Baylin *et al.*, 2004; Baylin, 2005; Robertson, 2005; Weber *et al*., 2005; 2007). Genes are silenced if they are methylated at the promoter regions of genes, where transcription begins (Baylin, 2005; Weber *et al*., 2005). Epigenetic silencing is thought to play a role in early cancer development and occurs as often as mutations and deletions in cancers, resulting in the dysregulation and silencing of tumour suppressor genes (Baylin, 2005; Weber *et al*., 2005; Lin *et al*., 2010c; Deaton and Bird, 2011). The promoter region in the GR (exon 1) consists of many CpG islands that have the potential to be methylated (Duma *et al.*, 2006; Turner *et al*., 2010).

1.5.1.2 The mechanism of DNA methylation regulation

DNA methylation is controlled at a number of different levels in normal cells (Baylin, 2005; Weber *et al*., 2005; Klose and Bird, 2006; Weber *et al*., 2007). DNA methyltransferases (DNMTs) are enzymes that add methyl groups to cytosine residues in DNA (Baylin, 2005; Weber *et al*., 2005; Klose and Bird, 2006; Lin *et al*., 2010c). Other factors also affect methylation patterns, such as the chromatin structure near promoter regions, which are affected by nucleosome spacing and histone acetylases, affecting the access of transcriptional factors (Baylin, 2005).

The DNA methyltransferases identified in mammalian cells include DNMT1, DNMT3a and DNMT3b (Momparler and Bovenzi, 2000; Baylin, 2005; Klose and Bird, 2006; Weber *et al*., 2007). CpG modifications take place after DNA replication, when the template DNA is hemi-methylated and the methylation pattern is maintained by DNMT1 after each DNA replication (Momparler and Bovenzi, 2000; Baylin, 2005; Klose and Bird, 2006; Weber *et al*., 2007). The function of DNMT1 is to maintain the identical methylation pattern, which is tissue specific, throughout the genome and is also involved in *de novo* methylation. DNMT3a and DNMT3b have been found to methylate hemimethylated and also unmethylated DNA which has led to the conclusion that they are responsible for *de novo* methylation (Momparler and Bovenzi, 2000; Baylin, 2005; Klose and Bird, 2006; Lin *et al*., 2010c). DNMT3b expression is also

significantly increased in tumours suggesting that it has a role in tumour formation (Momparler and Bovenzi, 2000; Baylin, 2005). This means that, in cancer cells, DNMT1 and DNMT3b may both be responsible for the abnormal methylation patterns (Baylin, 2005). DNMT1 carries out DNA methylating activity throughout the genome (including CpG islands) and it has been reported to be over-expressed in lung and liver cancer patients that are cigarette smokers (Lin *et al.*, 2010b). The promoters of tumour suppressor genes (TSGs) are often hypermethylated at the CpG regions in tumour cells (Baylin *et al.*, 2004; Vaissière *et al.*, 2009; Lin *et al.*, 2010b).

1.6 NNK - a key carcinogen in cigarette smoke

There are over 60 known carcinogenic compounds in cigarettes. Nicotine, although toxic and highly addictive is not carcinogenic (Hecht, 2003). Chemicals from the *N*-nitrosamine family are considered to be most carcinogenic compounds found in cigarettes and are thought to play a major role in tumour formation (Hecht, 2003; Maser, 2004; Akopyan and Bonavida, 2006). These *N*-nitrosamines are produced during the curing process of tobacco (Maser, 2004; Akopyan and Bonavida, 2006) and are considered to be a group 1 carcinogen by the International Agency for Research on Cancer (IARC) (IARC, 2014). Nitrosamine 4-(methylnitrosamino)-1-(3-pyridyl)-1-butanone, also known as nicotine-derived nitrosamine ketone (NNK), is the most potent cancer causing molecule in the nitrosamine family and is a biomarker of cigarette smoke exposure (Carmella *et al.*, 1995; Akopyan and Bonavida, 2006; Lin *et al.*, 2010b). NNK is an aromatic compound with a molecular formula of $C_{10}H_{13}N_3O_2$ (Fig. 1.6) (Maser, 2004; Akopyan and Bonavida, 2006).

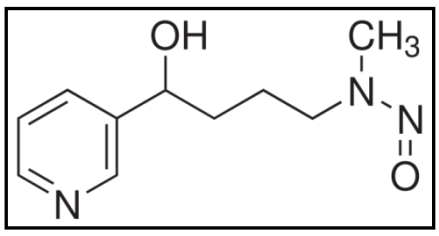

Figure 1.6. Chemical structure of NNK, a key carcinogen in cigarette smoke. Taken from http://www.sigmaaldrich.com/catalog/product/fluka/59773?lang=en&region=ZA

1.6.1 The link between NNK and carcinogenesis

Exposure to NNK induces pulmonary carcinomas in rodents and humans (Carmella *et al*., 1993; Carmella *et al*., 1995; Maser, 2004; Akopyan and Bonavida, 2006; Lin *et al.*, 2010b). NNK

exposure has been linked to gene mutation and hypermethylation of multiple TSG promoters in lung and liver cancers, such as cyclin-dependent kinase inhibitor 2A (p16, inhibits CDK4) (*p16*^{INK4a}), death-associated protein kinase 1 (*DAPk1*), retinoic acid receptor β (*RARB*), and runt-related transcription factor 3 (*Runx*) (Carmella *et al*., 1995; Pulling *et al*., 2004; Belinsky, 2005; Turner *et al*., 2008; Lin *et al*., 2010b). NNK exposure also causes changes in many signalling pathways such as the EGFR, AKT, MAPK, ERK1/2, and NFκB pathways (Lin *et al*., 2010b). Lin *et al*. (2010b) found that NNK induced nuclear accumulation of DNMT1 and subsequent hypermethylation of multiple TSG promoters; this in turn may lead to tumourigenesis and poor prognosis, thus providing a possible link between smoking and lung cancer.

1.7 Aims and Objectives

SCLC cells express low levels of the usually ubiquitously expressed GR, accounting for their Gc resistance. Restoration of GR expression in human SCLC cells (via infection with adenovirus) ultimately results in apoptosis of the cancer cells, suggesting that silencing of the *GR* gene may confer a tumour survival advantage in SCLC (Sommer *et al*., 2007; 2010). This means that the loss of GR expression provides a survival advantage in SCLC cells and may be a TSG in SCLC (Sommer *et al*., 2010). DNA methylation patterns of the alternative GR promoters regulate tissue-specific GR isoform expression (Turner *et al*., 2008), suggesting that GR expression is controlled by methylation. It has recently been shown that the *GR* promoter region (particularly promoter 1C) in SCLC shows evidence of methylation (Kay *et al*., 2011).

Recent data suggest that the *GR* promoters in SCLC cells are silenced by DNA hypermethylation (Kay *et al*., 2011). The deoxyribonucleoside triphosphate, 5-Aza-2'-deoxycytidine, is a DNMT inhibitor that can be incorporated into DNA (Baylin, 2005; Ghoshal *et al*., 2005; Lyko and Brown, 2005; Stresemann and Lyko, 2008). 5-Aza-2'-deoxycytidine is a simple derivative of the DNA nucleoside, cytosine, and DNMT cannot methylate DNA that has the 5-Aza-2'-deoxycytidine nucleoside incorporated (Baylin, 2005; Ghoshal *et al*., 2005; Lyko and Brown, 2005). When SCLC cells are treated with a demethylating agent, the GR is re-expressed; leading to the apoptotic cell death of the SCLC cells (Kay *et al*., 2011). GR tissue-specific protein isoform expression has been suggested to mediate the repression or expression of apoptotic genes (Wu *et al*., 2013).

DNMT1 carries out methylating activity and is known to be over-expressed in lung and liver cancer patients who are cigarette smokers (Lin *et al.*, 2010b). NNK, a major carcinogenic agent in cigarette smoke, has been linked in the nuclear accumulation of DNMT1 and thus responsible for the hypermethylation of multiple TSGs in lung cancers (Baylin, 2005; Lin *et al.*, 2010b). Therefore, it is possible that NNK is linked to the silencing of the *GR* gene through hypermethylation in SCLC.

The aims of this study were:

1. To determine which GRα isoforms are re-expressed in SCLC cells after exposure to a demethylation agent.

2. To determine whether treatment with the cigarette carcinogen, NNK, results in GRα expression changes due to the nuclear accumulation of DNMT1 in normal lung fibroblast MRC-5 cells.

    2.1. To determine whether the tobacco carcinogen, NNK, down-regulates *GR*α mRNA expression.

    2.2. To determine whether NNK treatment down-regulates GRα protein expression.

    2.3. To determine whether the mechanism by which the *GR* gene is silenced, after NNK treatment, is due to DNMT1 accumulation at the *GR* promoter.

The SCLC cell line, DMS 79; the Gc-sensitive non-SCLC cell line, A549; and the Gc-resistant HEK 293 cell lines, were be treated with 5-Aza to determine which GRα isoforms are re-expressed in SCLC cells and compared to the control cell lines. Normal lung fibroblast cells (MRC-5) were treated with NNK, to determine whether the GR is affected at the gene and protein level, due to the nuclear accumulation of DNMT1 at the *GR* promoter region.

2. Materials and Methods

2.1 Tissue culture

2.1.1 Cell lines

A small cell lung cancer (DMS 79), non-small cell lung cancer (A549), human embryonic kidney (HEK 293) and normal lung fibroblast (MRC-5) cell line were used in this study. All of the cell lines were obtained from the American Type Culture Collection (ATCC). The DMS 79 cell line was derived from a patient diagnosed with an ACTH-producing SCLC. This cell line produces very low levels of the GR below the threshold level required for functionality. The cells are insensitive to Gc administration. The HEK cells are also GR deficient and are thus also resistant to Gcs. The A549 express high levels of the GR and are Gc sensitive. The MRC-5 cells are normal, non-cancerous, lung fibroblast cells and thus express "normal" lung levels of the GR.

2.1.2 Tissue Culture Techniques

All tissue culture techniques and treatments were carried out in a Class II (Type A2) laminar flow, biological safety cabinet (Logic Purifier® Labconco®) under sterile conditions. The cell lines were incubated at 37°C in a humidified CO_2 incubator (Forma Scientific) containing 5 % CO_2. The non-adherent (grown in suspension) DMS 79 cells were cultured in T-75 (75 cm^3) flasks (Corning®) with 20 mL RPMI 1640 culture medium containing 10 mmol/L HEPES buffer and L-glutamine (BioWhittaker™, Lonza) supplemented with 10% heat-inactivated foetal bovine serum (FBS) (HyClone™, Thermo Scientific™), and 100 units/mL of penicillin/streptomycin (BioWhittaker™, Lonza). The adherent A549, HEK 293 and MRC-5 cell lines were cultured in 10 cm^3 Corning® culture dishes containing 10 mL of Dulbecco's Modified Eagle's Medium (DMEM) (BioWhittaker™, Lonza) supplemented with 10% FBS and 100 units/mL of penicillin/streptomycin (BioWhittaker™, Lonza).

Cell culture growth was assessed using an inverted microscope (Nikon TMS) at 40 × and 100 × magnification. When the adherent cells were confluent, they were passaged by the addition of 1 mL of Trypsin-EDTA (1x) solution (BioWhittaker™, Lonza) (Appendix B.1) to a T-75 flask or a 10 cm^3 culture dish (Corning®). Culture medium was added to neutralise the Trypsin-EDTA solution in a 1:1 ratio and the cells were split accordingly. When the non-adherent DMS 79 cellswere confluent, excess medium was removed whilst the remaining medium (with cells) was

transferred to a 15 mL centrifuge tube (Corning®) and centrifuged at 1000 × *g* for 3 minutes (Eppendorf Centrifuge 5810R, Merck). The cell pellet was re-suspended in 1 mL of medium and the cells split accordingly.

2.1.3 Tissue culture experimental design

2.1.3.1 5-Aza-2'-deoxycytidine stock preparation

5-Aza-2'-deoxycytidine (5-Aza) was purchased from Sigma-Aldrich®. The 5-Aza was dissolved in 500 µL of filter sterilised acetic acid and 500 µL of water (in a 1:1 ratio) (Appendix B.2). From this stock, a 1:100 working solution was prepared by adding 1 µL of 5-Aza stock solution and 99 µL of the respective media. A 0.5:100 dilution of the vehicle (control) was made with 0.5 µL of filter sterilised glacial acetic acid and 99.5 µL of medium.

2.1.3.2 5-Aza Treatments

The A549 and HEK 293 cell lines were split into two 10 cm^3 culture dishes per treatment and the DMS 79 cell line was split into one T-75 flask per treatment for protein extraction. When the cells were ~60% confluent they were either treated with a vehicle (control), 0.5 µmol/L, 1 µmol/L or a 5 µmol/L of 5-Aza for 72 hour/s (h) (Appendix B.2).

2.1.3.3 NNK stock preparation

4-(Methylnitrosoamino)-1-(3-pyridinyl)-1-butanone, NNK was purchased from Sigma-Aldrich®. The NNK was dissolved in 200 µL of dimethyl sulfoxide (DMSO) (Appendix B.3). From this stock, a 1:100 working solution was made by adding 1 µL of NNK stock solution and 99 µL of the respective media. When the cells were ~60% confluent they were either treated with vehicle (control) or 10 µmol/L of NNK for 2, 4, 6, 24, 48 or 72 h.

2.1.3.4 NNK Treatments

For qPCR assays, the MRC-5 cell line was split into one 10 cm^3 culture dishes per treatment. For Western blot and Chromatin Immunoprecipitation (ChIP) assays, two 10 cm^3 culture dishes were used per treatment. The MRC-5 cells were treated with 10 µmol/L of NNK for 0 minutes (vehicle control/DMSO), 2, 4, 6, 24 or 48 h to examine the effect of NNK treatment on GRα expression. The cells used for the ChIP-PCR assay were either treated with a vehicle (control)

or 10 µmol/L of NNK for 24 or 48 h. The cells used in the Western blot analysis were either treated with a vehicle (control) or 10 µmol/L of NNK for 24, 48 or 72 h (Appendix B.3).

2.2 RNA Extraction

Total RNA was extracted from the MRC-5 cells using the RNeasy® Mini spin column kit (QIAGEN). The cell culture medium was removed from the culture dishes and the cells were washed with 2 mL of 1 × phosphate buffered saline (PBS) (Appendix B.4). Trypsin-EDTA (1 ×) solution (1 mL) was added to each dish, which was incubated for 4-5 minutes at 37°C, until the cells were detached from the bottom surface of the dish. Culture medium (1 mL) was added to the cell dishes, to inactivate the trypsin, and the cells were then transferred to a 15 mL centrifuge tube (Corning®). The tube was centrifuged for 3 minutes at 1000 × *g* (Eppendorf Centrifuge 5810R, Merck).

The RNA was extracted from cells using the RNeasy® Mini spin column kit, as per manufacturer's instructions for animal cells. After the cells were collected by centrifugation, the supernatant was discarded and the cell pellet was re-suspended in 350 µL of RLT lysis buffer. The cell mixture was pipetted up and down, and vortexed (Vortex Genie 2, Lastec SA) for 15 seconds to loosen the cell pellet and lyse the cells. The mixture was transferred to a QIAshredder spin column (QIAGEN), to purify the RNA lysate, and centrifuged at full speed for 2 minutes (Eppendorf Centrifuge 5418). One volume (350 µL) of 70% ethanol (Appendix B.5) was added to the cell lysate (supernatant fraction) which was mixed well by pipetting (~20 times) to homogenise the lysate.

The RNA cell lysate was then transferred into an RNeasy spin column with a 2 mL collection tube and centrifuged at 8000 × *g* for 15 seconds after which the flow-through was discarded. RW1 buffer (700 µL) was added to the spin column to wash the membrane. The sample was centrifuged at 8000 × *g* for 15 seconds and the flow-through discarded. RPE buffer (500 µL) was added to the spin column, which was then centrifuged at 8000 × *g* for 15 seconds. The flow-through was discarded and 500 µL of RPE buffer was added to the spin column, which was centrifuged at 8000 × *g* for 2 minutes to wash the spin column membrane. The spin column was then placed into a new 2 mL collection tube and centrifuged at 13,000 × *g* for 1 minute to remove any leftover RPE buffer and ethanol which may interfere with the RNA isolation. The spin column was then placed into a new 1.5 mL microcentrifuge tube and 30 µL of RNase free water (GIBCO®) was added directly to the spin column membrane. The spin column was

centrifuged at 8000 × *g* for 1 minute to elute the RNA. RNA concentration was measured using a Nanodrop spectrophotometer ND-1000 version 3.5.2 (NanoDrop Technologies) (Appendix A.3.1). The RNA samples were then aliquoted and stored at -80°C.

2.2.1 Evaluation of RNA Integrity

The integrity of each RNA sample was evaluated by RNA agarose gel electrophoresis in accordance with the Minimum Information for Publication of Quantitative Real-time PCR Experiments (MIQE) guidelines. Prior to RNA gel casting, all electrophoresis gel apparatuses and glassware were soaked in hydrogen peroxide overnight to remove RNAses. The samples were prepared by adding 2 µg of RNA to 2 volumes of RNA loading buffer (Sigma-Aldrich®) into a 1.5 mL microcentrifge tube (Starlab). The samples were incubated at 65°C for 10 minutes in a dry bath incubator (Polychem supplies cc). The samples were resolved on a 1.5% RNA agarose/2.2 mol/L formaldehyde gel (Appendix B.6). The 1 kb O'GeneRuler™ DNA ladder mix (0.5 µg/µL) (Fermentas) molecular weight marker (MWM) was used. A 1 × MOPS buffer was used for the running buffer (Appendix B.6). The gel was viewed using the ChemiDoc™ XRS$^+$ Imaging System with Image lab™ software version 2.0.1 (Bio-Rad). Two distinct bands of 18 S rRNA and 28 S rRNA were used to verify the integrity of the RNA samples.

2.3 cDNA Synthesis

cDNA was synthesised from RNA samples using the Tetro cDNA Synthesis Kit (Bioline). The RNA was defrosted on ice prior to cDNA synthesis and a Bio-Rad MyCycler™ thermal cycler was used for all the incubation steps as per the cDNA synthesis protocol below. All buffers and reagents were thawed, vortexed and centrifuged as per manufacturer's instructions before use. A standard concentration of 2 µg RNA was used for cDNA synthesis.

2.3.1 Poly (A) tail priming

The poly(A) tail priming step was prepared on ice. An RNA concentration of 2 µg, 1 µL of Oligo $(dT)_{18}$ primer mix, 1 µL of dNTP mix, and DEPC-treated water were added to a final volume of 10 µL per reaction. The samples were centrifuged and incubated at 70°C for 5 minutes after which the samples were immediately put on slushy ice for 5 minutes.

2.3.2 First strand cDNA synthesis

A reaction master mix was prepared whilst the samples were incubating on ice. The master mix was made up with: 4 µL of 5 × RT buffer, 4 µL of DEPC-treated water, 1 µL Ribosafe RNase Inhibitor and 1 µL Tetro reverse transcriptase (RT) (200 units/µL) per reaction. A volume of 10 µL of the reaction master mix was added to each sample after ice incubation, mixed by gentle pipetting and centrifuged. The PCR tubes were then incubated at 45°C for 60 minutes and the reaction was terminated incubating the samples at 85 °C for 5 minutes. The tubes were cooled on ice and 20 µL of RNase free water was added to each sample. cDNA aliquots were made and stored at -20°C. A no-RT control sample was prepared for each RNA sample (per treatment and cell line) in which no reverse transcriptase was added; this was used as a negative control for cDNA synthesis and qPCR analysis.

2.4 CpG plot mapping of *GR* promoter

The CpG island content within the *GR* promoter region was evaluated. The *GR* gene sequence was obtained from the UCSC genome browser site (http://genome.ucsc.edu/); range = chr5:142661454-142787754 (ref. = uc003lmy.3). The 5'-UTR was 4500 base pairs (bp) long. The input sequence, ranging from the 5'-UTR to the beginning of exon 2 (+ 3000 bp), was entered into the EMBOSS CpG Plot finder software. The CpG Plot finder software was accessed on the EBI website, an outstation of the European Molecular Biology Laboratory (http://www.ebi.ac.uk/Tools/seqstats/emboss_cpgplot/). The parameters used to analyse the *GR* sequence were as follows: the ratio of observed to expected of CpG islands was set to 0.60, the percentage of 5'-CpG-3' must be equal to or more than 50% and CpG island length must be equal to or greater than 200.

2.5 Polymerase Chain Reaction (PCR)

2.5.1 Primers

Primer sets specific for the human glucocorticoid receptor alpha (*GRα*), human *GR* promoter regions (1B, 1C, 1F, and 1J), glyceraldehyde-3-phosphate dehydrogenase (*GAPDH*), and beta actin (*β-actin*) were used in PCR analysis. The primer sets for the human *GR* promoter regions: 1B, 1C, 1F and 1J were not obtained from published material and were designed using the Primer 3 Plus tool (Rozen and Skaletsky, 2000) in conjunction with the NCBI database

(www.ncbi.nlm.nih.gov) using the Primer BLAST resource (Appendix A.5.1) (Table 2.1). The primer sets were selected on the basis of primer specificity, GC %, and similar melting temperatures of individual primers within a set and by a desired product size. The primer sets were aligned against the human genome, using the NCBI database, in order to ensure that they were specific for the desired product. Primers, purchased from Inqaba Biotech, were reconstituted in TE buffer (Appendix B.8) into 100 µmol/L stock solutions, as per manufacturer instructions, and stored at -20°C. The primer stock solutions were diluted in a 1:10 ratio with nuclease free water and used at a final concentration of 10 µmol/L. Conventional PCR was initially performed to optimise the primers sets, prior to qPCR analysis.

2.5.2 Conventional PCR

Conventional PCR was performed to assess the specificity and optimal annealing temperature of each primer set in a temperature gradient. A 20 µl reaction was made up of 1 µl of cDNA/DNA, 2 µl of 10 × *Taq* $(NH_4)_2SO_4$ buffer, 1.8 µl $MgCl_2$ (25 mmol/L), 1 µl of forward (10 mmol/L) and 1 µL of reverse primer (10 mmol/L) (Appendix B.9), 2 µl of dNTP mix (2 mmol/L) (Appendix B.10), 0.2 µl of *Taq* recombinant DNA polymerase (5 units/µl) and 11 µl of nuclease free water. All PCR reagents were purchased from Fermentas. As a negative control, a no template control, in which cDNA/DNA was excluded, was run for each primer set. The incubation steps for the conventional PCR reactions were performed in a Bio-Rad MyCycler™ thermal cycler.

For standard PCR tests or runs, the following PCR protocol was used: Initial denaturation at 95°C for 4 minutes; 35 cycles of 95°C for 30 seconds, 60°C for 1 minute and 72°C for 1 minute; and a final elongation step for 7 minutes at 72°C. For the ChIP analysis, conventional PCR was used to verify the presence of the *GR* promoter regions. The following protocol was used with 2 µl of DNA: Initial denaturation at 95°C for 3 minutes; 35 cycles of 95°C for 30 seconds, 59°C for 45 seconds and 72°C for 1 minute; and a final elongation step for 7 minutes at 72°C. When amplification was completed, all PCR products were collected by centrifugation and stored at 4°C.

Table 2.1. List of primer sequence information used in PCR and qPCR.

Primers/Gene	**Sequences (5'-3')**	**Product Size (base pairs-bp)**	**Annealing Temperature (T_a) (°C)**	**Source**
GRα	Fwd: CCATTGTCAAGAGGGAAGGA Rev: CAGCTAACATCTCGGGGAAT	173	60	Sommer *et al.* (2007)
GR promoter 1B	Fwd: CAACTTCCTTCGAGTGTGAGC Rev: AGAGAAGTTGCAAAGCAGAACC	160	59	Primer 3 Plus Rozen and Skaletsky (2000)
GR promoter 1C	Fwd: AACTCGGTGGCCCTCTTAAC Rev: ATGCAACCTGTTGGTGACG	247	60	Primer 3 Plus Rozen and Skaletsky (2000)
GR promoter 1F	Fwd: CCCCTTTCGAAGTGACACAC Rev: CCACCGAGTTTCTCCAGTTT	165	59	Primer 3 Plus Rozen and Skaletsky (2000)
GR promoter 1J	Fwd: TATGAACGTGATAGGGTGAGCA Rev: CAAGTTGCAGGCGAAATAGTAA	177	59	Primer 3 Plus Rozen and Skaletsky (2000)
β-actin	Fwd: GGCCACGGCTGCTTC Rev: GTTGGCGTACAGGTCTTTGC	208	60	Alt *et al*. (2010)
GAPDH	Fwd: TACTAGCGGTTTTACGGGCG Rev: TCGAACAGGAGGAGCAGAGAGCGA	166	59	EZ ChIP™ kit (Millipore) Catalog # 22-004

2.5.2.1 Agarose gel electrophoresis

PCR products were resolved on a 1.5% agarose (TopVision™, Fermentas) gel (Appendix B.11) in 1 × Tris-base EDTA (TBE) running buffer (Appendix B.12). A 50 bp O'GeneRuler DNA Ladder molecular weight marker was resolved in the first lane of all gels and 3 µL of 6 × loading dye (Thermo Scientific) was added to each sample prior to loading. Each sample (12 µL), containing loading dye, was added to each well. The gels were run at 85 V for 50 minutes. Gels were visualised using a ChemiDoc® XRS+ Imaging System with the software package Image Lab™ (Bio-Rad).

2.6 Quantitative Real-Time PCR (qPCR)

The relative expression levels of the *GRα* gene and *GR* promoter regions (1B, 1C, 1F and 1J) were quantified using qPCR analysis. The primers sets for *GRα* and the two reference genes: *β-actin* and *GAPDH* (ChIP analysis only) were used where appropriate for each qPCR run. qPCR experimental design and procedures were based on the MIQE guidelines (Bustin *et al*., 2009). The MIQE guidelines ensure the accurate evaluation and reporting of qPCR data by making a standard manner in which the results are interpreted (Bustin *et al*., 2009). The detailed information satisfying the MIQE guidelines for the experiments are outlined in Appendix A.

No-template/cDNA controls and no-RT controls were performed to ensure that no contamination was present and that the results were obtained were true reflections of expression levels reported (Appendix A.8.4). Primer set specificity was evaluated by melt curve analysis of each qPCR product (Appendix A.7.1). The qPCR products were also confirmed by agarose gel electrophoresis. qPCR was performed using SYBR® Green JumpStart™ *Taq* ReadyMix™ (Sigma-Aldrich®) in a MiniOpticon™ Real-Time PCR Detection System (Bio-Rad) using the CFX Manager™ Program Software package version 2.1 (Bio-Rad). Florescence was read using a baseline of 0.2 RFU for all qPCR runs (Appendix A.6).

One 25 µL qPCR reaction consisted of 12.5 µL SYBR® Green JumpStart™ *Taq* ReadyMix™, 9.5 µL of nuclease free water, 1 µL forward primer (10 µmol/L), 1 µL reverse primer (10 µmol/L) and 1 µL cDNA. The qPCR reaction protocol was: Initial denaturation step at 95°C for 2 minutes; followed by 40 cycles of 95°C for 15 seconds, 60°C for 30 seconds, 72°C for 1 minute with a plate read step; and an extra 72°C extension step for 10 minutes. The melt curve

analysis ranged from 50 °C - 95 °C, with a temperature increase of 1°C every 5 seconds and a plate read.

2.6.1 qPCR analysis

The results of the qPCR runs were analysed using the CFX Manager™ package version 2.1 (Bio-Rad). The data was transformed using the $2^{-\Delta\Delta C_T}$ method as outlined by Livak and Schmittgen (2001) and gene expression levels in treatments were represented as bar graphs (made in Microsoft Excel) along with standard error of the mean. The average threshold cycle (Ct) values for each of the genes of interest in a single experimental run were calculated, these values were then normalised against the average Ct values for the corresponding internal reference gene (*β-actin* or *GAPDH*) in order to obtain fold change values for treatments relative to the control (Appendix A).

2.6.1.1 The $2^{-\Delta\Delta C_T}$ analysis method of qPCR Data

Two biological repeats were performed per experiment, where each biological repeat consisted of 3 experimental runs with 3 technical repeats within each run (n=3). The use of the $2^{-\Delta\Delta C_T}$ method was performed according to the MIQE guidelines. Each primer set was tested for reaction efficiency by making a dilution series of cDNA and quantifying the Ct values. Fresh undiluted cDNA was used to make a 10-fold series of dilutions which was analysed using primer sets for GRα and β-actin. The reaction efficiencies of each primer set were between 90-110% and the r^2 value was close to 1 (Appendix A.7.2).

2.7 Western blot analysis

2.7.1 Protein extraction and sample preparation

For the adherent cell lines, MRC-5, HEK and A549s, two 10 cm^3 dishes were used per treatment. The cell culture medium was removed from the dishes. The lightly adherent HEK cells were washed off with 2 mL of 1 × PBS. The MRC-5 and A549 cells were removed from the 10 cm^3 dishes by using a cell scraper (Biologix Research Company) and washed off the dishes with 1 × PBS. The cells were combined in a single 15 mL centrifuge tube. One T75 flask per treatment was used for the DMS 79 cells. The suspension cells were collected by centrifugation in a 15 mL centrifuge tube. The 15 mL tubes containing the cells were

centrifuged at room temperature for 5 minutes at 1800 rpm (Eppendorf Centrifuge 5810R, Merck). The supernatant was discarded. The pellet was re-suspended in 1 mL of 1 × PBS and centrifuged at 4°C for 3 minutes at 1800 rpm. The supernatant was discarded.

RIPA buffer (Sigma-Aldrich®) (50 µL) containing protease and phosphate inhibitors (Appendix C.1) was added to each tube and mixed by vortexing at medium speed. The tubes were incubated for 5 minutes at room temperature and then plunged into ice for 30 minutes. The tubes were then centrifuged at 4°C for 15 minutes at 4000 rpm. The protein lysate (supernatant) was removed, ready for sample preparation. Some of the protein lysate (10 µL) was removed before sample preparation, to be used for protein quantification.

The protein lysate samples were prepared by adding the reducing sample treatment buffer (Appendix C.2) to each protein lysate in a 1:1 ratio. The mixture was vortexed to mix the samples and centrifuged before being placed on a heating block (Polychem Supplies cc) at 95°C for 5 minutes. Thereafter, the samples were vortexed, centrifuged and stored at -80°C.

2.7.2 Protein quantification

The protein concentration was measured using the Pierce® Bicinchoninic Acid (BCA) protein assay kit (Thermo Scientific), using the 'microplate procedure'. A standard curve was generated using known dilutions and concentrations of bovine serum albumin (BSA) (Appendix C.3). The unknown protein sample concentrations were determined based on the standard curve.

2.7.2.1 BCA Working Reagent (WR) Preparation

The 10 µL of protein lysate, that was removed previously, was prepared for protein quantification by dilution in RNase free water in a 1:10 ratio (90 µL of RNase free water added to 10 µL of lysate).The total working reagent (WR) consisted of a mixture of Reagent A and Reagent B, and was calculated using the following equation:

WR required = [(number of standards × number of replicates) + (number of samples × number of replicates) + 1 extra for pipetting error] × 200 µL

The WR is made up by mixing Reagent A and Reagent B. The WR is prepared by mixing 50 parts of Reagent A with 1 part of Reagent B (Reagent A: Reagent B, 50:1).

2.7.2.2 Microplate procedure

The BSA standards were made up according to the manufacturers' instructions (Appendix C.3). The BSA standards and samples were all mixed and centrifuged. Each standard or sample was pipetted into a 96-well microplate (Sero-Well), 25 µL of each. There were 2 replicates per BSA standard concentration and 3 replicates were performed per unknown protein sample. WR (200 µL) was added to each well and the plate was gently mixed by brief agitation for 30 seconds. The microplate was covered with cling wrap and incubated at 37°C for 30 minutes. After incubation, the microplate was allowed to cool to room temperature and read on a microplate reader (PowerWave XS plate reader, Bio-Tek®), using the KC4™ v.3.2 program. The absorbance readings were read at 562 nm. A standard curve was generated from the known BSA protein standard concentrations, which was used to determine the unknown sample concentrations.

2.7.2.3 Generation of the BSA standard curve and unknown protein concentrations

A standard curve was constructed by plotting the mean absorbance vs. concentration of BSA standards (Appendix C.3). Each BSA standard series was loaded onto the microplate in duplicate. The absorbance values for the 'blank' readings were subtracted from the mean absorbance values for the BSA standard reading. A straight line equation was generated from the standard curve, which was used to calculate the unknown protein concentrations (Appendix C.3).

The absorbance values for unknown protein samples run in triplicate were averaged and the 'blank' reading was subtracted from each mean. The unknown protein concentrations were calculated using the straight line equation generated from the standard curve and concentration was multiplied by 10 (due to 1:10 dilution of protein lysate done previously) to determine the protein stock concentration. This value was further divided by 2 because of the protein dilution by the addition of the reducing sample treatment buffer (1:1 dilution). The amount (in µL) of prepared protein lysate to achieve a final concentration of 40 µg of protein was calculated, as this was the final concentration loaded into the PAGE gels.

2.7.3 Polyacrylamide Gel Electrophoresis (PAGE)

2.7.3.1 Polyacrylamide Gel Assemblage

The Mini-PROTEAN 3 cell system (Bio-Rad) was used to perform PAGE. The glass plates (1.5 mm) were cleaned thoroughly and wiped with 70% ethanol. The two glass plates were put together and were held with two pieces of parafilm (Pechiney Plastic Packaging) over each other to ensure a complete seal was achieved. The sealed plates were placed into a Bio-Rad casting gel frame which was secured onto a Bio-Rad gel casting stand, tightly pressed into the casting foam (to prevent leaking).

In this study, a 13.5% resolving SDS polyacrylamide gel was found to be most effective to visualise the GRα isoforms effectively and 12.5% SDS polyacrylamide gels were sufficient to visualise overall GRα protein expression. The resolving gel was made in a 15 mL centrifuge tube (Appendix C.4) and gently mixed by inverting the tube. The resolving gel solution was then carefully added to the middle of the two glass plates using a 1 mL pipette. After all of the resolving gel had been added, 1 mL of deionised water was added, very slowly (drop wise), on top of the resolving gel solution. The resolving gel was given 30 minutes to solidify. When the gel had solidified, the deionised water was poured off and residual water absorbed by a piece of sterile filter paper.

The stacking gel (Appendix C.4) was prepared in a 15 mL centrifuge tube and gently mixed by inverting the tube. The stacking gel solution was then added on top of the casted resolving gel with a 1 mL pipette until it overflowed. A 15-well (1.5 mm thick) comb was inserted into the stacking gel solution (between the two glass plates). The gel was allowed 30 minutes to solidify. After the stacking gel had solidified, the comb was carefully removed, the parafilm was removed and the plates were cleaned of any gel debris present on the outside of the plates. The wells of the gels were rinsed in 1 × Electrode (Tank) buffer (Appendix C.5) to ensure that they were free of any gel debris. The gel was then inserted into the Mini-PROTEAN 3 cell tank system, with the short plate facing the gasket. The whole Mini-PROTEAN 3 cell tank was placed into a plastic container containing ice to ensure that the gel system did not heat up during electrophoresis.

Figure 2.1. Equipment used during gel assembly and PAGE. Image adapted from www.bio-rad.com.

2.7.3.2 PAGE and Protein Transfer

The protein samples were thawed from -80°C, warmed to 37°C and centrifuged at 12000 × *g* for 2 minutes (to remove protein aggregates). The protein samples (40 µg per sample) were loaded in duplicate for the 5-Aza treated cells and triplicate for the NNK treated cells per treatment on each gel. The PageRuler™ Prestained Protein Ladder (Fermentas, Thermo Scientific) was used as a molecular weight marker and 2.5 µL was added to the first and last wells in each gel. The proteins were separated for 30 minutes at 90 V (to get through the stacking gel) and thereafter for 60 minutes at 120 V (PowerPac™ Basic; Bio-Rad) in 1 L of 1 × Electrode (tank) buffer (Appendix C.5).

After PAGE, the gels were taken out of the apparatus and soaked in ice cold protein transfer buffer for 2-5 minutes (Appendix C.6). The glass plates, on either side of the gel, were separated using a Bio-Rad gel separator and the gel was lifted off of the plate. The stacking gel was removed and discarded.

The protein transfer sandwich cassette (see Fig. 2.2) was laid out and the foam pad/sponge (Bio-Rad) was soaked in protein transfer buffer and placed on the black side (cathode) of the protein transfer sandwich cassette. Three pieces of filter paper, cut to size (7.5 cm/ 10.5 cm), were soaked in protein transfer buffer and laid on top of the foam pad. A fourth piece of filter paper was used to gather the gel and was placed on top of the rest of the filter paper pieces. A 1 mL pipette tip (Tip One, Starlab) was used to smooth the gel out and remove any air bubbles or spaces between the gel and the filter paper pieces (to ensure an even transfer of protein). A nitrocellulose membrane (0.45 µm pore size, Amersham™ Hybond™ ECL nitrocellulose

membrane, GE Healthcare), cut to size (7.5 cm/ 10.5 cm), was soaked in protein transfer buffer and then placed on top of the gel. The 1 mL pipette tip was used again to remove air bubbles that may be present. Another 4 pieces of filter paper were soaked and placed on top of the nitrocellulose membrane, each piece smoothed by a 1 mL pipette tip. Another foam pad was soaked in protein transfer buffer which was placed on top of the stack. The protein transfer sandwich cassette was closed and placed into the Mini-PROTEAN 3 cell tank with the protein electrode system apparatus. The tank was filled with ice cold protein transfer buffer and an ice brick was inserted into the tank. The tank was placed into a plastic container (with ice in the container, surrounding the tank), to prevent heating. A magnetic stirrer was placed into the tank, to ensure even ion transfer, and the tank system was placed on an IKA® Big Squid stirrer. The proteins were transferred for 70 minutes at 100 V.

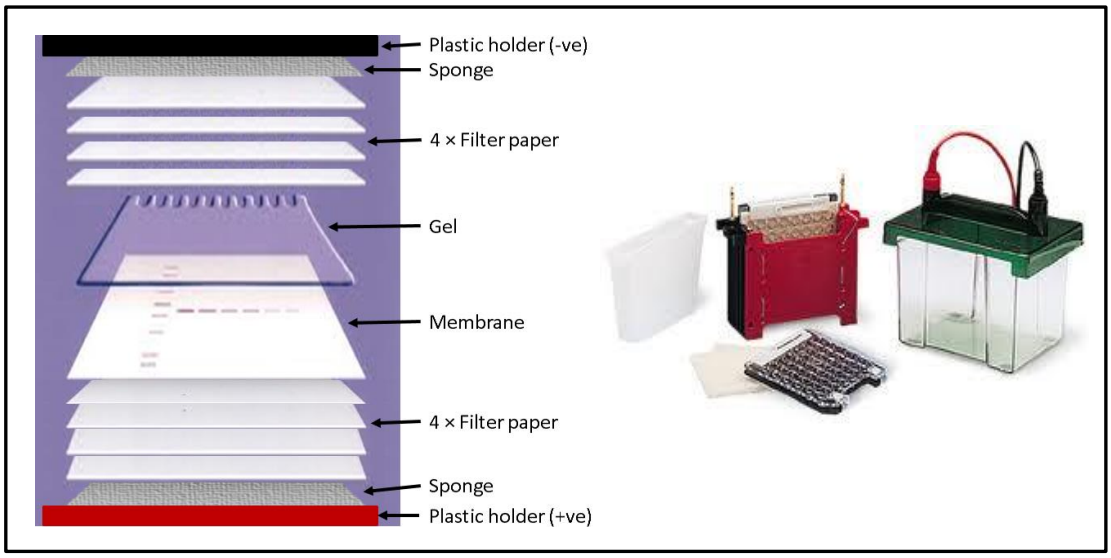

Figure 2.2. Equipment used during protein transfer onto nitrocellulose membrane. The protein transfer sandwich assembly is shown in detail, and the tank and protein transfer sandwich cassette are shown. Image adapted from www.bio-rad.com.

2.7.4 Membrane blocking and antibody incubations

Two proteins were probed for, GRα and GAPDH. GAPDH was used as the reference protein and loading control. The GAPDH protein is found between 30-40 kDa, whilst GRα is found between 60-94 kDa. When the protein transfer was complete, the nitrocellulose membrane was cut into two pieces at ~55 kDa, using the molecular weight marker as a guide. This was done so that the different antibodies could be probed for simultaneously.

The nitrocellulose membranes were rinsed twice in Tris-Buffered Saline with tween (TBS-T; Appendix C.7) to remove any excess protein transfer buffer. The TBS-T was discarded and the membranes were put into a 6% skim milk (Sigma-Aldrich®) blocking buffer solution (Appendix C.8) for an hour at room temperature with agitation (MiniMix, Enduro™, Labnet). This was done to block for non-specific primary antibody binding. After the blocking procedure, the nitrocellulose membranes were rinsed twice in TBS-T to remove excess blocking solution.

The nitrocellulose membranes were then probed with the primary antibodies: purified mouse anti-GRα, Clone 41 (1:24000; 611227, BD Biosciences) and rabbit anti-GAPDH (1:3000; 14C10, Cell Signalling) (Appendix C.9). The nitrocellulose membranes were incubated overnight at 4°C with agitation on an IKA® KS 130 Basic at 160 rpm.

The antibody solutions were removed the next day. The nitrocellulose membranes were rinsed 3 times quickly with TBS-T to remove residual antibody solution. The nitrocellulose membrane probed with the GRα primary antibody was washed 5 times for 8 minutes on the IKA® KS 130 Basic at 320 rpm with TBS-T, to remove any unbound or non-specifically bound primary antibody. In between each wash, the membrane probed with GRα was given an additional vigorous rinse with fresh TBS-T. The nitrocellulose membrane probed with GAPDH was washed 3 times for 8 minutes in TBS-T.

After the washes were completed, the TBS-T was removed completely. The nitrocellulose membranes were probed with the secondary antibodies, goat anti-mouse horseradish peroxidase (HRP) IgG for GRα (1:2000; 554002, BD Biosciences) and anti-rabbit HRP for GAPDH (1:4000; 7074, Cell Signalling) (Appendix C.9) at room temperature for an hour, with agitation on an IKA® KS 130 Basic at 160 rpm.

As above after the primary antibody incubation, the membranes were washed with TBS-T. This was performed as described. The GRα membrane was washed 6 times and the GAPDH membrane washed 3 times for 8 minutes each to remove non-specific secondary antibody binding.

2.7.4.1 Imaging and Densitometry

The nitrocellulose membrane was then visualised using the Immun-Star™ HRP Chemiluminescent kit (Bio-Rad) on the ChemiDoc™ XRS+ Imaging System with Image lab™

software version 2.0.1 (Bio-Rad). The chemiluminescent solution was made by combining stable HRP peroxide buffer with Immun-Star™ HRP luminol/Enhancer in a 1:1 ratio. The membranes were visualised individually for each protein. The membranes were dabbed on tissue paper on one side to remove excess TBS-T. 300 µL of the chemiluminescent mixture was pipetted onto the blot and evenly distributed. The images were captured with the ChemiDoc™ XRS+ Imaging System's supercooled high-resolution CCD camera. A colorimetric image was taken of the molecular weight marker as this does not show up in the chemiluminescent signal image. These two images of the membrane were merged and flipped so that the image was in the same orientation as when the protein was loaded onto the polyacrylamide gel. Ponceau S staining was performed on the nitrocellulose to examine total protein presence. The nitrocellulose was stained for 5 minutes with 1 × Ponceau S stain (Sigma-Aldrich®; Appendix C.10) with agitation and then rinsed with a Ponceau destain (Appendix C.10) for 30 seconds at room temperature with agitation. A colorimetric image was taken.

Densitometric analysis was performed on the nitrocellulose images using the Image lab™ software. The local pixel or band intensity was determined by constructing a rectangle (all the same size for each blot) around each band of interest. This value was subtracted from background "noise". The band intensities were exported into Microsoft Excel and the GRα band intensity was calculated relative to the GAPDH or total protein content (Ponceau S stain) band intensity with standard error of the mean (SEM). Statistical analyses were performed on the densitometry as explained in section 2.9.

2.8 Chromatin Immunoprecipitation

Chromatin Immunoprecipitation (ChIP) was performed according to the manufacturer's instructions using the EZ-ChIP™ kit (Millipore, Upstate, #17-371), with minor modifications. All components and reagents used were provided in the kit.

2.8.1 Crosslinking, Cell lysis and Sonication

Two 10 cm^3 dishes (with 10 mL culture medium) were used per treatment (vehicle (control), and 10 µmol/L of NNK for 24 or 48 h) for the adherent MRC-5 cells. The MRC-5 cells were fixed with 300 µL of 37% formaldehyde per 10 mL of medium for 10 minutes. After fixing the cells, 1 mL of 10 × glycine (0.125 mol/L) was used per 10 mL of medium to quench the unreacted formaldehyde for 5 minutes at room temperature.

The medium was aspirated from the adherent MRC-5 and the cells washed with 4 mL of ice cold 1 × PBS. Ice cold 1 × PBS (2 mL) (with protease inhibitor cocktail added - 10 µL per 2 mL) was added to each dish of MRC-5 cells which were then scraped off with a cell scraper (Biologix). The cells were then put into a 15 mL centrifuge tube (Corning®). The cells were centrifuged at 700 × *g* at 4°C for 2 minutes (Eppendorf Centrifuge 5810R, Merck) and the supernatant was removed. The cells were re-suspended in 1 mL of SDS lysis buffer (5 µL protease inhibitor cocktail added per 1 mL of SDS lysis buffer). 500 µL aliquots were made for sonication.

Sonication was performed to shear the chromatin into ~200-1000 bp fragments (verified by agarose gel electrophoresis) (see Appendix D). The 500 µL cell aliquots in SDS lysis buffer were sonicated on ice with ten 15 second pulses with 50 second rests (on wet ice) in between pulses, at power setting 6 (Misonix ultrasonic liquid processor XL 2000). Once the DNA was sheared, it was centrifuged at 13,000 × *g* for 10 minutes to remove insoluble material. The supernatant was then aliquoted into a fresh 1.5 mL microcentrifuge tube.

2.8.2 Immunoprecipitation of crosslinked protein/DNA complexes

The sheared chromatin was aliquoted into 200 µL per immunoprecipitation (IP) and diluted with 800 µL of the dilution buffer provided containing 4.5 µL of the protease inhibitor cocktail. The recommended positive control (Anti-RNA polymerase II), negative control (Normal Mouse IgG) and Input control were included in each experiment/IP. To each IP tube, 60 µL of ChIP blocked protein G agarose (in a gel slurry) was added and incubated for 1 hour at 4°C with agitation on an IKA® KS 130 Basic at 400 rpm. This step removes proteins and DNA that may bind non-specifically to the ChIP blocked protein G agarose. After incubation, the agarose was pelleted by brief centrifugation for 1 minute at 4000 × *g* (Eppendorf Centrifuge 5418). The supernatant was then removed and placed into a fresh microfuge tube (the agarose pellet was discarded) and the immunoprecipitating antibody was then added to each tube. Prior to the antibody addition, 10 µL of the IP was put in the fridge to be used later as an input control. Anti-RNA polymerase II was added (1 µg per 1 mL) to the positive control while normal mouse IgG was added (1 µg per 1 mL) to the negative control. The monoclonal mouse anti-DNMT1 (2 µg per 1 mL; IMG-261A) was added to the experimental IP. These tubes were then incubated overnight at 4°C with agitation (at 400 rpm). 60 µL of protein G agarose was added to each IP and incubated for 1 hour at 4°C with agitation (at 400 rpm) to collect the antibody/antigen/DNA

complex onto the beads. The tubes were then centrifuged to remove the supernatant by brief centrifugation for 1 minute at 4000 × *g*. The beads were then washed by re-suspending the beads in 1 mL of each of the cold buffers that were provided, in the order that they are stated below, and incubating for 4 minutes with agitation followed by brief centrifugation for 1 minute at 4000 × *g* and careful removal of the supernatant. One wash with Low Salt Immune Complex Wash Buffer, 1 wash with High Salt Immune Complex Wash Buffer, 1 wash with LiCl Immune Complex Wash Buffer, and 2 washes with TE Buffer.

2.8.3 Elution of the protein/DNA complexes and reversal of protein/DNA crosslinks

An elution buffer was made up with 10 µL of 20% SDS, 20 µL of 1 mol/L $NaHCO_3$ and 170 µL of RNase free water (GIBCO®) to a final volume of 200 µL (at room temperature) for each IP. Elution buffer (100 µl) was added to each IP tube as well as the input control tube (input was removed prior to antibody addition). The tubes were gently mixed by flicking the tubes and incubated for 15 minutes at room temperature. The pellets were collected by brief centrifugation for 1 minute at 4000 × *g* and the supernatants transferred into a new microfuge tube. The pellets were re-suspended in another 100 µL of the elution buffer and gently mixed by flicking the tubes and incubated for 15 minutes at room temperature. The pellets were collected by brief centrifugation for 1 minute at 4000 × *g*. The supernatants were transferred into the corresponding microfuge tube stated before to have a total of 200 µL of eluted IP.

The IP tubes were incubated at 65°C for 4.5 h with 8 µL of NaCl (5 mol/L) to reverse the DNA/protein complex crosslinks. The IP tubes were then stored at -20°C overnight. After reversal of the DNA/protein complex crosslinks, the IP tubes were incubated at 37°C for 30 minutes with 1 µL of RNase A. 4 µL of 0.5 mol/L EDTA, 8 µL of 1 mol/L Tris-HCL and 1 µL of Proteinase K were added to each tube and the tubes were incubated for 2 h at 45°C.

2.8.4 DNA Purification

1 mL of Bind Reagent A was added to each IP tube and mixed well by pipetting. Up to 600 µL of the mixture was added to a spin column/collection tube, provided in the kit, which was centrifuged for 30 seconds at 13,000 × *g*. The flow through was discarded, and the remaining 600 µL mixture was added to the spin column and centrifuged as before. 500 µL of Wash Reagent B was then added to each spin column and centrifuged for 30 seconds at 13,000 × *g*.

The flow through was discarded and the tubes were centrifuged again at the same speed to remove any further flow through. The spin column was placed into a fresh microfuge and 50 µL of Elution Buffer C was added directly onto the spin filter membrane which was then centrifuged for 30 seconds at 14,000 × *g*. The microfuge tube contained the purified DNA.

2.9 Statistical Analyses

The statistical analyses were performed using in IBM SPSS statistical software version 21. A one-way analysis of variance (ANOVA) was performed to make comparisons or a one sample t-test, where appropriate. The assumptions of an ANOVA apply to the residuals of the test. The assumptions of the ANOVA were that the residuals are normally distributed (determined by a one-sample Kolmogorov-Smirnov test), the variance of the residuals are equal in all treatments (determined using a Levene's test), and that the treatments are independent. A multiple comparisons test was performed to determine whether there were any significant differences between treatments. The assumptions of the t-test were that the data was normally distributed and the variances are equal. The assumptions were met for all statistical tests.

3. Results

3.1 Validation of RNA integrity

The MRC-5 cell line was used for qPCR gene expression analyses. RNA was extracted and cDNA synthesised for use in qPCR analyses. In accordance with the MIQE guidelines (Bustin *et al.*, 2009), the integrity all of the RNA samples were validated before use in qPCR analyses. RNA samples (2 µg) were run on 1.5% agarose/2.2 mol/L formaldehyde gels. A 1 kb O'GeneRuler^{TM} DNA ladder mix (0.5 µg/µL) (Fermentas) MWM was used and run in each gel and gels were stained with ethidium bromide. The presence of two distinct, intact bands (18 S rRNA and 28 S rRNA subunits) was used to verify good quality RNA and integrity (Fig. 3.1). The MIQE guideline requirements are presented in detail in Appendix A.

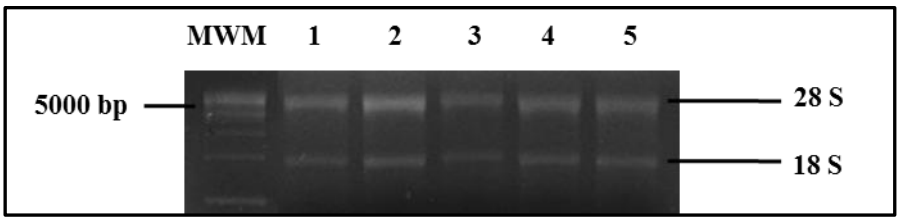

Figure 3.1. RNA integrity of samples extracted from MRC-5 cells, treated with NNK (10 µmol/L) or the vehicle (control). MWM - Molecular weight marker 1- Control; 2 - 2 h; 3 - 4 h; 4 - 6 h; and 5 - 24 h treatment with 10 µmol/L of NNK. The RNA extracted (second biological repeat) for qPCR is shown.

3.2 GRα protein expression with 5-Aza-2'-deoxycytidine treatment

Treatment with the demethylating agent, 5-Aza-2'-deoxycytidine (5-Aza) removes methyl marks and allows re-expression of hypermethylated genes (Baylin, 2005). The GR in SCLC is known to be silenced by methylation and treatment with 5-Aza results in its re-expression (Kay *et al.*, 2011). Western blot analyses were performed to establish which GRα isoforms were present and are re-expressed in SCLC cells (DMS 79s) after exposure to 5-Aza. The DMS 79, HEK and A549 cells were either treated with vehicle (control), 0.5 µmol/L, 1 µmol/L or 5 µmol/L of 5-Aza for 72 h. The protein was extracted and run on a 13.5% SDS PAGE gel, which was transferred onto a nitrocellulose membrane. The membrane was probed with a primary human monoclonal GRα or GAPDH antibody, and detected using the appropriate secondary HRP antibody.

3.2.1 5-Aza-2'-deoxycytidine treatment decreases presence of GRα protein in A549 cells

3.2.1.1 Presence of GRα isoforms in A549 cells

The Western blot image in Fig. 3.2 shows the GRα and GAPDH protein present in A549 cells. Two distinct GRα bands were seen in the A549 cells, representing two GRα isoforms GRα-A (~94 kDa) and GRα-B (~91 kDa).

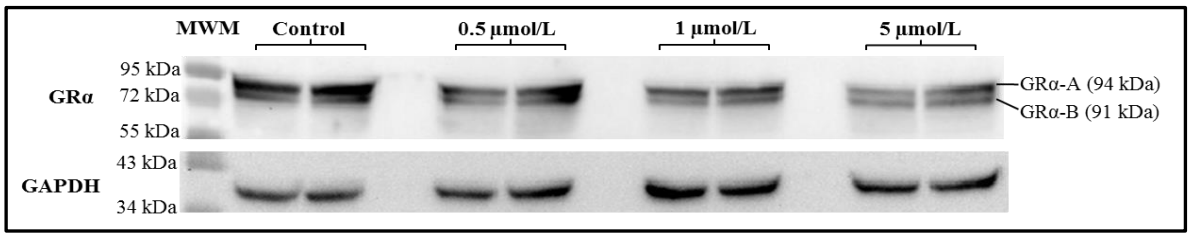

Figure 3.2. Western blot image probed for GRα and GAPDH in A549 cells treated either with vehicle (control), 0.5 µmol/L, 1 µmol/L and 5 µmol/L of 5-Aza for 72 h. MWM = Protein molecular weight marker (kDa). The different GRα isoforms are indicated.

3.2.1.2 Effect of 5-Aza-2'-deoxycytidine on GRα protein expression in A549 cells

Densitometry was performed on the Western blot image to quantitate band intensity. Band intensity indicates the amount of GRα protein present. Total GRα protein levels were normalised against the relative GAPDH (reference protein) levels. The relative GRα/GAPDH protein was then represented as fold change relative to the control. There was a significant difference in total GRα protein expression in the A549 cell line between the vehicle (control), 0.5 µmol/L, 1 µmol/L and 5 µmol/L 5-Aza treatments (F = 38.17; df = 3; p = 0.0021; Fig. 3.3). A multiple comparisons test indicated that the significant difference was between the control and all of the other treatments with a $p < 0.05$. This shows that all treatments with 5-Aza significantly down-regulated GRα protein expression in A549 cells.

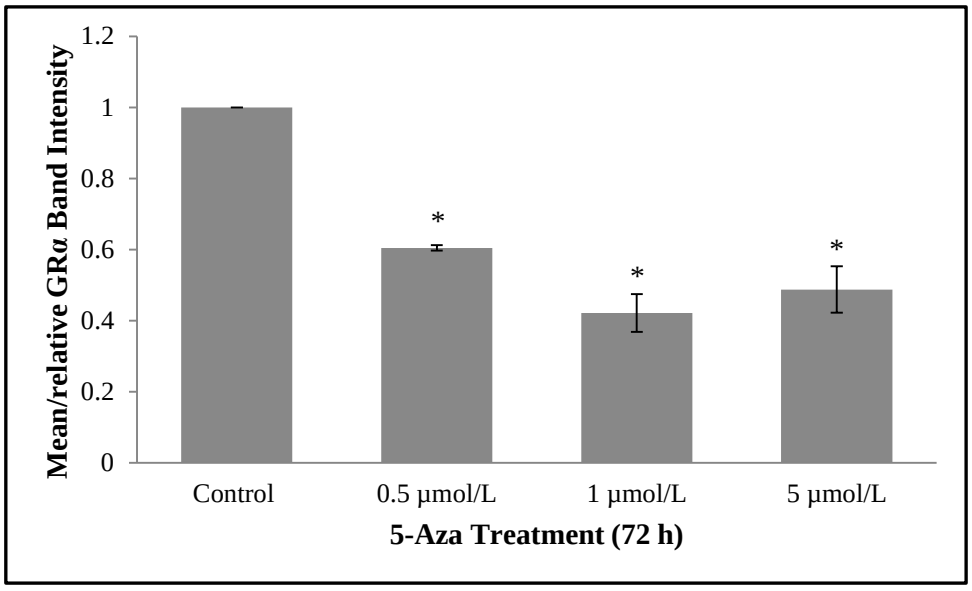

Figure 3.3. Densitometric analysis of total GRα protein expression relative to GAPDH expression in A549 cells. The mean ± SEM is displayed (n = 2; * indicates $p < 0.05$ compared to the vehicle (control)).

3.2.2 5-Aza-2'-deoxycytidine treatment has no effect on GRα protein in HEK 293 cells

3.2.2.1 Presence of GRα isoforms in HEK 293 cells

The Western blot image in Fig. 3.4 shows the GRα and GAPDH protein present in HEK 293 cells. Three distinct GRα bands were seen in the HEK 293 cells, representing three GRα isoforms, at GRα-A (~94 kDa), GRα-B (~91 kDa) and GRα-C (~78 kDa).

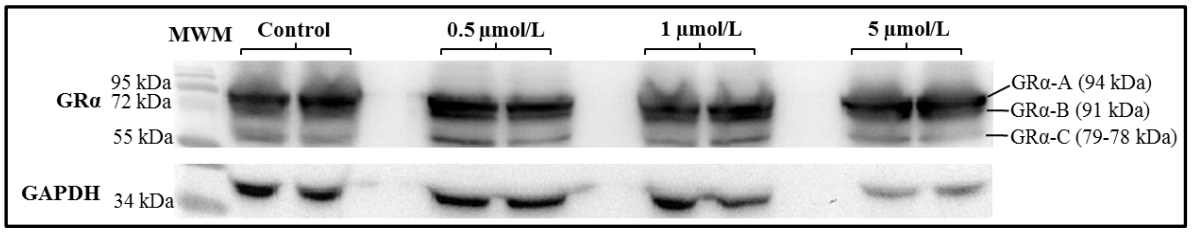

Figure 3.4. Western blot image probed for GRα and GAPDH in HEK 293 cells treated with vehicle (control), 0.5, 1 and 5 µmol/L of 5-Aza for 72 h. MWM = Protein molecular weight marker (kDa). The different GRα isoforms are indicated.

3.2.2.2 Effect of 5-Aza-2'-deoxycytidine on GRα protein expression in HEK 293 cells

Densitometric analysis showed that there was no significant difference in total GRα protein expression in the HEK 293 cell line between the vehicle (control), 0.5 µmol/L, 1 µmol/L and 5 µmol/L 5-Aza treatments (F = 0.23; df = 3; p = 0.87; Fig. 3.5). These data show that 5-Aza treatment has no effect on GRα expression in HEK cells.

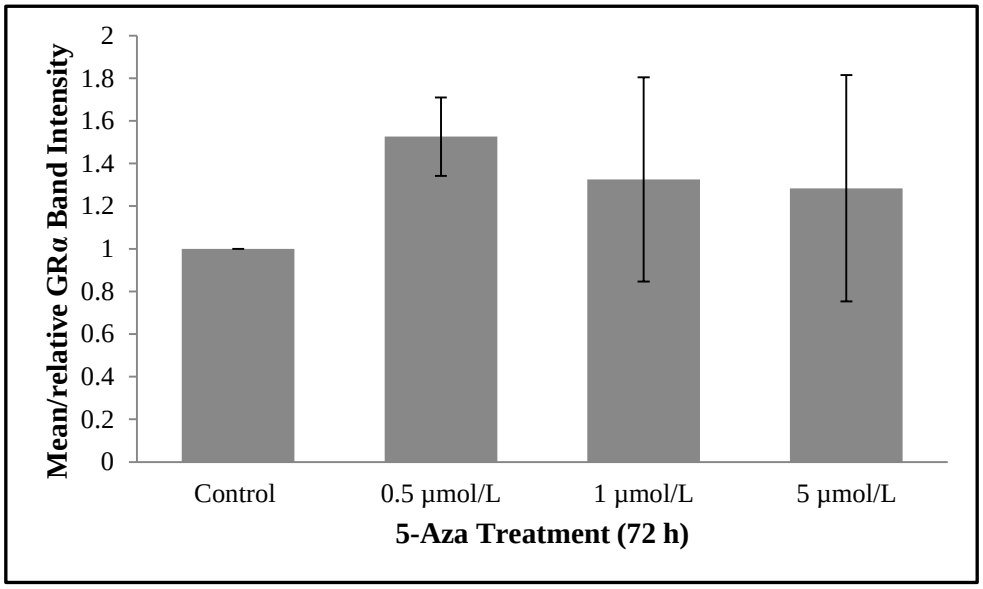

Figure 3.5. Densitometric analysis of the total GRα protein expression relative to GAPDH expression in HEK 293 cells. The mean ± SEM is displayed (n = 2).

3.2.3 5-Aza-2'-deoxycytidine treatment has no effect on GRα protein in DMS 79 cells

3.2.3.1 Presence of GRα isoforms in DMS 79 cells

The Western blot image in Fig. 3.6 shows the GRα and GAPDH protein present in DMS 79 cells. Four distinct GRα bands were seen in the DMS 79 cells, representing four GRα isoforms, at GRα-A (~94 kDa), GRα-B (~91 kDa) and two at GRα-C (~79-78 kDa).

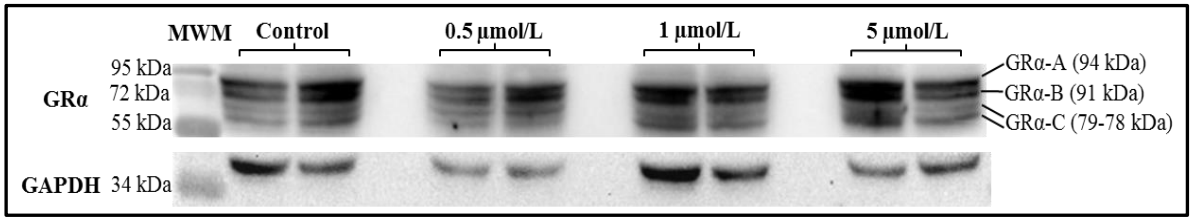

Figure 3.6. Western blot image probed for GRα and GAPDH in DMS 79 cells treated with a vehicle (control), 0.5, 1 and 5 µmol/L of 5-Aza for 72 h. MWM = Protein molecular weight marker (kDa). The different GRα isoforms are indicated.

3.2.3.2 Effect of 5-Aza-2'-deoxycytidine on GRα protein expression in DMS 79 cells

Previous work has shown that the GR is silenced by methylation in the SCLC cell line, DMS 79, and that treatment with the demethylating agent, 5-Aza results in GR re-expression (Kay *et al.*, 2011). Despite evidence of a trend indicating an increase in GRα expression with 5-Aza treatment, densitometric analysis showed that there was no significant difference in total GRα protein expression in the DMS 79 cell line between the vehicle (control), 0.5, 1 and 5 µmol/L 5-Aza treatments ($F = 0.659$; $df = 3$; $p = 0.6$; Fig. 3.7). This suggests that 5-Aza treatment has no effect on GRα protein expression in DMS 79 cells. These results are inconsistent with published data from Kay *et al*. (2011) showing that 5-Aza treatment restored GRα expression. The lack of significance in these data may be been due to degraded 5-Aza stocks, as a result of the late discovery of a bio-freezer failure.

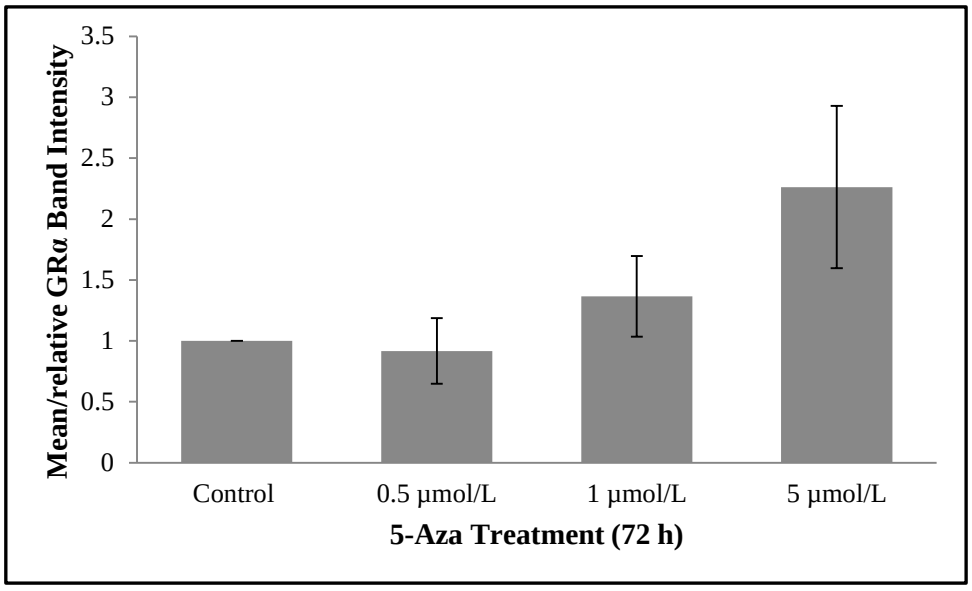

Figure 3.7. Densitometric analysis of the total GRα protein expression relative to GAPDH expression in DMS 79 cells. The mean ± SEM is displayed (n = 3).

3.3 The effect of NNK treatment on *GRα* mRNA expression in the non-cancerous lung fibroblast cell line, MRC-5

3.3.1 Short term exposure to NNK leads to reduced *GRα* expression in MRC-5 cells

Lin *et al*. (2010b) found that the tobacco smoke carcinogen, NNK, induced nuclear accumulation of DNMT1 which subsequently resulted in hypermethylation and thus silencing of multiple TSG promoters. Lin *et al*. (2010b) found that a 10 µmol/L dose of NNK was sufficient to elicit a change in expression of various genes. As the *GR* is silenced by methylation in small cell lung cancers, our aim was to determine whether NNK treatment could result in the repression of *GRα* expression in normal lung cells. The normal lung fibroblast (MRC-5) cell line was treated with 10 µmol/L of the tobacco smoke carcinogen, NNK, for various time intervals. RNA was extracted, cDNA synthesised and qPCR was run with primers specific for *GRα* and for the reference gene *β-actin*.

The data showed a significant down-regulation of *GRα* expression normalised to *β-actin* when the MRC-5 cells were treated with 10 µmol/L of NNK ($F = 3.976$; $df = 3$; $p = 0.038$; Fig. 3.8). A multiple comparisons test (Tukey HSD) indicated that the significant difference was between the vehicle (control) and the 2 h treatment with NNK ($p = 0.026$). Although not significant, both

4 and 6 h treatments show reduced *GRα* expression following NNK treatment. Therefore, short term (2 h) treatment with NNK significantly down-regulates *GRα* mRNA expression levels in the MRC-5 cells.

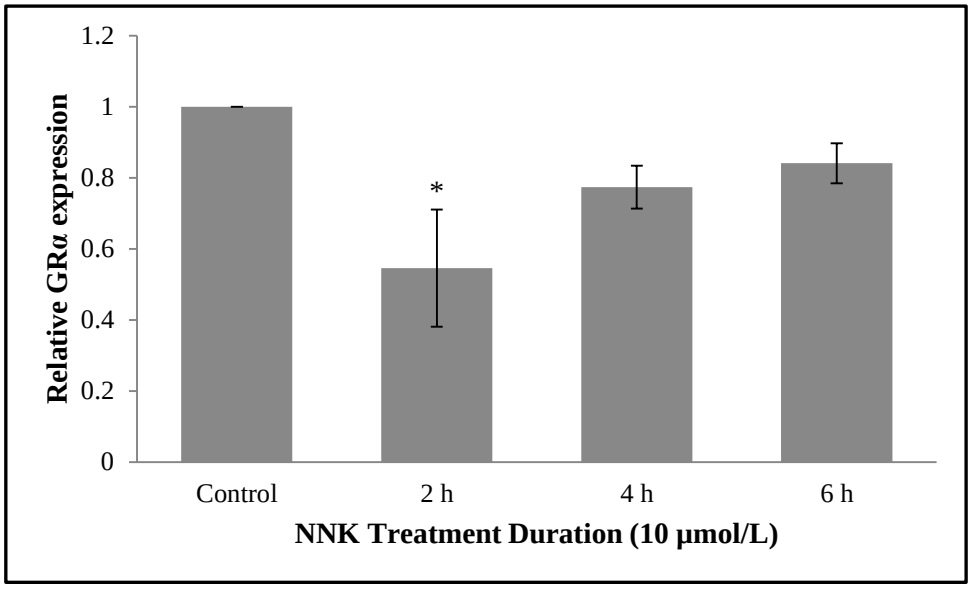

Figure 3.8. The relative fold change of *GRα* expression in MRC-5 cells when treated with 10 µmol/L of NNK for 2, 4 and 6 h. *GRα* expression was normalised against *β-actin* expression. The mean ± SEM is displayed (n = 3; * indicates $p < 0.05$ compared to the vehicle (control)).

3.3.2 Long term treatment with NNK in MRC-5 cells leads to decreased *GRα* expression

There was a significant down-regulation of *GRα* expression when the MRC-5 cells were treated with 10 µmol/L of NNK for 24 h ($t = 33.3$; $df = 13$; $p < 0.001$; Fig. 3.9). There was also a significant decrease in *GRα* mRNA expression when the MRC-5 cells were treated with 10 µmol/L of NNK for 48 h ($t = 14.591$; $df = 7$; $p < 0.001$; Fig. 3.9). This means that long term NNK exposure down-regulates *GRα* mRNA expression levels in the MRC-5 cell line ($r^2 = 0.9909$; Fig. 3.9).

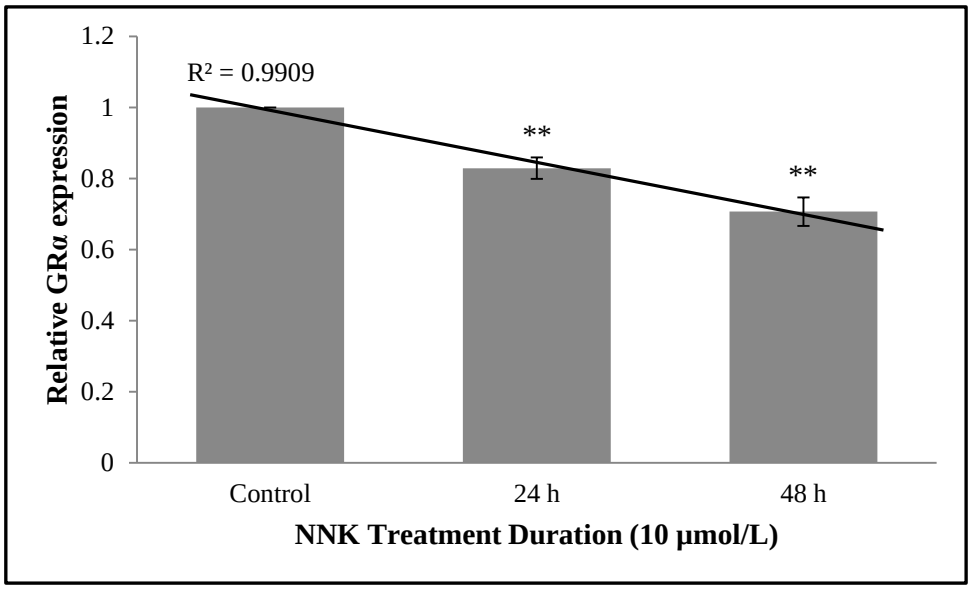

Figure 3.9. The relative fold change of *GRα* expression in MRC-5 cells when treated with 10 µmol/L of NNK for 24 and 48 h, showing prolonged exposure further decreases *GRα* mRNA. *GRα* expression was normalised against *β-actin* expression. The mean ± SEM is displayed (n = 3;** indicates $p < 0.001$ compared to the vehicle (control)).

3.4 The effect of NNK treatment on GRα protein expression

Western blot analyses were performed to establish whether NNK exposure affects GRα at the protein level. The MRC-5 cells were treated with 10 µmol/L of NNK for 0 (vehicle (control)), 24 h, 48 h or 72 h. The protein was extracted and run on a 13.5% SDS PAGE gel, which then was transferred onto a nitrocellulose membrane. The membrane was probed with a primary human monoclonal GRα and GAPDH antibody. Specific binding was detected with the appropriate secondary HRP antibody.

3.4.1 NNK treatment decreases the presence of GRα protein in MRC-5 cells

3.4.1.1 The effect of NNK treatment on GRα isoforms in MRC-5 cells

The Western blot image in Fig. 3.10 shows the GRα protein present in MRC-5 cells. Two distinct GRα bands were seen in the MRC-5 cells, representing the GRα isoforms, at GRα-A (~94 kDa) and GRα-B (~91 kDa).

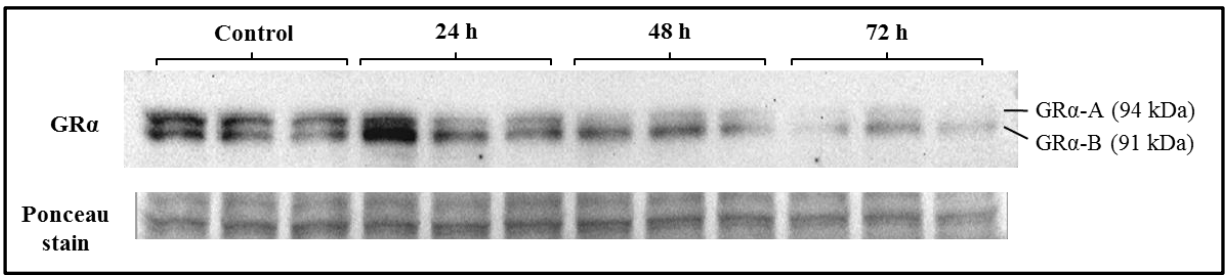

Figure 3.10. Western blot image probed for GRα shown with Ponceau stained blot (as a loading control) of MRC-5 cells treated with NNK (10 μmol/L) for 24, 48 and 72 h or vehicle (control). The different GRα isoforms are indicated.

3.4.1.2 The effect of NNK on GRα protein expression in MRC-5 cells

Densitometry was performed on the Western blot images to quantitate band intensity. Band intensity indicates the amount of GRα protein present. Total GRα protein levels were normalised against the relative GAPDH (reference protein) levels and total proteins as obtained by Ponceau staining of the nitrocellulose. GAPDH normalisation against the GRα was compared to the total protein normalisation. It was found that normalising against total proteins produced a more consistent and reliable result per experiment, producing the same trend for each experiment. This suggested that GAPDH was not a suitable reference protein for this experiment. This finding was consistent with Aldridge *et al.* (2008) who found that total protein stains are often more suitable as loading controls than single proteins. The relative GRα/Ponceau stain was represented as fold change relative to the control (expressed as 1). There a was significant difference in total GRα protein expression in the MRC-5 cell line between the vehicle (control) and all NNK treated cells ($F = 30.77$; $df = 3$; $p < 0.001$; Fig. 3.11). A multiple comparisons test (Tukey HSD) indicated that there was a significant difference between the control and all of the NNK treatments. There was also a significant difference between the 24 h and 48 h treatment ($p = 0.004$; Fig. 3.11 - a) and between the 24 h and 72 h treatments ($p = 0.001$; Fig. 3.11 - b), suggesting that long term exposures are more effective in down-regulating GRα expression. These data show that NNK treatment results in a down-regulation of GRα protein expression in the MRC-5 cells and that it appears to be exposure dependent.

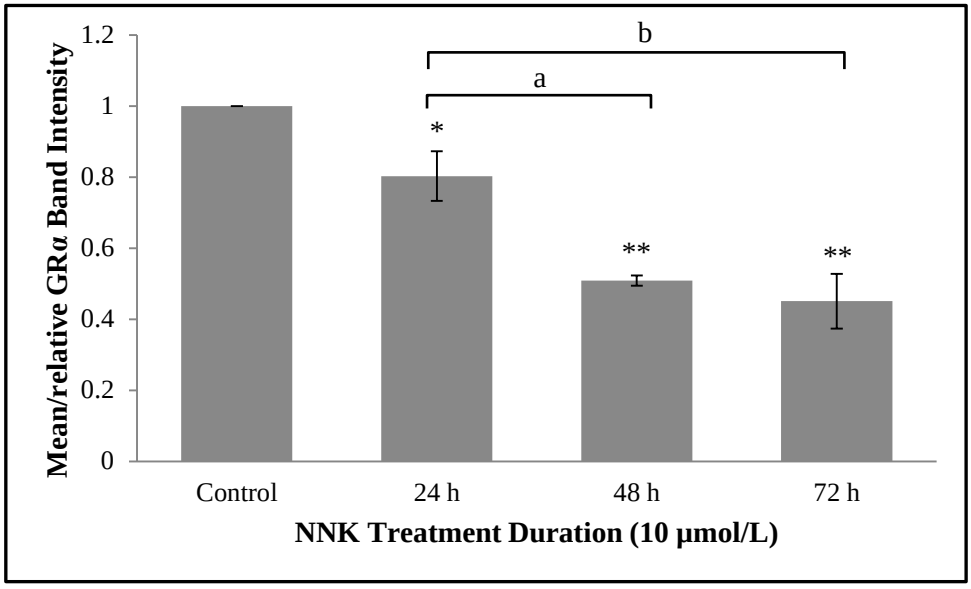

Figure 3.11. Densitometric analysis of the total GRα protein expression relative to total protein loaded (Ponceau staining) in MRC-5 cells. The mean ± SEM is displayed (n = 3;* = $p < 0.05$; ** = $p < 0.001$ compared to the vehicle (control); a = $p < 0.05$; b = $p < 0.05$).

3.5 DNA methylation of the GR promoter

The CpG islands present within the GR gene promoter region were confirmed by entering the GR nucleotide sequence into the EBI EMBOSS CpG plot finder software. The CpG plot finder output indicated that there were putative CpG islands between 2646 – 2930 base pairs (bp) and 3541 bp - 4795 bp (Fig. 3.12). The promoter 1B, 1C and1F regions are found within the 3541 - 4795 bp region and the promoter 1J region is found between 2930 - 3541 bp (Fig. 3.12). It was concluded that promoter 1B, 1C and1F may contain a high proportion of CpG islands whereas promoter 1J may contain less CpG islands.

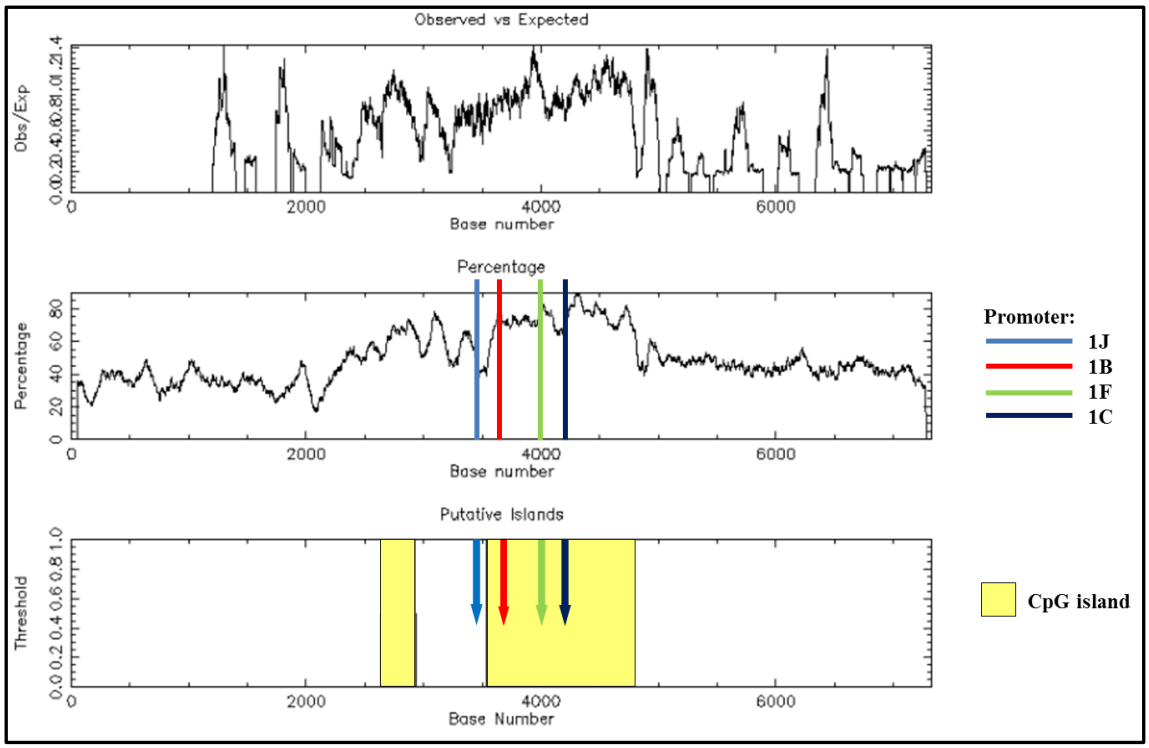

Figure 3.12. Predicted CpG islands within the *GR* gene promoter region. CpG islands are shown with the positions of promoter 1J, 1B, 1F and 1C that lie within the *GR* promoter.

3.6 Preliminary ChIP analysis results

As shown by Lin *et al*. (2010b), NNK appears to induce the nuclear accumulation of DNMT1 which subsequently results in the hypermethylation and silencing of TSGs. As we showed that NNK treatment results in reduced GRα expression and that the GR promoters are housed in predicted CpG islands, our aim was to determine whether NNK treatment could result in the nuclear accumulation of DNMT1 at the promoter region of the GR gene in normal lung fibroblast MRC-5 cells. The MRC-5 cells were treated with 10 μmol/L of NNK for 24 and 48 h. ChIP analysis was performed and PCR or qPCR was run with primers specific for the GR promoter region and for the reference gene GAPDH.

Conventional PCR (Fig. 3.13) indicated that ChIP analysis was successful (positive controls present). The Input control and Input 24 h (NNK treatment) DNA were used to assess whether the primer sets would work and showed that promoters 1B, 1F and 1J were present without DNMT1 antibody selection (Fig. 3.13). After selection with the DNMT1 antibody and conventional PCR using primers for promoters 1B, 1F and 1J; 1B and 1F amplified in the

vehicle treated cells while only 1F was present after 24 h NNK treatment. These data show that, under normal conditions, DNMT1 is associated with promoters 1B and 1F, suggesting that these promoters are methylated under normal conditions. After NNK treatment, only promoter 1F is amplified. It is surprising that 1B did not amplify as 1B is present in the control cells. Thus, 1B should be present in the NNK treated cells as well as it seems unlikely that NNK treatment would prevent DNMT1 accumulation at promoter 1B. These conventional PCR results are not quantitative and only indicate the presence of product, limited by the resolving power of the gel and imaging system.

Therefore qPCR was performed after ChIP on the vehicle control and NNK treated DNA after DNMT1 selection to determine whether there were quantitative differences in the amount of the promoters present. We used primers for 1B, 1F and 1J.

To ensure that each promoter was indeed present, each sample was analysed using the no-template control (NTC), melt curve and agarose gel electrophoresis data of each sample. Although the presence of promoter 1B was shown by conventional PCR, this promoter region failed to amplify using qPCR. It is possible that there were contaminants present which inhibited the qPCR reaction. Although promoter 1J did not amplify under conventional PCR conditions, it did amplify in qPCR analysis. Promoters 1F and 1J amplified successfully using qPCR and were normalised against the corresponding Input DNA control's *GAPDH* presence. There was no significant difference in *GR* promoter 1F presence compared to the vehicle (control) after 24 and 48 h treatments with NNK ($F = 3.619$; $df = 2$; $p = 0.159$; Fig. 3.14). There was no significant difference in *GR* promoter 1J presence compared to the vehicle (control) after 24 and 48 h treatments with NNK ($F = 0.917$; $df = 2$; $p = 0.489$; Fig. 3.14). However, the general trend suggests that NNK treatment results in the presence of more promoter 1F and 1J after 24 h and more 1F after 48 h, suggesting that NNK treatment results in more accumulation of DNMT1 at these promoters.

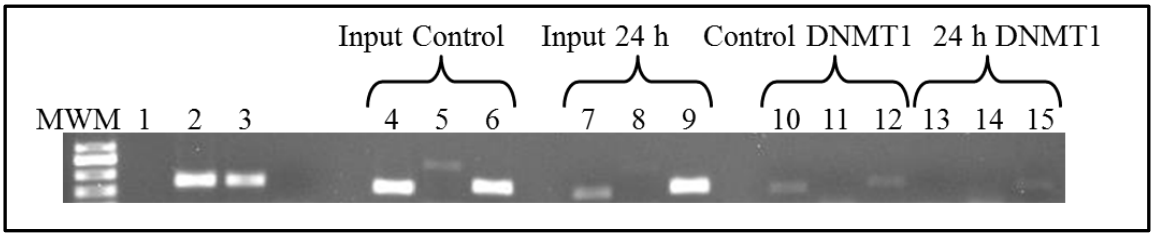

Figure 3.13. Agarose gel showing the PCR products of ChIP analysis with primer sets 1B, 1F, 1J and GAPDH. 1 - Negative control; 2 – Positive control (GAPDH); 3 – GAPDH Input control; Input Control primer test: 4 – 1B, 5 – 1J, 6 – 1F; Input 24 h primer test: 7 – 1B, 8 – 1J, 9 – 1F; Control DNMT1: 10 – 1B, 11 – 1J, 12 – 1F; 24 h DNMT1: 13 – 1B, 14 – 1J, 15 – 1F.

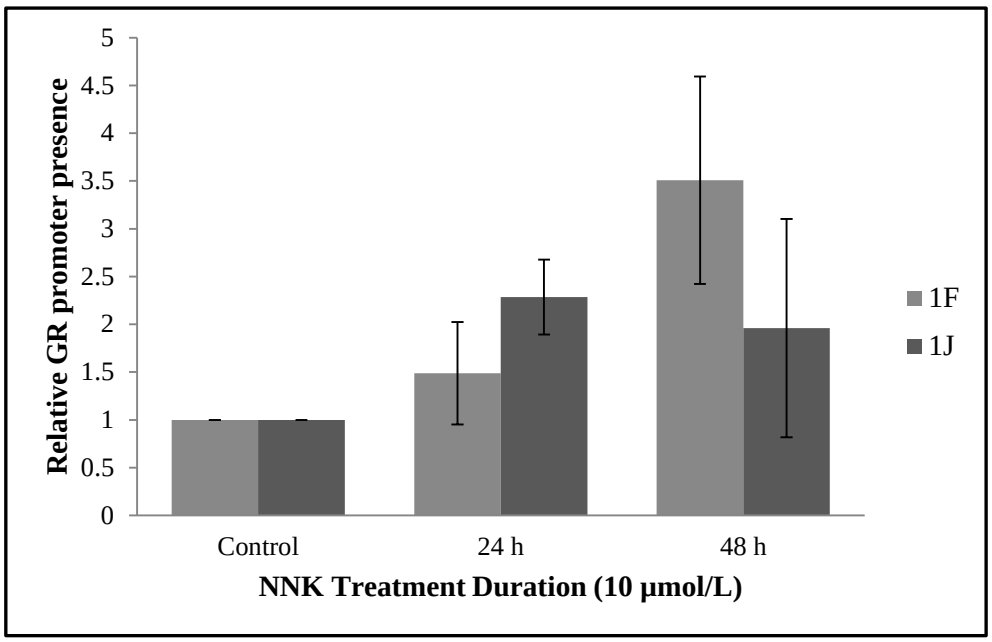

Figure 3.14. The relative fold change of GR promoters 1F and 1J associated with DNMT1 in MRC-5 cells treated with 10 µmol/L of NNK for 24 and 48 h and subjected to ChIP. Each GR promoter was normalised against GAPDH in the corresponding input DNA. The mean ± SEM is displayed (n = 3).

4. Discussion

Lung cancer is considered the most common cancer type and has the highest rate of cancer-related deaths worldwide (Panani and Roussos, 2006; Vaissière *et al*., 2009). Lung cancers are closely associated with cigarette smoking (Maser, 2004; Akopyan and Bonavida, 2006; Vaissière *et al*., 2009). SCLC, is an aggressive disease and encompasses up to 20% of all lung cancers (Panani and Roussos, 2006; Tessema and Belinsky, 2008; Kay *et al*., 2011). Patients with SCLC tumours initially respond well to chemotherapy, however, the prognosis is very poor as SCLC tumours develop chemoresistance (Jackman and Johnson, 2005; Panani and Roussos, 2006; Tessema and Belinsky, 2008; Kay *et al*., 2011). SCLC is a neuroendocrine tumour that ectopically secretes neuropeptides, such as ACTH. The ectopic secretion of ACTH by SCLCs is resistant to the normal negative feedback by Gcs, thus SCLC is thought to be Gc resistant (Ray *et al*., 1994; Ilias *et al.*, 2005; Sommer *et al*., 2007; 2010).

The SCLC cell line, DMS 79, is Gc-resistant and shows reduced GR expression (Ray *et al.*, 1996). Thus, the insensitivity of SCLC cells to Gcs is thought to be attributed to the reduced GR expression in SCLC. When the GR is overexpressed in human SCLC cells (via infection with adenovirus), the SCLC cells undergo apoptosis, suggesting that silencing of the *GR* gene may confer a tumour survival advantage and may be a key TSG in SCLC development (Sommer *et al*., 2007; 2010). In many tumours TSG expression may be silenced via epigenetic mechanisms (Baylin *et al.*, 2004; Baylin, 2005; Weber *et al*., 2005; Vaissière *et al.*, 2009; Lin *et al*., 2010c). Recent data in our laboratory suggests that the *GR* is epigenetically silenced by DNA methylation in SCLC cells and that treatment with a demethylating agent results in the re-expression of the GR (Kay *et al.*, 2011).

4.1 GRα protein expression in A549, HEK and DMS 79 cells treated with a demethylating agent

Epigenetic gene silencing of tumour suppressor and other cancer-related genes via hypermethylation plays a crucial role in tumourigenesis. The deoxyribonucleoside triphosphate, 5-Aza-2'-deoxycytidine (5-Aza), is a DNMT inhibitor that competes with cytosine residues and can be incorporated into DNA. DNMTs cannot methylate DNA that have the 5-Aza nucleoside incorporated (Baylin, 2005; Ghoshal *et al*., 2005; Lyko and Brown, 2005; Stresemann and Lyko, 2008). 5-Aza is one of the drugs used in epigenetic cancer therapies to restore gene

function by demethylating genes silence via methylation (Stresemann and Lyko, 2008). Kay *et al.* (2011) used 5-Aza to demethylate the GR promoter in the DMS 79 SCLC cell line which resulted in the reversal of DNA methylation and restored GR expression. Concentrations of 0.5 µmol/L, 1 µmol/L and 5 µmol/L of 5-Aza were for cell treatments for 72 h. These concentrations were in a study which also treated the SCLC DMS 79, the NSCLC A549, and the HEK cell lines (Kay *et al.*, 2011). The 5-Aza treatment concentrations were also based on a study by Stresemann and Lyko (2008) which found that cells treated with 2 µmol/L of 5-Aza for 48 h achieved the highest rate of demethylation with prolonged treatments.

The *GR* is a complex gene consisting of 9 exons. Only exons 2-9 are translated. Exon 9 can be alternatively spliced to generate three functional 3' splice variants, GR-α or –β and GR-P. The 5'UTR of the GR contains 9 alternative first exons, 1A, B, 1C, 1E, 1F, 1H, 1I and 1J (Duma *et al.*, 2006; Turner *et al*., 2010). These promoter regions do not contain TATA boxes; instead, they contain many GC rich regions (Duma *et al.*, 2006; Turner *et al*., 2010). Regardless of which promoter used, authentic full length GR is generated as the common translation start site is located in exon 2 (Turner *et al*., 2010). From the 3' splice variants, GR-α and –β, multiple GR isoforms are generated via the use of alternative translation initiation sites, RNA splicing or shunting and post-translational modifications (Duma *et al.*, 2006; Turner *et al*., 2010). GRα appears to be the major transcriptionally active and functional GR isoform. Eight different GRα isoforms are generated from the full length GRα mRNA transcript namely: GRα-A, B, C1 - C3, and D1 - D3 (Duma *et al.*, 2006; Turner *et al*., 2010; Wu *et al*., 2013).

4.1.1 GRα isoform expression in A549, HEK and DMS 79 cells

Western blots were performed to determine which GRα isoforms are expressed in the SCLC cell line, DMS 79, before and after exposure to a demethylating agent. DMS 79 (SCLC) and HEK cells have a low GR expression, whereas A549 (NSCLC) cells display abundant GRα expression (Kay *et al*., 2011). In these experiments, the HEK and A549 cell lines served as controls for GRα protein expression.

The A549 cell line expressed abundant GRα protein with two distinct bands at ~94 and ~91 kDa (Fig. 3.2). GRα-A and –B are approximately 94 and 91 kDa respectively (Zhou and Cidlowski, 2005; Duma *et al.*, 2006). The HEK cells displayed three protein bands, at ~94, ~91 and ~78 kDa, representing GRα-A, –B and –C respectively (Fig. 3.4). This confirms the findings of Zhou and Cidlowski (2005).

The DMS 79 cells displayed four distinct GRα protein bands between 95 kDa and 55 kDa (Fig. 3.6). The isoforms were found at ~94, ~91 and two bands at ~79/78 kDa. GRα-A and –B are approximately 94 and 91 kDa respectively (Zhou and Cidlowski, 2005; Duma *et al.,* 2006), whereas GRα-C is below ~82 kDa (Duma *et al.,* 2006). The GRα antibody used in this study is specific for the N-terminal domain (NTD) which is not present in the GRα-D isoform and therefore GRα-D could not be detected. Therefore, GRα isoforms –A, -B and two GRα-C isoforms were expressed in the DMS 79 cell line (Fig. 3.6). Treatment with 5-Aza did not appear to affect the individual GRα isoform expression in any of the cell lines, when analysed separately and compared.

These experiments were performed to determine which GRα isoforms are expressed in DMS 79 cells as a study done by Lu *et al*. (2007), aimed at describing the GRα gene, revealed that the eight different translational GRα isoforms appeared to have distinct gene-regulatory abilities. Lu *et al.* (2007) showed that in osteosarcoma U-2 OS cells, when specific GRα isoforms were re-expressed, they induced apoptosis. Lu *et al.* (2007) and Wu *et al*. (2013) found that the GRα-C isoforms were the most effective at inducing apoptosis in U-2 OS cells and Jurkat cells (T-lymphocytes); however the apoptotic pathways were different for each cell type indicating cell-specific gene regulation of apoptotic pathways. GRα –A and –B were less effective at inducing apoptosis, whereas GRα-D was the least effective at inducing apoptosis in U-2 OS and not effective in T-cells (Lu *et al*,. 2007; Wu *et al*., 2013). We show that the DMS79 cells express GRα-A, -B and –C (Fig 3.6).

When the full length GRα was re-expressed and Gcs administered, the pro-survival genes, Bcl-2 and Bcl-xL, were repressed and pro-apoptotic genes were induced in U-2 OS cells and T cells (Lu *et al.,* 2007; Wu *et al*., 2013). This was also found to be the case in SCLC cells when GR was over-expressed, ultimately leading to apoptosis in these cancer cells (Sommer *et al.,* 2010). Since Lu *et al.* (2007) and Wu *et al*. (2013) found that GRα-C was more effective at inducing apoptosis, it would be interesting to examine whether this isoform is specifically responsible for inducing apoptosis in DMS 79 cells since they express GRα-C.

4.1.2 The effect on GRα protein expression in A549, HEK and DMS 79 cells exposed to a demethylating agent

Densitometric analyses were performed on the Western blots to determine whether GRα protein expression in A549, HEK and DMS 79 cells was affected after 5-Aza treatment. GRα protein

expression was normalised against the reference protein, GAPDH. The NSCLC, A549, cells indicated that the untreated (vehicle control) cells expressed significantly more total GRα protein than the cells treated with 0.5, 1 and 5 µmol/L of 5-Aza for 72 h (Fig. 3.3). This indicated that 5-Aza treatment down-regulated total GRα expression in A549 cells. A549 cells normally exhibit abundant GR expression and the GR gene is not methylated in these cells. Treatment with 5-Aza has been shown to be toxic and can inhibit cell proliferation in cancer cells (Stresemann and Lyko, 2008). Yuan *et al*. (2004) showed that treatment with 5-Aza in NSCLCs *in vitro* caused growth inhibition. This was believed to have been due to 5-Aza inducing DNA demethyaltion which caused changes in the expression of multiple genes, leading to cell death. This may have occurred in the A549 cells, leading to a decrease in GR protein expression. In the other control cell line, HEK 293, densitometric analysis revealed that there was no significant change in GRα protein expression when treated with 0.5, 1 and 5 µmol/L of 5-Aza for 72 h compared to the vehicle (control) (Fig. 3.5). This was expected as the *GR* promoter is known to be unmethylated in HEK cells and the GR gene and protein are known to be non-functional. This is in accordance with what Kay *et al*., (2011) found. At these concentrations, 5-Aza did not appear to affect the HEK cells and suggests that different cell types respond differently to demethylation activity.

The SCLC DMS 79 cell line has been shown to be GR deficient due to the epigenetic silencing of the *GR* gene as treatment with a demethylation agent results in the re-expression of the GR in SCLC cells (Kay *et al.*, 2011). Re-expression of the GR induces apoptosis in SCLC cells (Sommer *et al.*, 2007; 2010); this indicates that the loss of the GR provides a survival advantage in the cancer cells. Densitometric analyses performed on the DMS 79 Western blots indicated that there was no significant difference in the total GRα protein expression when treated with 0.5, 1 and 5 µmol/L of 5-Aza for 72 h compared to the vehicle (control) (Fig. 3.7). However, there did appear to be an increase, although not significant, in total GRα protein when treated with higher doses of 5-Aza (1 µmol/L and 5 µmol/L) (Fig. 3.7). This was also found to be the case when GRα-C expression was analysed separately by densitometric analysis. Thus, 5-Aza treatment had no effect on the re-expression of GRα protein in the DMS 79 cell line.

These results were unexpected and inconsistent with the results from Kay *et al*. (2011), who revealed that 5-Aza treatment restored GRα expression in the DMS 79 cells. As 5-Aza inhibits DNA methylation and the *GR* promoter in the DMS 79 cells is likely methylated (Kay *et al.*, 2011), 5-Aza was expected to demethylate the *GR* promoter and subsequently up-regulate the overall GRα protein expression. The lack of a significant difference in the data from this study

may be been due to (1) degraded 5-Aza stocks, due to an undiscovered (at the time) bio freezer power failure and (2) the use of an inappropriate reference protein. Although GAPDH is commonly used as a reference protein, it is possible that GAPDH was not an appropriate reference protein for these experiments. In subsequent Western blots we compared total protein loaded (Ponceau staining) and GAPDH, which revealed GAPDH to be an unsuitable loading control, giving inconsistent results when compared to the Ponceau staining. A study conducted by Aldridge *et al.* (2008) found that at the protein concentrations normally used to quantify proteins of interest, single-protein loading controls, such as GAPDH and β-actin, did not accurately reflect differences in protein concentration. They came to the conclusion that total protein staining, in conjunction with the use of the BCA assay to quantify protein concentration before loading, was more reliable in determining protein loading quantities (Aldridge *et al.*, 2008).

4.2 The effect of a cigarette carcinogen on GRα expression in normal lung fibroblast cells

The close association between lung carcinoma development and cigarette smoking is due to the vast number (> 60) of carcinogens found in cigarettes. A highly carcinogenic compound in cigarette smoke and tobacco products, NNK, has been connected to carcinogenesis (Hecht, 2003; Baylin, 2005). One of the enzymes responsible for DNA methylation, DNMT1, has been shown to be over-expressed in cancer patients who smoke, and is correlated with a poor prognosis. NNK has been shown to cause the nuclear accumulation of DNMT1 and subsequent hypermethylation of several TSGs in lung cancers (Lin *et al.*, 2010b).

The *GR* promoter region contains many CpG islands and, in SCLC, shows evidence of being silenced by DNA methylation (Kay *et al.*, 2011). Since NNK has been shown to induce the DNA methylation of many TSGs in cancers, we attempted to determine whether NNK is capable of inducing *GR* gene inactivation by DNA methylation. This could be a link between NNK and the silencing of the *GR* gene through promoter hypermethylation in SCLC.

4.2.1 The short and long term effects of a cigarette carcinogen on *GRα* mRNA expression in normal lung fibroblast cells

In mouse and rat studies, NNK exposure not only lead to tumour formation, but also induced the hypermethylation of multiple TSG promoters, shown later to be reversible after exposure to a demethylation agent (Pulling *et al*., 2004; Belinsky, 2005). Pulling *et al*. (2004) performed a study on mice to determine whether the inactivation of the *DAP-kinase* gene in adenocarcinomas was induced by exposure to cigarette smoke and NNK. The study found that methylation of the *DAP-kinase* gene was induced by NNK, suggesting that the inactivation of this gene is one pathway for lung tumour development in mice (Pulling *et al*., 2004). Similarly, in 94% of lung adenocarcinomas, induced by NNK, promoter hypermethyaltion of *p16* was seen (Belinsky, 2005). The mechanism surrounding NNK-induced DNMT1 accumulation and promoter hypermethylation will elucidate the process of carcinogenesis. Lin *et al.* (2010b) showed that NNK induced DNMT1 protein stability by AKT/GSK-3β/βTrCP signalling and AKT/hnRNP-U/βTrCP nucleocytoplasmic shuttling (Fig. 4.1). NNK-induced hypermethylation of the promoter of TSGs may lead to tumourigenesis and poor prognosis and provide an important link between tobacco smoking and lung cancer (Lin *et al.*, 2010b).

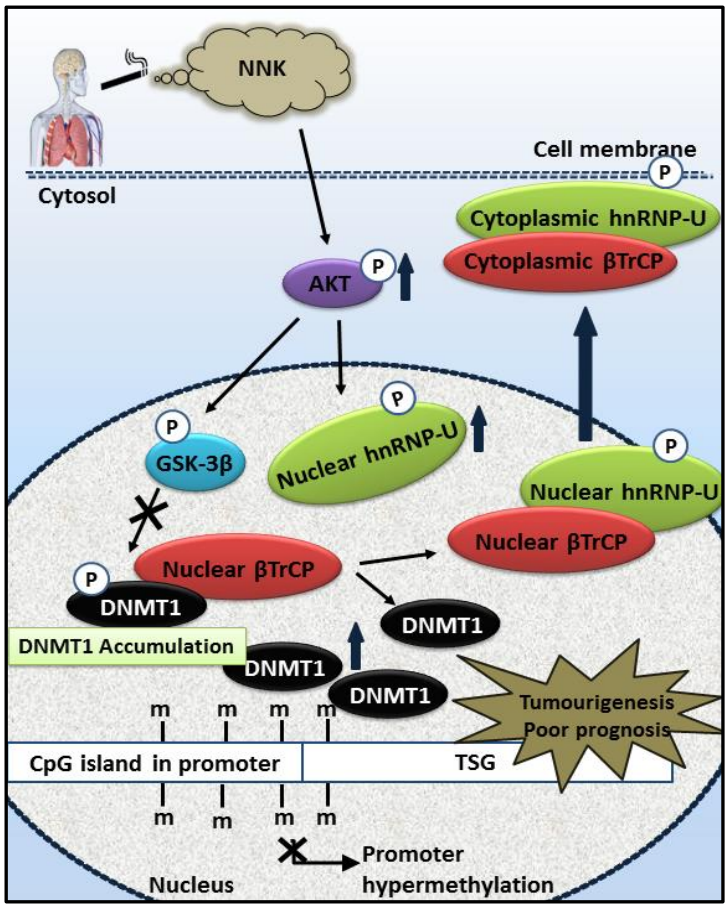

Figure 4.1. Proposed model illustrating the nuclear accumulation of DNMT1 via NNK-induced signalling, leading to TSG promoter hypermethylation, which ultimately leads to tumourigenesis. NNK induces DNMT1 protein accumulation in the nucleus through AKT/GSK3β/βTrCP/hnRNP-U signalling. βTrCP is an E3 ubiquitin ligase that interacts with and degrades DNMT1. NNK induces AKT activation, and promotes GSK3β phosphorylation-inactivating GSK3β, which subsequently reduces the ability of βTrCP to degrade DNMT1 protein. In addition, NNK activates AKT to induce interaction between phosphorylated hnRNP-U and βTrCP, which disrupts βTrCP/ DNMT1 interaction. The hnRNP-U/βTrCP complex translocates to the cytoplasm, leading to DNMT1 accumulation in the nucleus. Adapted from Lin *et al*. (2010b).

Our study aimed to determine whether NNK affects *GRα* gene expression via NNK-induced inactivation of the *GR* due to DNMT1 accumulation at the *GR* promoter region. The normal human lung fibroblast MRC-5 cells were exposed to NNK for 2, 4, 6, 24 and 48 h. *GRα* expression was normalised against the reference gene, *β-actin*.

This study showed that NNK treatment appeared to down-regulate *GRα* expression in the MRC-5 cells. There was a significant decrease in *GRα* expression when the cells were treated for 2 h with 10 µmol/L of NNK compared to the vehicle (control) (Fig. 3.8). There was no significant

difference between the vehicle (control) and the 4 and 6 h treatments with 10 µmol/L of NNK; however the *GRα* mRNA levels are consistently reduced with NNK treatment compared to the vehicle (control) (Fig. 3.8). This indicates that although the cells were only exposed to NNK for short periods, *GRα* expression was affected. Quite interestingly, *GRα* expression was decreased, suggesting that NNK treatment inhibits *GRα* expression as it does other TSGs (Pulling *et al*., 2004; Belinsky, 2005; Lin *et al.*, 2010b).

After the preliminary results indicated that short term NNK exposure resulted in decreased *GRα* expression levels, long term exposures with NNK were performed. This was done to ensure that the cells were affected by NNK exposure after long term exposure because although short term exposure reduced *GRα* expression, a trend was seen with the cells appearing to acclimatise to NNK treatment after 4 and 6 h. There was a significant decrease in *GRα* expression when the cells were treated for 24 and 48 h with 10 µmol/L of NNK compared to the vehicle (control) (Fig. 3.9). A trend was seen with a decrease in *GRα* expression after 24 h and then a further decrease after 48 h (Fig. 3.9). This verified that NNK exposure did decrease *GRα* mRNA expression, especially after an extended treatment period.

Lin *et al*. (2010b) confirmed that patients who ceased smoking displayed a lower nuclear accumulation of DNMT1, compared to patients who smoked continuously, suggesting that NNK-induced DNMT1 accumulation was reversible. This was confirmed *in vitro* where DNMT1 protein expression returned to basal levels after as little as 6 h of discontinuing NNK use (Lin *et al*., 2010b).

Therefore, our data showed that *GRα* mRNA expression was reduced following treatment with NNK. This does not necessarily mean that GRα protein expression is reduced after NNK treatment. Western blots were carried out to determine whether treatment with NNK results in the down-regulation of GRα protein.

4.2.2 The effect on GRα protein expression in normal lung fibroblast cells exposed to a cigarette carcinogen

The half-life of GRα protein, which depends on the presence of the Gc hormone, can be ~8-9 h in the presence of hormone or anything between ~18-32 h without hormone (Bodwell *et al.*, 1998; Lu and Cidlowski, 2004). Due to this long half-life, it was important to treat the MRC-5 cells for periods longer than this, in order for GRα protein expression changes to be seen.

The normal human lung fibroblast MRC-5 cells were exposed to a cigarette carcinogen to determine whether GRα protein expression is affected. In the MRC-5 cells, two distinct protein bands were seen at ~94 kDa and ~91 kDa, representing the GRα isoforms –A and –B respectively (Fig. 3.10). Importantly, the Western blot appeared to indicate that there was less GRα protein with prolonged NNK treatment.

Densitometric analyses were performed on the MRC-5 Western blots. GRα protein expression was normalised against the total proteins present (Ponceau staining of nitrocellulose). Initially, GAPDH was also probed for and compared to the Ponceau stain of total protein present (as a loading control); however when these loading controls were compared to each other, it was found that GAPDH was not a suitable reference protein for these experiments, producing different results on occasion.

Densitometric analysis showed that there was a significant decrease in total GRα protein expression after treatment with 10 µmol/L of NNK for 24, 48 and 72 h when compared to the vehicle (control) (Fig. 3.11). There was more of a decrease in GRα protein when treatment with NNK was prolonged, especially in the 48 and 72 h treatment exposures. This suggests that long term exposures with NNK are more effective in down-regulating GRα protein expression. This may be due to the GRα half-life, since it would take longer to see a decrease in total GRα protein levels even if the gene was down-regulated at the mRNA level.

In this study, NNK treatment down-regulates GRα expression at both mRNA and protein level, particularly after prolonged exposure. Other studies have found that TSGs are inactivated by DNA methylation, induced by NNK treatment (Pulling *et al*., 2004; Belinsky, 2005; Lin *et al.*, 2010b). To determine whether, as with other TSGs (Lin *et al*., 2011), NNK inhibition of GRα expression is due to DNMT1 accumulation at the *GR* promoter, ChIP analysis was performed to establish whether DNMT1 accumulated at the *GR* promoter.

4.3 NNK treatment may result in the accumulation of DNMT1 at the *GR* promoter in normal lung fibroblast cells

Lin *et al*. (2010b) investigated NNK-induced DNMT1 accumulation and binding to TSG promoters, which consequently resulted in the 5'CpG hypermethylation of bound TSGs. In these experiments, the normal lung cell line IMR90 was treated with NNK and it was found that

NNK increased the binding of DNMT1 to the TSG promoters: *FHIT, p16*^{INK4a} and *RARB*. This was confirmed by ChIP-PCR.

The 5'UTR promoter region of the *GR* gene (exon 1) contains many CpG islands that have the potential to be methylated (Duma *et al.,* 2006; Turner *et al*., 2010). CpG plotting indicated that there are at least two areas predicted to contain CpG islands, with a large portion (spanning ~1200 bp) predicted to have CpG islands. The *GR* promoters 1B, 1C and 1F were predicted to contain a high probability of CpG islands while 1J was predicted to have fewer CpGs due to being housed in between the two CpG island predicted sites (Fig. 3.12). Kay *et al*. (2011) examined promoters 1D, 1E and 1C and found evidence of methylation in SCLC cells.

Our aim was to determine whether NNK treatment results in the nuclear accumulation of DNMT1 at the *GR* promoter in MRC-5 cells. The MRC-5 cells were exposed to NNK for 24 and 48 h and ChIP analysis was performed. ChIP-PCR and qPCR were performed with primers specific for the *GR* promoter 1B, 1F and 1J. Primer sets were designed for the *GR* promoter 1C; however, we were unable to optimise them for this experiment. Under conventional PCR conditions, *GR* promoters 1B, 1F and 1J were present in the input controls. After selection with the DNMT1 antibody, 1B and 1F amplified and were seen on the gel. This suggests that under normal conditions, these two promoters show evidence of DNMT1 accumulation, suggesting possible methylation. Treatment with NNK for 24 h and selection with the DNMT1 antibody revealed the presence of only promoter1F. This suggests that 1F is therefore associated with DNMT1 accumulation after 24 h treatment. However, 1F is present in the vehicle control and 1B is absent. The absence of 1B may be due to technical problems as it seems unlikely that NNK treatment would prevent DNMT1 accumulation at the 1B promoter. Conventional PCR is dependent on the resolving power of the gel and imaging system. Therefore, to determine whether there was a quantitative difference in the amount of promoter 1B, 1J and 1F DNA in the control and NNK treated cells, we performed qPCR analysis.

Promoter 1B failed to amplify under qPCR reaction conditions; however 1F and 1J amplified successfully. The data reveal a possible trend with an increase in promoters IF and 1J, compared to the vehicle (control), however the difference was not significant (Fig. 3.14). This preliminary data suggests that there appears to be more 1F and 1J promoter presence after NNK treatment. It is important to note that both promoters 1F and 1J were present with some DNMT1 at these promoters; however the amount of DNMT1 present at these promoters seemed to increase after NNK treatment. Unfortunately, due to technical problems, this experiment only consisted of two

data points/readings per treatment and will need to be verified as a significant difference might be reached with the repetition. The *GR* promoter 1F is known to be highly expressed in the human hippocampus and is expressed in immune cells (Turner and Muller, 2005) and it has been shown to be methylated in response to stress in rats and humans while little is known about promoter 1J. Recent data in our laboratory has indicated that when the *GR* is re-expressed by treatment with 5-Aza in SCLC cells, inducing apoptosis, the use of promoters 1F and 1J may be responsible for inducing apoptosis in these cells. Here, we show that treatment of non-cancerous lung fibroblasts with a cigarette carcinogen, results in a possible increase in DNMT1 accumulation at these promoters. These preliminary data may provide insight into the mechanism of cigarette carcinogen induced SCLC carcinogenesis.

5. Conclusion and future research

Glucocorticoids are important in treating inflammation and certain cancers, although their side effects limit their use. The GR has a wide range of gene targets; however, only one *GR* gene has been discovered. This is mostly likely because the *GR* gene generates several GR translational isoforms (Wu *et al*., 2013). Wu *et al*. (2013) proposed that GR isoforms play a key role in tissue-specific glucocorticoid responses. This was due to the revelation that GR isoforms have tissue-specific expression patterns which have unique gene targets (Wu *et al*., 2013). Tissue-specific expression and functions of GR isoforms may provide a basis for developing improved glucocorticoids for targeted therapies.

SCLC has a poor prognosis therefore, it is important to understand the pathways involved in carcinogenesis and apoptosis. Apoptosis is a key mechanism by which cancer drugs kill tumour cells, and is a promising pathway target for lung cancer therapy. DNA methylation is a significant contributor to carcinogenesis. In SCLC cells when the *GR* (thought to be methylated) is re-expressed, it induces apoptosis in these cells (Sommer *et al*., 2007; 2010). We found that 5-Aza treatment had no significant effect on GRα protein re-expression in SCLC cells; although a general trend of increased GR expression after 5-Aza exposure was seen. The lack of significance may be due to degraded 5-Aza or inappropriate reference protein use.

It is interesting that the concentration of NNK in cigarettes is not monitored or limited by health organisations, considering its carcinogenic classifications. Smoking not only causes cancer, but is also correlated with a poor prognosis in cancers. Gray *et al*. (2000) showed a 3- to 9- fold variation in NNK dosage within and between cigarette brands, without warnings of said dosage. This clearly indicates that cigarettes can be produced to contain lower NNK levels (Gray *et al*., 2000).

Lin *et al*. (2010b) found that NNK-mediated DNMT1 accumulation is reversible. This is promising for patients who quit smoking, improving their survival. Drugs aimed at reducing DNMT protein levels, such as AKT or demethylating agents may be good therapeutic strategies in certain cancer treatments (Lin *et al.*, 2010b). We found that, with NNK treatment, the *GRα* gene was down-regulated at the transcriptional level and that prolonged exposure caused a further decrease in GRα mRNA and protein presence. Preliminary data suggests that NNK treatment leads to the accumulation of DNMT1 at the *GR* promoters 1F and 1J, inducing DNA methylation and silencing of the *GR* gene. This may be achieved as Lin *et al*. (2010b) explained,

via AKT/GSK3β/βTrCP/hnRNP-U signalling. This may provide an important link between smoking and lung cancer development.

According to Kay *et al*. (2011), the *GR* promoter 1C appears to be methylated in SCLC cells. We failed to design working primer sets for promoter 1C in this experiment, therefore, primer sets for *GR* promoter 1C and other promoter regions should be re-designed. ChIP analysis will need to be repeated for more data points, to determine whether there is a significant increase in DNMT1 binding to the *GR* promoter regions. Western blots can be performed to determine whether there is an increase in DNMT1 protein presence due to increased protein stability and accumulation in the nucleus after NNK treatment. Methylation specific bisulfite assays can be used to confirm the presence of methylation at 5'CpGs after NNK treatment.

GRα may be an important TSG in SCLC which could be fundamental in the development of SCLC. Illuminating the pathways involved in SCLC development and the identification of mechanisms that induce apoptosis could lead to more targeted therapies in treating this disease. As it is possible, we hope that government and health organisations will in the near future monitor and regulate the carcinogenic levels in cigarettes to reduce the occurrence of these deadly diseases.

6. References

Akopyan, G., Bonavida, B., 2006. Understanding tobacco smoke carcinogen NNK and lung tumorigenesis (Review). International Journal of Oncology 29, 745-752.

Aldridge, G. M., Podrebarac, D. M., Greenough, W. T., Weiler, I. J., 2008. The use of total protein stains as loading controls: an alternative to high-abundance single protein controls in semi-quantitative immunoblotting. Journal of Neuroscience Methods 172, 250–254.

Alt, S.R., Turner, J.D., Klok, M.D., Meijer, O.C., Lakke, E.A.J.F., DeRijk, R.H., Muller, C.P., 2010. Differential expression of glucocorticoid receptor transcripts in major depressive disorder is not epigenetically programmed. Pyschoneuroendocrinology 35, 544-556.

Baylin, S.B., 2005. DNA methylation and gene silencing in cancer. Nature Clinical Practice Oncology 2, S4-S11.

Baylin, S.B., Futscher, B.W., Gore, S.D., 2004. Understanding DNA methylation and epigenetic gene silencing in cancer. Current Therapeutics 1, 1-25.

Belinsky, S.A., 2005. Silencing of genes by promoter hypermethylation: key event in rodent and human lung cancer. Carcinogenesis 26, 1481-1487.

Bell, J., Spector, D.T., 2011. A twin approach to unravelling epigenetics. Trends in Genetics 27, 116-125.

Bodwell, J.E., Webster, J.C., Jewell, C.M., Cidlowski, J. A., Hu, J., Munck, A., 1998. Glucocorticoid receptor phosphorylation: Overview, function and cell cycle-dependence. The Journal of Steroid Biochemistry and Molecular Biology 65, 91–99.

Bustin, S.A., Benes, V., Garson, J.A., Hellemans, J., Huggett, J., Kubista, M., Mueller, R., Nolan, T., Pfaffl, M.W., Shipley, G.L., Vandesompele, J., Wittwer, C.T., 2009. The MIQE guidelines: Minimum Information for Publication of Quantitative Real-Time PCR Experiments. Clinical Chemistry 55, 611-622.

Carmella, S.G., Akerkar, S., Hecht, S.S., 1993. Metabolites of the Tobacco-specific Nitrosamine 4-(Methylnitrosamino)-1-(3-pyridyl)-1 butanone in Smokers' urine. Cancer Research 53, 721-724.

Carmella, S.G., Akerkar, S.A., Richie, J.P., Hecht, S.S., 1995. Intraindividual and Interindividual Differences in Metabolites of the Tobacco-specific Lung Carcinogen 4-(Methylnitrosamino)-1-(3-pyridyl)-1-butanone (NNK) in Smokers' Urine. Cancer Epidemiology, Biomarkers and Prevention 4, 635-642.

Chrousos, G.P., 2004. Is 11β-hydroxysteroid dehydrogenase type 1 a good therapeutic target for blockade of glucocorticoid actions? Proceedings of the National Academy of Sciences of the USA 101 (17), 6329-6330.

Deaton, A.M., Bird, A., 2011. CpG islands and the regulation of transcription. Genes and Development 25, 101-1022.

Duma, D., Jewel, C.M., Cidlowski, J.A., 2006. Multiple glucocorticoid receptor isoforms and mechanisms of post-translational modification. Journal of Steroid Biochemistry and Molecular Biology 102, 11-21.

Elmore, S. 2007. Apoptosis: A review of programmed cell death. Toxicologic Pathology 35, 495-516.

Ghobrial, I.M., Witzig, T.E., Adjei, A.A., 2005. Targeting Apoptosis Pathways in Cancer Therapy. CA Cancer Journal for Clinicians 55, 178–194.

Ghoshal, K., Datta, J., Majumder, S., Bai, S., Kutay, H., Motiwala, T., Jacob, S.T., 2005. 5-Aza-Deoxycytidine Induces Selective Degradation of DNA Methyltransferase 1 by a Proteasomal Pathway That Requires the KEN Box, Bromo-Adjacent Homology Domain, and Nuclear Localization Signal. Molecular and Cellular Biology 25, 4727–4741.

Gray, N., Zaridze, D., Robertson, C., Krivosheeva, L., Sigacheva, N., Boyle, P., 2000. Variation within global cigarette brands in tar, nicotine, and certain nitrosamines: analytic study. Tabacco Control 9, 351-354.

Hecht, S., 2003. Tobacco carcinogens, their biomarkers and tobacco-induced cancer. Nature Reviews Cancer 3, 733-744.

Ilias, I., Torpy, D.J., Pacak, K., Mullen, N., Wesley, R.A., Nieman, L.A., 2005. Cushing's syndrome due to ectopic corticotropin secretion: Twenty years' experience at the National Institutes of Health. The Journal of Clinical Endocrinology and Metabolism 90, 4955–4962.

International Agency for Research on Cancer (IARC), 2014. Agents classified by the *IARC monographs* 1-109, 1-33. http://monographs.iarc.fr/ENG/Classification/ClassificationsGroupOrder.pdf. (Accessed 20/1/14).

Jackman, D.M., Johnson, B.E., 2005. Small-cell lung cancer. Lancet. 366, 1385-1396.

Jeong, Y., Xie, Y., Xiao, G., Behrens, C., Girard, L., Wistuba, I.I., Minna, J.D., Mangelsdorf, D.J., 2010. Nuclear Receptor Expression Defines a Set of Prognostic Biomarkers for Lung Cancer. Public Library of Science Medicine 7, 1-13.

Kay, P., Schlossmacher, G., Matthews, L., Sommer, P., Singh, D., White, A., Ray, D., 2011. Loss of Glucocorticoid Receptor Expression by DNA Methylation Prevents Glucocorticoid Induced Apoptosis in Human Small Cell Lung Cancer Cells. Public Library of Science 6, 1-11.

Klose, R.J., Bird, A.P., 2006. Genomic DNA methylation: the mark and its mediators. Trends in Biochemical Sciences 31, 89-97.

Kudielka, B.M., Kirschbaum, C., 2005. Sex differences in HPA axis responses to stress: a review. Biological Psychology 69, 113–132.

Laird, P.W., Jaenisch, R., 1994. DNA Methylation and Cancer. Human Molecular Genetics 3, 1487-1495.

Lin, R., Hsieh, Y., Lin, P., Hsu, H., Chen, C., Tang, Y., Lee, C., Wang, Y., 2010b. The tobacco-specific carcinogen NNK induces DNA methyltransferase 1 accumulation and tumor suppressor gene hypermethylation in mice and lung cancer patients. Journal of Clinical Investigation 120, 521-532.

Lin, R., Wu, C., Chang, J., Juan, L., Hsu, H., Chen, C., Lu, Y., Tang, Y., Yang, Y., Yang, P., Wang, Y., 2010c. Dysregulation of p53/Sp1 Control Leads to DNA Methyltransferase-1 Over expression in Lung Cancer. American Association for Cancer Research 14, 5807-5817.

Lin, P., Yu, S., Yang P., 2010a. MicroRNA in Lung Cancer. British Journal of Cancer 103, 1144-1148.

Livak, K.J., Schmittgen, T.D., 2001. Analysis of relative gene expression data using real-time quantitative PCR and the $2^{-\Delta\Delta C_T}$ method. Methods 25, 402-408.

Lu, N.Z., Cidlowski, J.A., 2004. The Origin and Functions of Multiple Human Glucocorticoid Receptor Isoforms. Annals of the New York Academy of Sciences 1024, 102–123.

Lu, N.Z., Cidlowski, J.A., 2006. Glucocorticoid receptor isoforms generate transcription specificity. Trends in Cell Biology 16, 301-307.

Lu, N.Z., Collins, J.B., Grissom, S.F., Cidlowski, J.A., 2007. Selective Regulation of Bone Cell Apoptosis by Translational Isoforms of the Glucocorticoid Receptor. Molecular and Cellular Biology 27, 7143-7160.

Lyko, F., Brown, R., 2005. DNA methyltransferase inhibitors and the development of epigenetic cancer therapies. Journal of the National Cancer Institute 97, 1498-1506.

Maser, E., 2004. Significance of reductases in the detoxification of the tobacco-specific carcinogen NNK. Trends in Pharmacological Sciences 25, 235-237.

Micke, P., Faldum, A., Metz, T., Beeh, K., Bittinger, F., Hengstler, J., Buhl, R., 2002. Staging small cell lung cancer: Veterans Administration Lung Study Group versus International Association for the Study of Lung Cancer/what limits limited disease? Lung Cancer 37, 271-276.

Molitoris, J.K., McColl, K.S., Distelhorst, C.W., 2011. Glucocorticoid-Mediated Repression of the Oncogenic microRNA Cluster miR-17~92 Contributes to the Induction of Bim and Initiation of Apoptosis. Molecular Endocrinology 25, 409–420.

Momparler, R.L., Bovenzi, V., 2000. DNA Methylation and Cancer. Journal of Cellular Physiology 183, 145–154.

Oakley, R.H., Cidlowski, J.A., 2011. Cellular Processing of the Glucocorticoid Receptor Gene and Protein: New Mechanisms for Generating Tissue-specific Actions of Glucocorticoids. The Journal of Biological Chemistry 286, 3177–3184.

Panani, A.D., Roussos, C., 2006. Cytogenetic and molecular aspects of lung cancer. Cancer Letters 239, 1-9.

Pariante, C.M., Lightman, S.L., 2008. The HPA axis in major depression: classical theories and new developments. Trends in Neurosciences 31, 464-468.

Parks, L.L., Turney, M.K., Detera-Wadleigh, S., Kovacs, W.J., 1998. An ACTH-producing small cell lung cancer expresses aberrant glucocorticoid receptor transcripts from a normal gene. Molecular and Cellular Endocrinology 142, 175-181.

Poirier, M. C., 2004. Chemical-Induced DNA Damage and Human Cancer Risk. Nature reviews, Cancer 4, 630-637.

Pulling, L.C., Vuillemenot, B.R., Hutt, J.A., Devereux, T.R., Belinsky, S.A., 2004. Aberrant Promoter Hypermethylation of the *Death-Associated Protein Kinase* Gene Is Early and Frequent in Murine Lung Tumors Induced by Cigarette Smoke and Tobacco Carcinogens. Cancer Research 64, 3844–3848.

Qui, J., 2006. Epigenetics: Unfinished symphony. Nature 441, 143-145.

Ray, D.W., Davis, J.R.E., White, A., Clark, J.L., 1996. Glucocorticoid receptor structure and function in glucocorticoid-resistant small cell lung carcinoma cells. Cancer Research 56, 3276-3280.

Ray, D.W., Littlewood, A.C., Clark, A.J.L., White, A., 1994. Human small cell lung cancer cell lines expressing the proopiomelanocortin gene have aberrant glucocorticoid receptor function. Journal of Clinical Investigations 93, 1625-1630.

Robertson, K.D., 2005. DNA Methylation and Human Disease. Nature Reviews, Genetics 6, 597-610.

Rozen, S., Skaletsky, H.J., 2000. Primer3 on the WWW for general users and for biologist programmers. In: Krawetz, S., Misener, S., (eds) Bioinformatics Methods and Protocols: Methods in Molecular Biology. Humana Press, Totowa, NJ, 365-386.

Salgado, L.R., Fragoso, M.C.B.V, Knoepfelmacher, M., Machado, M.C., Domenice, S., Pereira, M.A.A., de Mendonça, B.B., 2006. Ectopic ACTH syndrome: our experience with 25 cases. European Journal of Endocrinology 155, 25-733.

Schlossmacher, G., Stevens, A., White, A., 2011. Glucocorticoid receptor-mediated apoptosis: mechanisms of resistance in cancer cells. Journal of Endocrinology 211, 17–25.

Schmidt, S., Rainer, J., Ploner, C., Presul, E., Riml, S., Kofler, R., 2004. Glucocorticoid-induced apoptosis and glucocorticoid resistance: molecular mechanisms and clinical relevance. Cell Death and Differentiation 11, S45–S55.

Sethi, T., Rintoul, R.C., Moore, S.M., Mackinnon, A.C., Salter, D., Choo, C., Chilvers, E.R., Dransfield, I., Donnelly, S.C., Strieter, R., Haslett, C., 1999. Extracellular matrix proteins protect small cell lung cancer cells against apoptosis: A mechanism for small cell lung cancer growth and drug resistance *in vivo*. Nature Medicine 5, 662-668.

Sommer, P., Cowen, R.L., Berry, A., Cookson, A., Telfer, B.A., Williams, K.J., Stratford, I.J., Kay, P., White, A., Ray, D.W., 2010. Glucocorticoid receptor over-expression promotes human small cell lung cancer apoptosis *in vivo* and thereby slows tumour growth. Endocrine-Related Cancer 17, 203-213.

Sommer, P., Le Rouzic, P., Gillingham, H., Berry, A., Kayhara, M., Huynh, T., White, A., Ray, D.W., 2007. Glucocorticoid receptor overexpression exerts an antisurvival effect on human small cell lung cancer cells. Oncogene 26, 7111-7121.

Sommer, P., Ray, D.W., 2008. Novel therapeutic agents targeting the glucocorticoid receptor for inflammation and cancer. Current Opinion in Investigational Drugs 9, 1070-1077.

Stahn, C., Löwenberg, M., Hommes, D.W., Buttgereit, F., 2007. Molecular mechanisms of glucocorticoid action and selective glucocorticoid receptor agonists. Molecular and Cellular Endocrinology 275, 71–78.

Stresemann, C. Lyko, F., 2008. Modes of action of the DNA methyltransferase inhibitors azacytidine and decitabine. International Journal of Cancer 123, 8-13.

Tessema, M., Belinsky, S.A., 2008. Mining the Epigenome for Methylated Genes in Lung Cancer. Proceedings of the American Thoracic Society 5, 806-810.

Turner, B.M., 2000. Histone acetylation and an epigenetic code. BioEssays. John Wiley & Sons, Inc. 22, 836-845.

Turner, J.D., Alt, S.R., Cao, L., Vernocchi, S., Trifonova, S., Battello, N., Muller, C.P., 2010. Transcriptional control of the glucocorticoid receptor: CpG islands, epigenetics and more. Biochemical Pharmacology 80, 1860–1868.

Turner, J.D., Muller, C.P., 2005. Structure of the glucocorticoid receptor (NR3C1) gene 5' untranslated region: identification, and tissue distribution of multiple new human exon 1. Journal of Molecular Endocrinology 35, 283–292.

Turner, J.D., Pelascini, L.P.L, Macedo, J.A., Muller, C.P., 2008. Highly individual methylation patterns of alternative glucocorticoid receptor promoters suggest individualized epigenetic regulatory mechanisms. Nucleic Acids Research 36, 7207–7218.

Weber, M., Davies, J.J., Wittig, D., Oakeley, E.J., Haase, M., Lam, W.L., Schübeler, D., 2005. Chromosome-wide and promoter-specific analyses identify sites of differential DNA methylation in normal and transformed human cells. Nature Genetics 37, 853-862.

Weber, M., Hellmann, I., Stadler, M.B., Ramos, L., Pääbo, S., Rebhan, M., Schübeler, D., 2007. Distribution, silencing potential and evolutionary impact of promoter DNA methylation in the human genome. Nature Genetics 39, 457-466.

Wu, I., Shin, S.C., Cao, Y., Bender, I.K., Jafari, N., Feng, G., Lin, S., Cidlowski, J.A., Schleimer, R.P., Lu, N.Z., 2013. Selective glucocorticoid receptor translational isoforms reveal

glucocorticoid-induced apoptotic transcriptomes. Nature Publishing Group: Cell Death and Disease 4, 1-12.

Vaissière, T., Hung, R.J., Zaridze, D., Moukeria, A., Cuenin, C., Fasolo, V., Ferro, G., Paliwal, A., Hainaut, P., Brennan, P., Tost, J., Boffetta, P., Herceg, Z., 2009. Quantitative analysis of DNA methylation profiles in lung cancer identifies aberrant DNA methylation of specific genes and its association with gender and cancer risk factors. Cancer Research 69, 243-252.

Yuan, B., Jefferson, A.M., Popescu, N.C., Reynolds, S.H., 2004. Aberrant gene expression in human non-small cell lung carcinoma cells exposed to demethylating agent 5-Aza-2'-Deoxycytidine. Neoplasia 6, 412-419.

Zang, Y., He, J., 2013. The development of targeted therapy in small cell lung cancer. Journal of Thoracic Disease 5, 538-548.

Zhou, J., Cidlowski, J.A., 2005. The human glucocorticoid receptor: One gene, multiple proteins and diverse responses. Steroids 70, 407–417.

7. Appendix

A. MIQE Guidelines

qPCR experimental design was carried out according to the MIQE guidelines. The MIQE guidelines outline the minimum information that is required for qPCR experiments. This ensures that there is consistency in the scientific community and that the integrity of scientific literature is maintained. All the relevant experimental conditions are provided to allow reviewers to ensure that the experiments were valid (Bustin *et al*., 2009).

A.1 Experimental design

The effect of NNK on *GRα* expression was evaluated on the MRC-5 cell line (Normal lung fibroblast cells). The cells were treated with 10 µmol/L of NNK for 0 (vehicle control), 2, 4, 6, 24 or 48 h. The effect of NNK treatment on the *GRα* expression was evaluated using qPCR analyses. RNA was extracted from a confluent 10 cm^3 dish for each experiment/treatment. RNA was isolated using the RNeasy® Mini spin column kit (QIAGEN). RNA was only isolated from fully confluent 10 cm^3 dishes. cDNA was synthesised using the Tetro cDNA Synthesis Kit (Bioline). Two biological repeats were performed and three qPCR technical repeats within each repeat were performed. Each qPCR run consisted of three repeats per treatment. All qPCR analyses were performed by myself at the laboratory of my supervisor, Dr P. Sommer, in the School of Life Sciences, Biological and Conservation Building, University of KwaZulu-Natal, Durban, South Africa.

A.2 Sample Information

MRC-5, HEK and A549 cell stocks were frozen down from confluent 10 cm^3 culture dishes and were stored in 1 mL of media containing 10% DMSO in 1.5 mL cryovials (Corning®). DMS 79 cell stocks were frozen down from confluent T75 flasks and were stored in 1 mL of medium containing 5% DMSO in 1.5 mL cryovials. All of the cryovials were stored in a liquid nitrogen freezer at -196°C except for the DMS 79 cells that were stored at -80°C. The MRC-5, HEK and A549 cell lines were cultured in DMEM medium (BioWhittaker™, Lonza) whilst the DMS 79 cells were cultured in RPMI 1640 medium (BioWhittaker™, Lonza), supplemented with 10% FBS (HyClone™, Thermo Scientific™), and 100 units/mL of penicillin/streptomycin

(BioWhittaker™, Lonza). All of the cells were incubated at 37°C with 5% CO_2 in a humidified incubator (Forma Scientific).

A.3 Nucleic acid extraction

RNA was extracted using the RNeasy® Mini spin column kit (QIAGEN), as explained in section 2.2 (Materials and Methods). RNA concentration was quantified using a Nanodrop spectrophotometer (ND-1000) version 3.5.2 (NanoDrop Technologies) at 260/280 absorbance ratio. RNA integrity was evaluated by agarose/formaldehyde gel electrophoresis (see materials and methods section 2.2.1). The RNA samples were aliquoted immediately after quantification and stored at -80°C. RNA samples were subjected to only one freeze-thaw cycle.

The integrity of each RNA sample was validated before use in qPCR analyses. RNA samples (2 µg) were resolved on 1.5%/2.2 mol/L agarose formaldehyde gels (Appendix B.6), with a 1 kb O'GeneRuler™ DNA ladder mix (0.5 µg/µL) (Fermentas) resolved in each gel. The gels were imaged using the ChemiDoc™ XRS$^+$ Imaging System with Image lab™ software version 2.0.1 (Bio-Rad). The presence of two intact bands of 18 S rRNA and 28 S rRNA subunits were used to verify good quality RNA (see section 3.1 of the Results for RNA integrity gel images).

A.3.1 RNA concentration

RNA was quantified by spectrophotometry using a Nanodrop spectrophotometer (ND-1000) version 3.5.2 (NanoDrop Technologies). RNA concentration is shown in Table 7.1.

Table 7.1. Concentration of RNA isolated from MRC-5 cells. The MRC-5 cells were treated with 10 µmol/L of NNK for differing times.

Treatment	**Biological Repeat 1 Concentration (ng/µL)**	**Biological Repeat 2 Concentration (ng/µL)**
Control (6 h vehicle)	1049.8	692.1
Control (24 h vehicle)	581.5	769
Control (48 h vehicle)	273	319
2 h (10 µmol/L NNK)	893.4	402.4

4 h (10 µmol/L NNK)	1131.6	969.9
6 h (10 µmol/L NNK)	894.2	1101.4
24 h (10 µmol/L NNK)	1006	738.1
48 h (10 µmol/L NNK)	340.9	458.2

A.4 cDNA synthesis

cDNA synthesis was performed using the Tetro cDNA Synthesis Kit (Bioline) as described in section 2.3 in the Materials and Methods. A 2 µg concentration of RNA was used for each reaction. The cDNA was diluted with 20 µL of nuclease-free water and aliquoted immediately to ensure that only one freeze thaw was made per qPCR run. cDNA was stored at -80°C until use. All reagents are part of the Tetro cDNA Synthesis Kit purchased from Bioline (BIO-65042).

Table 7.2. Tetro cDNA Synthesis Kit reagents and concentrations.

Reagent	**Concentration**
5 × RT buffer:	
Tris-HCL (pH 8.6)	50 mmol/L
KCl	40 mmol/L
$MnSO_4$	1 mmol/L
DTT	1 mmol/L
dNTP mix	10 mmol/L
Oligo $(dT)_{18}$ primer mix	200 µmol/L
RNase inhibitor	10 u/µL
Reverse transcriptase	200 u/µL

A.5 Primer set information and qPCR target gene

qPCR target gene and primer information is presented in Table 2.1 in the Materials and Methods section. Primer stock solutions (100 µmol/L) were stored at -20°C. A working solution of 10 µmol/L for each primer set used in qPCR reactions was stored at -20°C.

A.5.1 Primer set blast specificity evaluation

Each primer set was evaluated by "BLASTing" them against the *Homo sapiens* genome on the NCBI database (www.ncbi.nlm.nih.gov) using the Primer BLAST tool (http://www.ncbi.nlm.nih.gov/tools/primer-blast/) to ensure specificity. The primer set specificity was confirmed by agarose gel electrophoresis of the conventional PCR products (Fig. 7.1). The qPCR products were also examined by agarose gel electrophoresis (A.7.1 of Appendix).

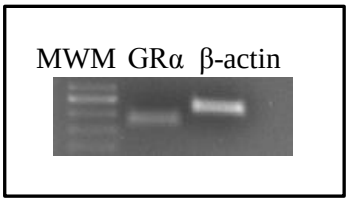

Figure 7.1. Validation of GRα and β-actin primer sets by agarose gel electrophoresis.

A.6 qPCR protocol

The protocol shown in Figure 7.2 was used for all qPCR runs that amplified target genes using SYBR® Green JumpStart™ *Taq* ReadyMix™ (Sigma-Aldrich®). Each SYBR Green reaction consisted of 1 µL of diluted cDNA which was synthesised from 2 µg of RNA, 1 µL of the forward and reverse primer, 9.5 µL nuclease-free H_2O, and 12.5 µL of SYBR® Green JumpStart™ *Taq* ReadyMix™, to a total standard reaction volume of 25 µL. The SYBR® Green JumpStart™ *Taq* ReadyMix™ consists of 20 mmol/L Tris-HCl at pH 8.3; 100 mmol/L KCl; 7 mmol/L $MgCl_2$; 0.4 mmol/L of each dNTP (dATP, dCTP, dGTP and dTTP); stabilisers; 0.05 units/mL *Taq* DNA polymerase; JumpStart *Taq* antibody; and SYBR Green I.

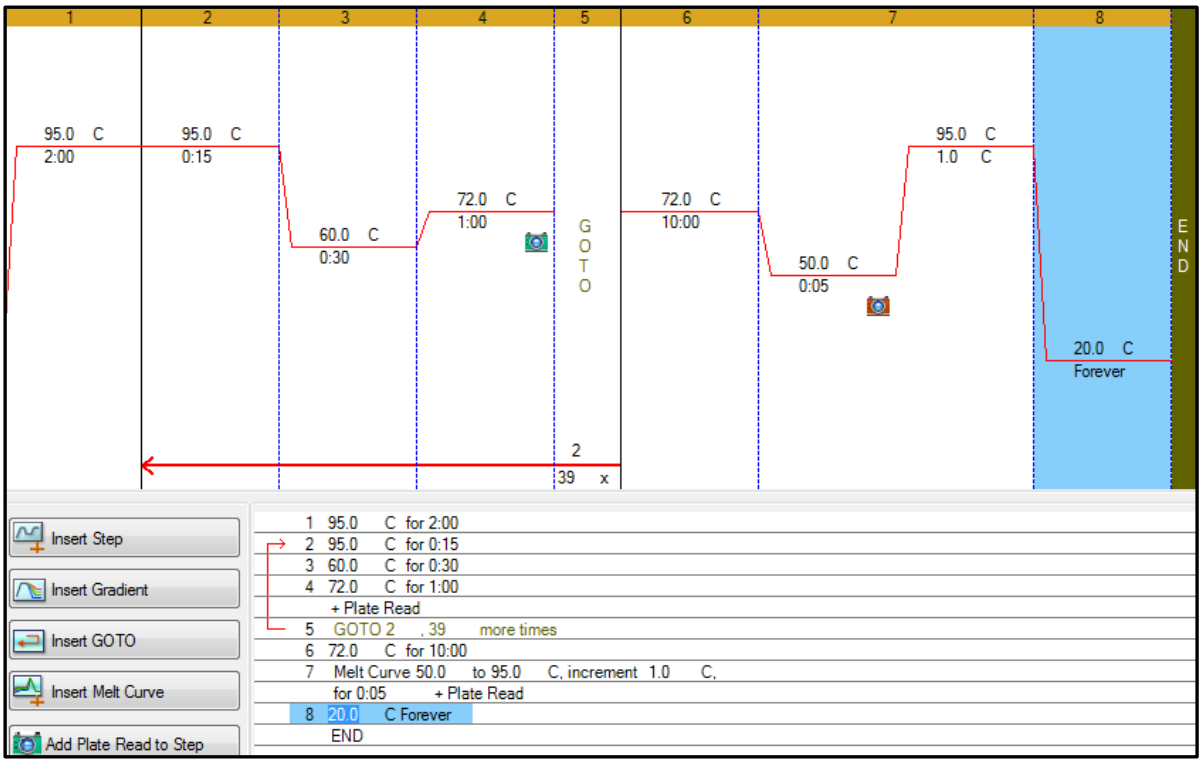

Figure 7.2. The qPCR protocol used for all qPCR runs.

Low profile (0.2 mL) white strip tubes (Bio-Rad) and optically clear flat cap strips (Bio-Rad) plastic ware was used for all qPCR reactions. The same set of Gilson Pipetman® starter kit micropipettes were used with TipOne bevelled filter tips (Starlab) for all qPCR experiments and runs. The reagents were kept and prepared on ice for the experiment set up. The MiniOpticon™ Real-Time PCR Detection System (Bio-Rad) using the CFX Manager™ Software version 2.1 (Bio-Rad) software package, which was used for all qPCR runs. C_t readings were determined by using the single threshold setting on the CFX manager software. Fluorescence was read in the FAM channel and the plate-type setting at MJ white for all experimental runs. The baseline value for fluorescence readings was set to a standardised value of 0.2 RFU for all experimental runs (Fig. 7.3).

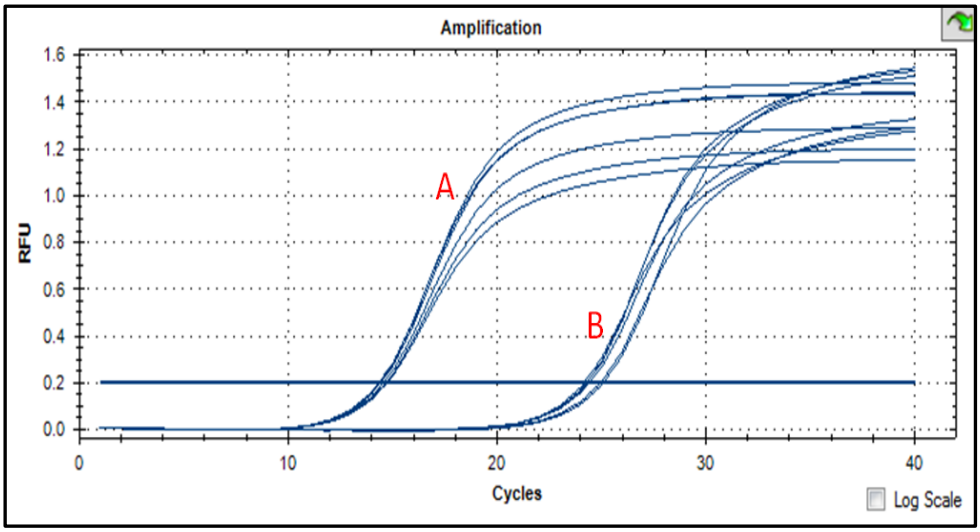

Figure 7.3. A representation of qPCR amplification curves using the FAM fluorescence channel at an RFU baseline of 0.2. **A** - β-actin; **B** - GRα.

A.7 qPCR validation

A.7.1 qPCR melt curve analysis verification

The melt curve analysis for each qPCR target and its verification by agarose gel electrophoresis are presented in the figures below (Fig. 7.4 and Fig. 7.5). A single melting temperature was observed and corresponded to a single product for each primer set. A 50-1000 bp GeneRuler™ DNA Ladder (Fermentas) was run as the MWM on each gel to confirm the size of the products.

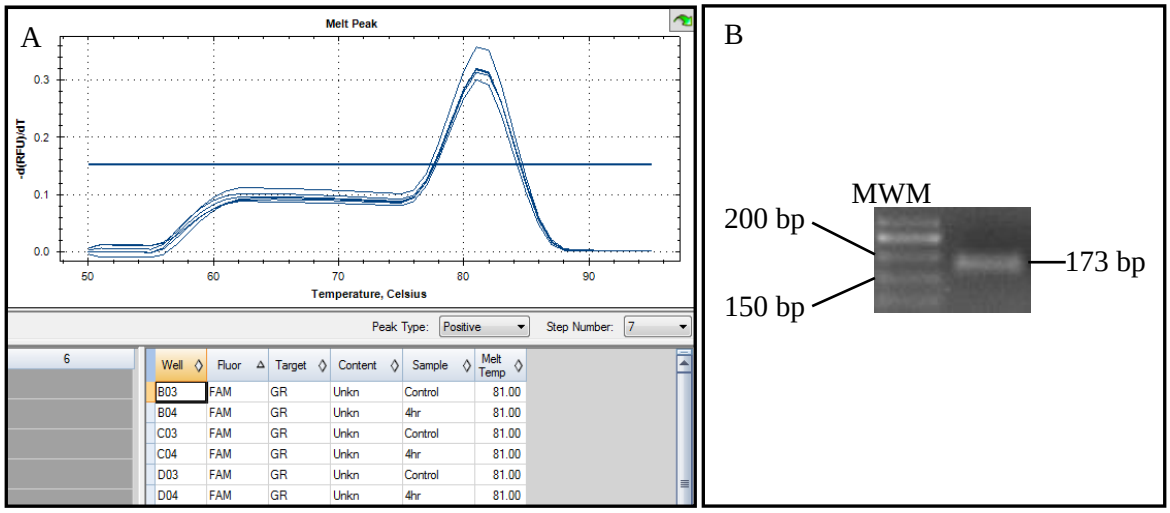

Figure 7.4. Melt curve analysis and gel verification of GRα primers. (A) GRα qPCR melting curve and temperature at 81°C and (B) validation of GRα (173 bp) qPCR product by agarose gel electrophoresis.

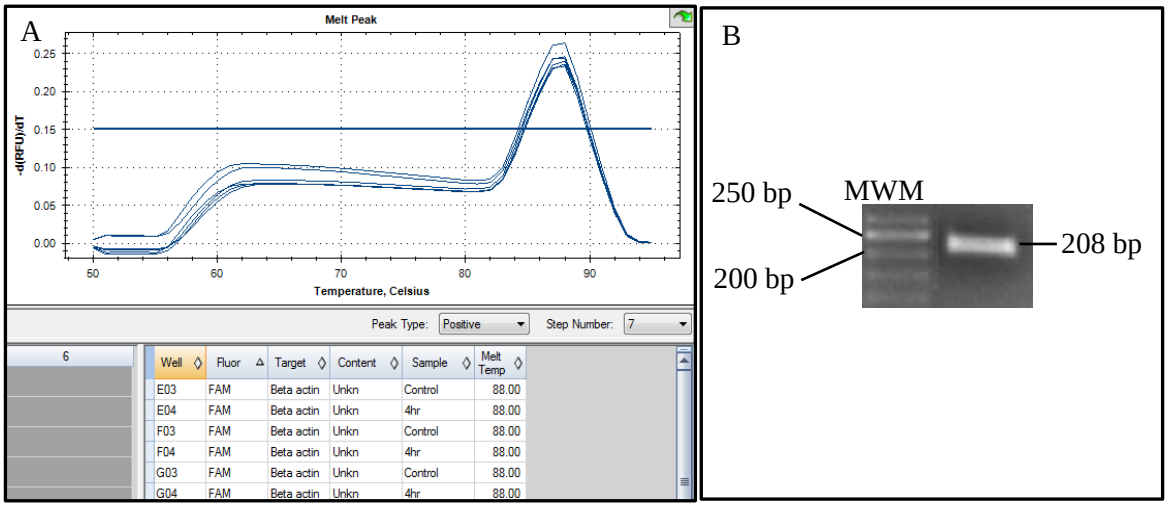

Figure 7.5. Melt curve analysis and gel verification of β-actin primers. (A) β-actin qPCR melting curve and temperature at 88°C and (B) validation of β-actin (208 bp) qPCR product by agarose gel electrophoresis.

A.7.2 Evaluation of qPCR reaction efficiencies

The $2^{-\Delta\Delta C_T}$ method is only applicable for analysis of qPCR data if the $r^2 > 0.98$ and the reaction efficiencies are between 90% and 110%. The reaction efficiency of the gene of interest (*GRα*) should be equal to that of the reference gene, β-actin (Livak and Schmittgen, 2001). As discussed in section 2.5.1.1 of the Materials and Methods, the reaction efficiencies of each

target gene were evaluated by qPCR analysis of 10-fold serial dilutions of template cDNA. The Ct values were averaged for both the target and reference genes, which was plotted against the cDNA concentration. Equal reaction efficiencies of the gene of interest and reference gene were denoted by a slope value close to zero in the linear analysis. The reaction efficiencies were calculated using the QPCR Standard Curve Slope to Efficiency Calculator on the Agilent Technologies website (http://www.genomics.agilent.com/biocalculators/calcSlopeEfficiency.jsp?_requestid=587799). The relevant r^2 value and reaction efficiency for each target gene are presented below (Fig. 7.6).

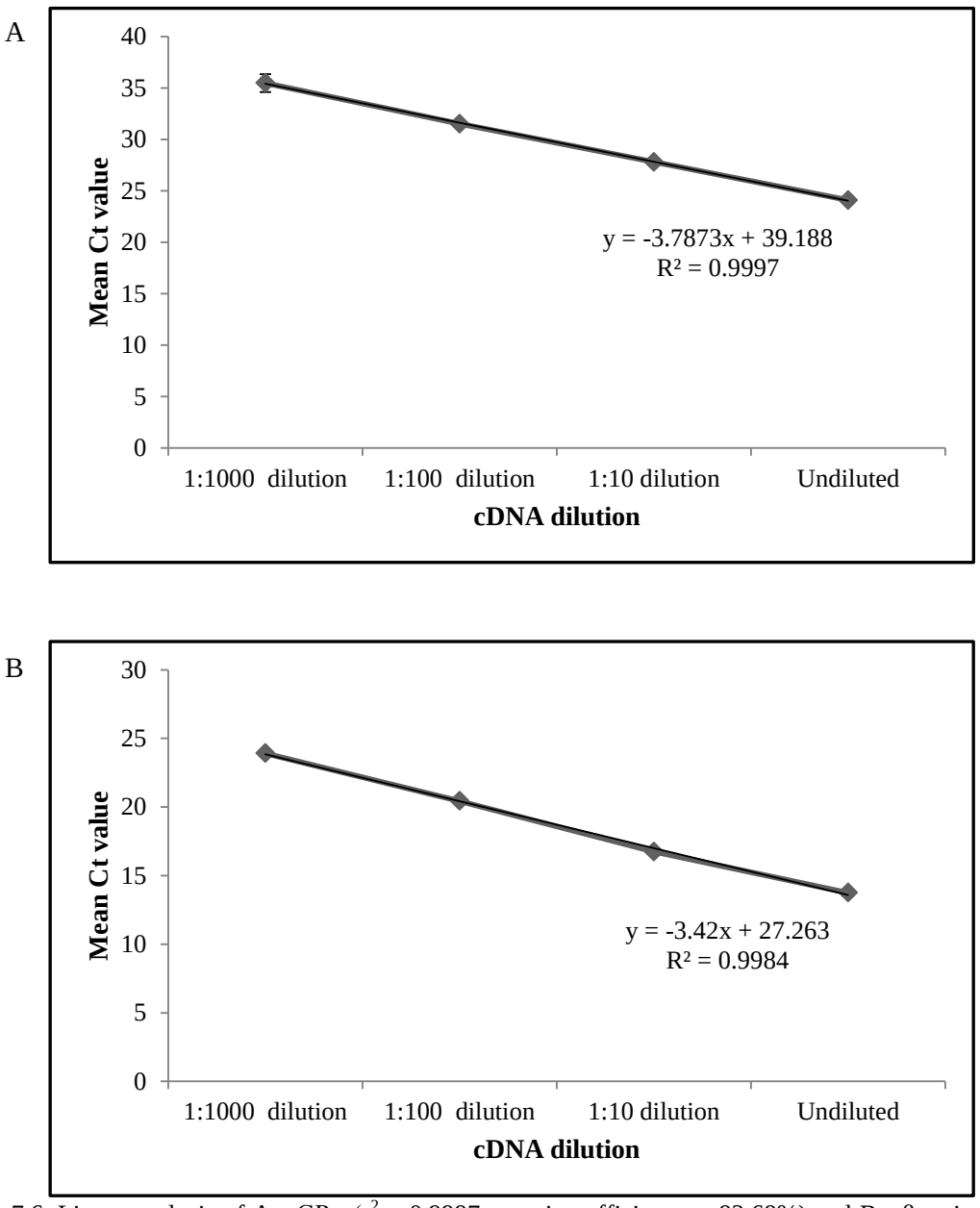

Figure 7.6. Linear analysis of A - GRα (r^2 = 0.9997; reaction efficiency = 83.68%) and B - β-actin (r^2 = 0.9984; reaction efficiency = 96.064%) qPCR reaction efficiencies.

A.8 Data analysis

The CFX Manager™ Software version 2.1 (Bio-Rad) was used to analyse all qPCR data. Ct values for each experiment were determined by fluorescence readings at the baseline 0.2 RFU for all experiments. Ct values that did not meet the criteria were excluded from analyses; the exclusion criteria for reactions are shown in Fig. 7.7. The NTC and no-RT controls for each qPCR were determined to either result in the formation of primer dimers, or to have no product (see Fig. 7.10 and Fig. 7.12). Primer dimer formation is evident by a melt temperature lower than 80°C, and by agarose gel electrophoresis.

β-actin is a well-known reference gene that have been widely used in experimental research. Alt *et al.* (2010) conducted a study in which qPCR was performed using primers for β-actin and GRα. β-actin confirmed to be a suitable reference gene (Alt *et al.*, 2010).

Description	Value	Use	Results	Exclude Wells
Negative control with a Cq less	38	☑		☐
NTC with a Cq less than	38	☑		☐
NRT with a Cq less than	38	☑		☐
Positive control with a Cq greate	30	☑		☐
Unknown without a Cq	N/A	☑		☐
Standard without a Cq	N/A	☑		☐
Efficiency greater than	110.0	☑		
Efficiency less than	90.0	☑		
Std Curve R^2 less than	0.980	☑		
Replicate group Cq Std Dev gre	0.20	☑		☐

Figure 7.7. Parameters used for reaction exclusions from $2^{-\Delta\Delta C_T}$ analyses (shown in CFX Manager™ Software program).

A.8.2 The $2^{-\Delta\Delta C_T}$ method of analysis for qPCR

The reactions for each target gene in each treatment/control were repeated in triplicate in a single qPCR experimental run. The average Ct for each target gene amplification in each treatment was normalised against β-actin (see Fig. 7.8). The fold change values were calculated by use of the $2^{-\Delta\Delta C_T}$ method, using the following equations:

Average Ct (target gene) – average Ct (reference gene) = ΔC_T

$\Delta\Delta C_T = \Delta C_T$ (treatment) – ΔC_T (control)

Thus, $\Delta\Delta C_T$ (control) = ΔC_T (control) – ΔC_T (control) = 0

Therefore $2^{-\Delta\Delta C_T}$ of control = 2^0 = 1 and for each treatment the fold change value = $2^{-(\Delta C_T \text{ (treatment)} - \Delta C_T \text{ (control)})}$

Example:

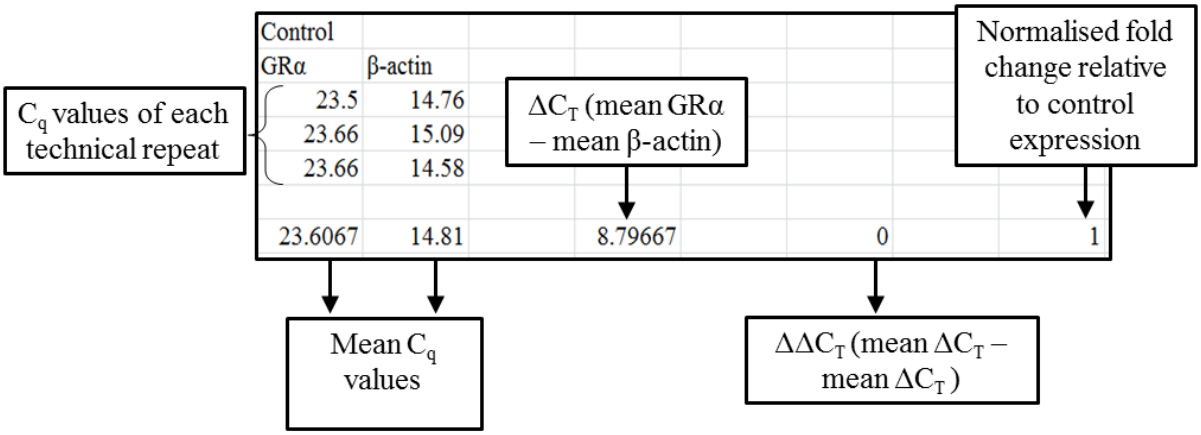

Figure 7.8. The $2^{-\Delta\Delta C_T}$ method example of equations used to calculate fold change.

A.8.3 Statistical analyses

The statistical significance of the relative fold change values for GRα expression of the treatments relative to the control were determined by either one sample t-test or one-way ANOVA, depending on the number of factors being analysed in each set of experimental run. The statistical analyses were analysed using IBM SPSS statistical software version 21.

The assumptions of an ANOVA and t-test were performed as explained in materials and methods section 2.9. The Tukey HSD test was performed for multiple comparisons analyses, to determine whether there was a significant difference between treatments for GRα expression. The assumptions were met for all statistical tests. A multiple comparisons test was performed to determine whether there were any significant differences between treatments. $p < 0.05$ was considered statistically significant. Fold change values were presented as bar graphs along with the standard error of the mean (SEM) (see results section 3.2).

A.8.4 No template cDNA control (NTC) and No-reverse transcriptase (RT) data

The relevant NTC and no-RT data for GRα and β-actin are shown below. The GRα NTC (Fig. 7.9 and Fig. 7.10) and no-RT quantitation data (Fig. 7.11) showed that NTC samples had no Cq values >, whereas β-actin had Cq values > 33.2 and the no-RT samples had no Cq values , whereas β-actin had Cq values > 31.99. The NTC and no-RT melt curve analyses for GRα and β-actin (Fig. 7.9, Fig. 7.10 and Fig. 7.12) showed that no product was amplified by the primer sets. The melt curve analyses and quantitation data of the NTC and no-RT controls thus suggest that there is no contamination present or that if there is, it cannot be amplified by the GRα and β-actin primer sets.

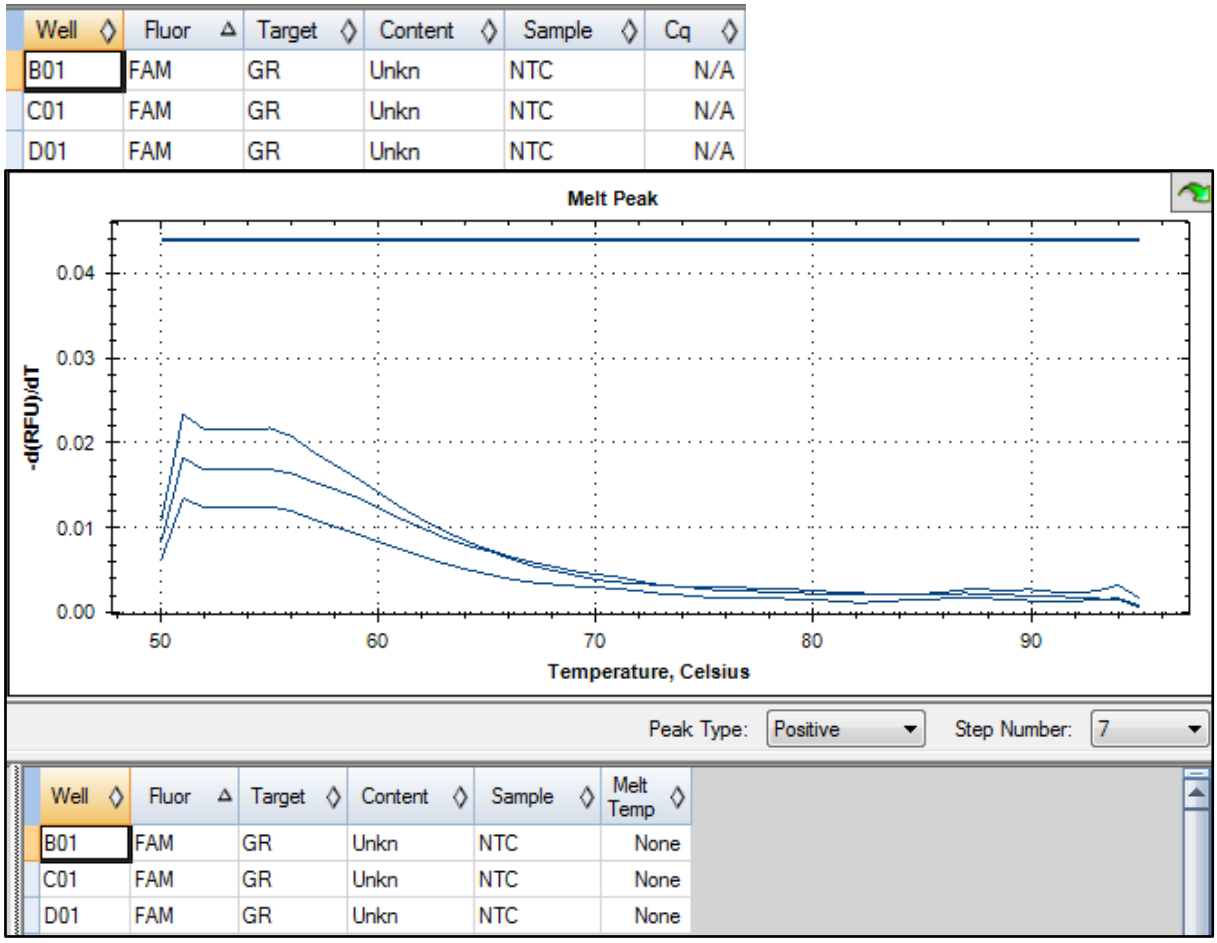

Figure 7.9. Quantitation data and Melt curve analyses for GRα NTC. Amplification of the NTC samples resulted in the formation of primer dimers or no amplification at all.

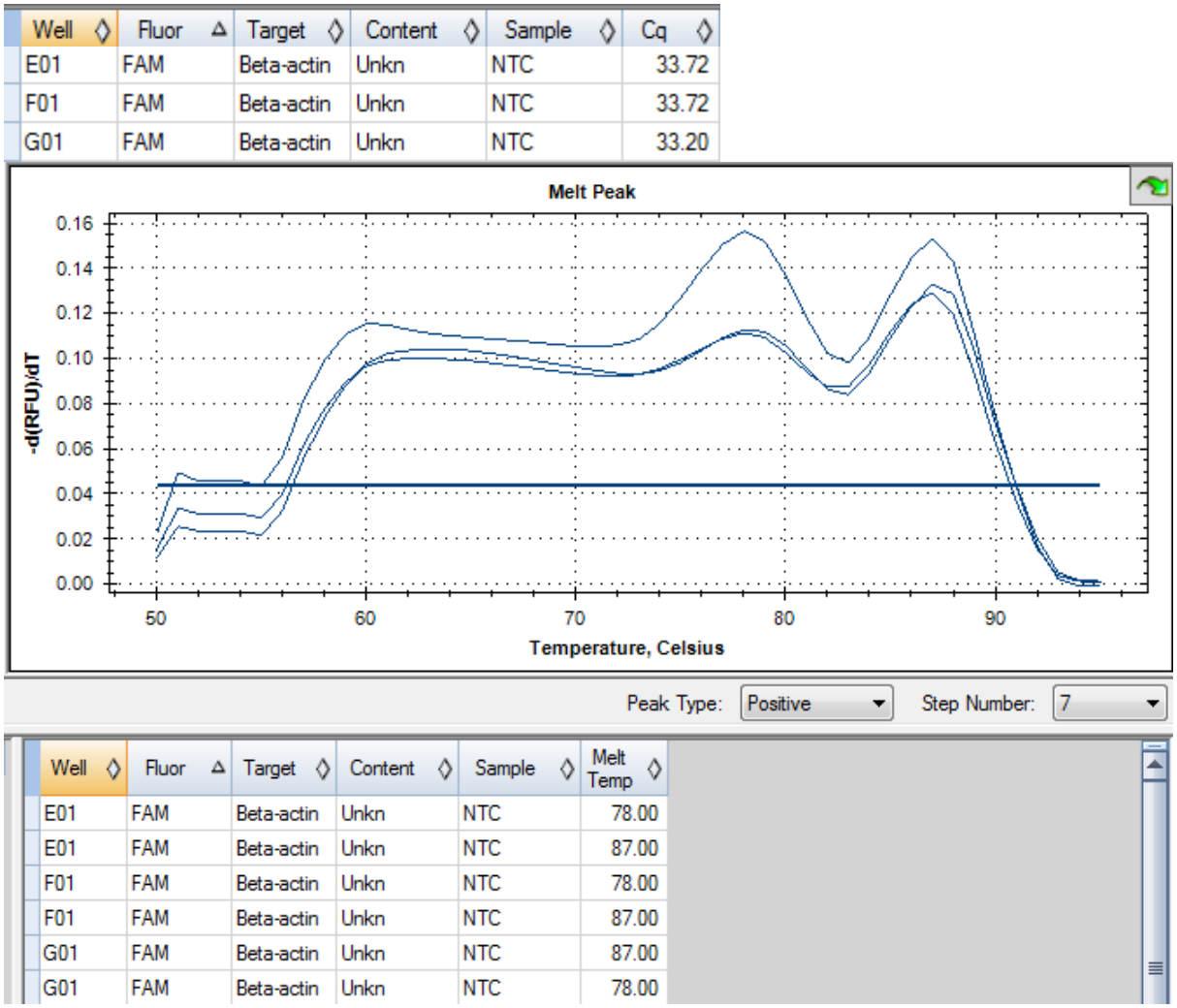

Figure 7.10. Quantitation data and Melt curve analyses for β-actin NTC. Amplification of the NTC samples resulted in the formation of primer dimers or no amplification at all.

Well	Fluor	Target	Content	Sample	Cq
B02	FAM	GR	Unkn	Control	N/A
B03	FAM	Beta-actin	Unkn	2 hr	31.59
B04	FAM	GR	Unkn	6 hr	N/A
B05	FAM	Beta-actin	Unkn	24hr	32.79
C02	FAM	GR	Unkn	Control	N/A
C03	FAM	Beta-actin	Unkn	2 hr	32.22
C04	FAM	GR	Unkn	6 hr	N/A
C05	FAM	Beta-actin	Unkn	24hr	32.16
D02	FAM	Beta-actin	Unkn	Control	33.17
D03	FAM	GR	Unkn	4 hr	N/A
D04	FAM	Beta-actin	Unkn	6 hr	32.31
D05	FAM	GR	Unkn	48 hr	N/A
E02	FAM	Beta-actin	Unkn	Control	32.61
E03	FAM	GR	Unkn	4 hr	N/A
E04	FAM	Beta-actin	Unkn	6 hr	31.99
E05	FAM	GR	Unkn	48 hr	N/A
F02	FAM	GR	Unkn	2 hr	N/A
F03	FAM	Beta-actin	Unkn	4 hr	32.63
F04	FAM	GR	Unkn	24hr	N/A
F05	FAM	Beta-actin	Unkn	48 hr	33.01
G02	FAM	GR	Unkn	2 hr	N/A
G03	FAM	Beta-actin	Unkn	4 hr	31.24
G04	FAM	GR	Unkn	24hr	N/A
G05	FAM	Beta-actin	Unkn	48 hr	32.49

Figure 7.11. Quantitation data for GRα and β-actin no-RT. Amplification of the no-RT samples resulted in the formation of primer dimers or no amplification at all.

A

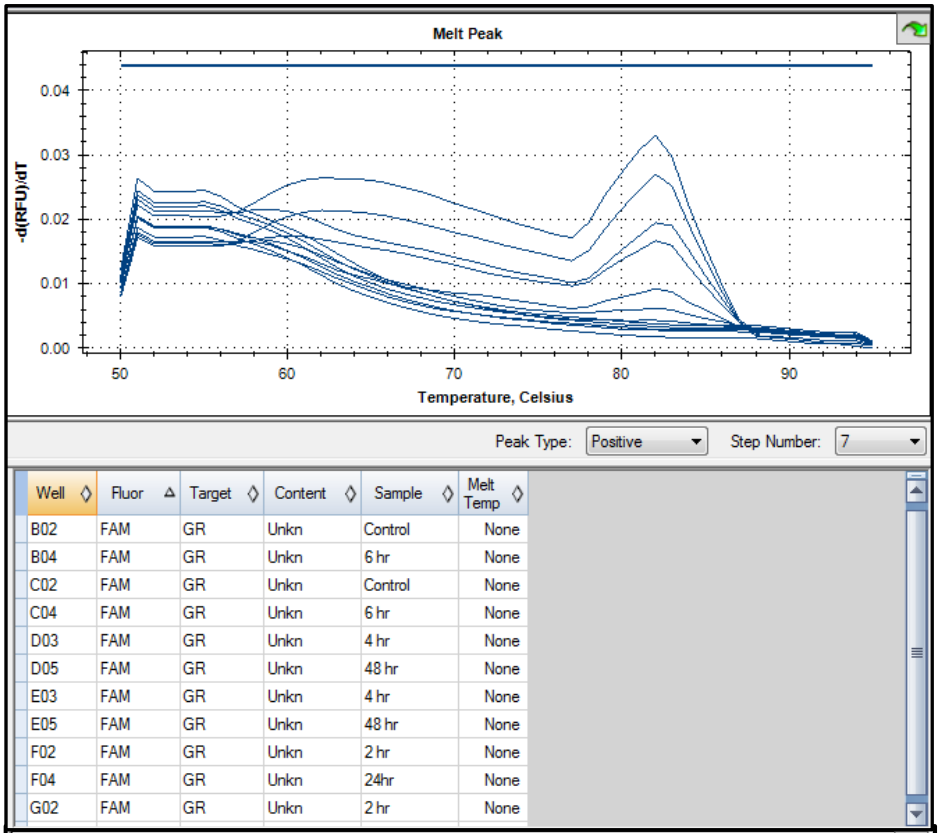

Well	Fluor	Target	Content	Sample	Melt Temp
B02	FAM	GR	Unkn	Control	None
B04	FAM	GR	Unkn	6 hr	None
C02	FAM	GR	Unkn	Control	None
C04	FAM	GR	Unkn	6 hr	None
D03	FAM	GR	Unkn	4 hr	None
D05	FAM	GR	Unkn	48 hr	None
E03	FAM	GR	Unkn	4 hr	None
E05	FAM	GR	Unkn	48 hr	None
F02	FAM	GR	Unkn	2 hr	None
F04	FAM	GR	Unkn	24hr	None
G02	FAM	GR	Unkn	2 hr	None

B

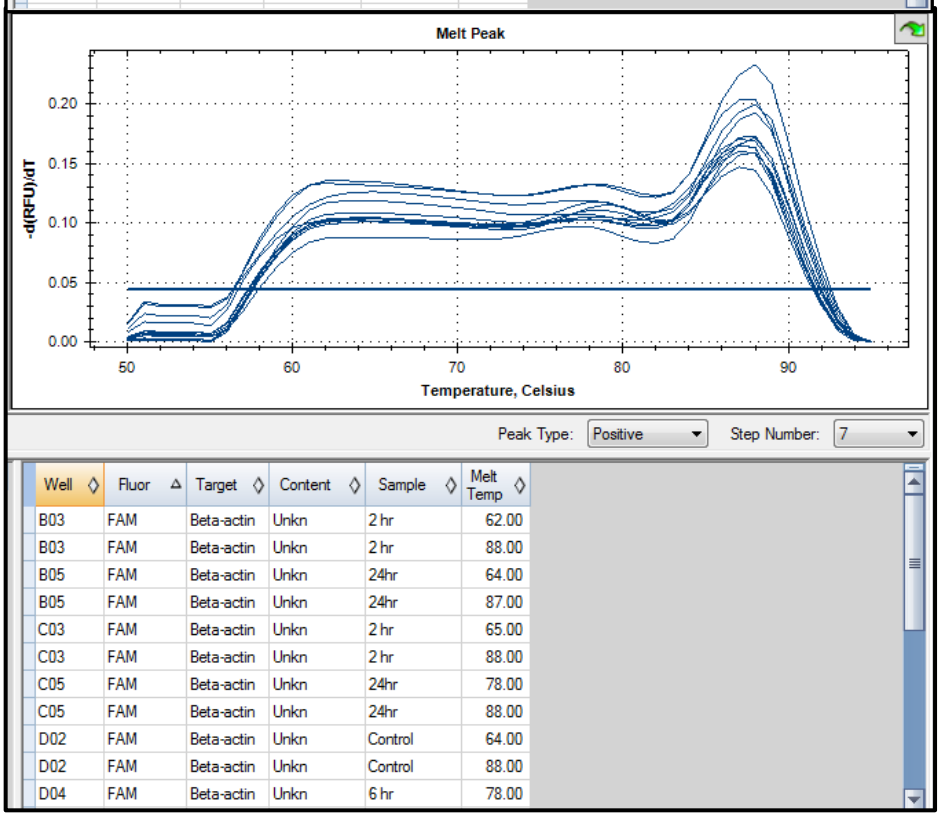

Well	Fluor	Target	Content	Sample	Melt Temp
B03	FAM	Beta-actin	Unkn	2 hr	62.00
B03	FAM	Beta-actin	Unkn	2 hr	88.00
B05	FAM	Beta-actin	Unkn	24hr	64.00
B05	FAM	Beta-actin	Unkn	24hr	87.00
C03	FAM	Beta-actin	Unkn	2 hr	65.00
C03	FAM	Beta-actin	Unkn	2 hr	88.00
C05	FAM	Beta-actin	Unkn	24hr	78.00
C05	FAM	Beta-actin	Unkn	24hr	88.00
D02	FAM	Beta-actin	Unkn	Control	64.00
D02	FAM	Beta-actin	Unkn	Control	88.00
D04	FAM	Beta-actin	Unkn	6 hr	78.00

Figure 7.12. No-RT Melt curve analyses for A - GRα and B - β-actin. Amplification of the no-RT samples resulted in the formation of primer dimers or no amplification at all.

B. Protocols

1. 1× Trypsin-EDTA

Reagents	Volume (10 mL)
10 × Trypsin (BioWhittaker™, Lonza)	1 mL
Sodium EDTA solution	9 mL

1 × Trypsin was made by dissolving 1 mL of 10 × Trypsin in 9 mL of sodium EDTA solution and stored at -20°C.

2. 5-Aza stock preparation

Reagents	Volume (1 mL)
5-Aza-2'-deoxycytidine (Sigma-Aldrich®)	50 mg
Glacial acetic acid (Saarchem)	500 µL
Distilled water	500 µL

The 5-Aza (50 mg) was dissolved in filter sterilised glacial acetic acid and distilled water in a 1:1 ratio. The stock solution was dissolved into the respective medium in a 1:100 ratio (e.g.1 µL of 5-Aza stock into 99 µL medium).

Amount of 1:100 diluted 5-Aza-2'-deoxycytidine used in treatments

Treatment concentration	DMS 79 (in 20 ml medium)	HEK 293 and A549 (in 10 ml medium)
Control (vehicle)	46 µL	23 µL
0.5 µmol/L	4.6 µL	2.3 µL
1 µmol/L	9.4 µL	4.7 µL
5 µmol/L	46 µL	23 µL

3. NNK stock preparation

Reagents	**Volume (200 µL)**
4-(Methylnitrosoamino)-1-(3-pyridinyl)-1-butanone, NNK (Sigma-Aldrich®)	10 mg
Dimethyl Sulfoxide (DMSO)	200 µL

The NNK was dissolved in DMSO. The stock solution was dissolved into the respective medium in a 1:100 ratio (e.g.1 µL of NNK stock into 99 µL medium). 41.5 µL was used from the NNK working solution into 10 mL of medium for a final concentration of 10 µmol/L of NNK.

4. Phosphate Buffered Saline (PBS)

10 × PBS

Reagents	**Volume (500 mL)**
NaH_2PO_4 (0.038M) (Merck)	2.28 g
Na_2HPO_4 (0.162 M) (Merck)	11.5 g
NaCl (Merck)	43.84 g
Distilled Water	Up to a final volume of 500 mL

The reagents were combined and dissolved in 450 mL distilled water. The pH of the solution was adjusted to pH 7.4. The solution was then made up to 500 mL with distilled water. The solution was autoclaved and allowed to cool before use.

1 × PBS

Reagents	**Volume (1000 mL)**
10 × PBS Buffer	100 mL
Distilled Water	900 mL

100 mL of 10 × PBS was added to 900 mL of sterile distilled water.

5. 70% Ethanol

Reagents	Volume (50 mL)
100% Ethanol (Merck)	35 mL
RNase Free Water	15 mL

The 70% Ethanol solution was prepared by mixing 100% Ethanol and RNase free water.

6. RNA Integrity gel solutions

1.5% Agarose/2.2 mol/L formaldehyde gel

Reagents	Volume (110 mL)
Agarose (TopVision™, Fermentas)	1.5 g
DEPC-treated water	72 mL
DEPC-treated Ethidium bromide	15 µL
10 × MOPS buffer	10 mL
Deionised formaldehyde (Merck)	18 mL

The agarose was melted in DEPC-treated water and cooled to ~55°C. In a fume hood; DEPC-treated ethidium bromine, 10 × MOPS buffer and formaldehyde was added to the agarose.

1M NaOAc (DEPC treated)

Reagent	Volume (100 mL)
NaOAc (Sigma®-Aldrich)	8.203 g
DEPC	100 µL
Distilled water	Up to 100 mL

0.5 mol/L EDTA (DEPC treated)

Reagents	**Volume (100 mL)**
EDTA (Merck)	18.6 g
DEPC	100 µL
Distilled water	Up to 100 mL

DEPC-treated water

Reagents	**Volume (1000 mL)**
DEPC	0.2 mL
Distilled Water	999.8 mL

0.2 mL of DEPC (Diethylpyrocarbonate) was mixed in 1000 mL of distilled water. The water was incubated at 37°C for 2 h with stirring (in a fume hood). The treated water was autoclaved to inactivate the DEPC in the water.

Ethidium bromide (DEPC-treated)

Reagents	**Volume (10 mL)**
Ethidium bromide working solution (0.05 mg/mL) (See Appendix B.7)	10 mL
DEPC	10 µL

Ethidium bromide was DEPC treated.

10 × MOPS Buffer

Reagents	**Volume (100 mL)**
0.5 mol/L EDTA (Merck) (In DEPC water)	2 mL
0.02 mol/L MOPS (Sigma®-Aldrich)	4.18 g
1 mol/L Sodium Acetate (NaOAc) (Sigma) (In DEPC water)	2 mL
DEPC-treated water	Up to a final volume of 100 mL

4.18 g MOPS, 2 mL NaOAc and 2 mL of EDTA was dissolved in DEPC treated water to a final volume of 100 mL. The solution was mixed and the pH was adjusted to 8.3.

1 × MOPS running buffer

Reagents	**Volume (100 mL)**
10 × MOPS buffer	10 mL
DEPC-treated water	90 mL

10 mL of 10 × MOPS buffer was dissolved in 90 mL of DEPC-treated water.

7. Ethidium Bromide

Ethidium Bromide Stock Solution

Reagents	**Volume (1 mL)**
Ethidium bromide	10 mg
Distilled water	Up to 1 mL

10 mg of Ethidium bromide was added to 1 mL of sterile distilled water.

Ethidium Bromide Working Solution (0.05 mg/mL)

Reagents	**Volume (200 mL)**
Ethidium bromide stock solution	1 mL
Distilled water	199 mL

A 0.05 mg/mL ethidium bromide working solution was made by adding 1 mL of ethidium bromide stock solution to 199 mL of sterile distilled water.

8. Tris-EDTA (TE) Buffer

1 × TE buffer

Reagents	**Volume (500 mL)**
1 mol/L Tris-HCL (Merck)	5 mL
0.5 mol/L EDTA (Merck)	1 mL
Distilled water	494 mL

Tris-HCL (1 mol/L)

Reagents	**Volume (50 mL)**
Tris-HCL (Merck)	7.9 g
Distilled water	Up to 50 mL

Tris-HCL was dissolved in distilled water and the pH adjusted to 7.5.

EDTA (*0.5 mol/L)*

Reagents	**Volume (50 mL)**
EDTA	9.3 g
Distilled water	Up to 50 mL

EDTA was dissolved in distilled water and the pH was adjusted to 8.0.

9. Primer Dilutions

10 µL of the 100 mmol/L primer stock was dissolved in 90 µL of nuclease free water (GIBCO). The primer dilutions (10 mmol/L) were aliquoted into microcentrifuge tubes at a volume of 25 µl and stored at -20°C.

10. dNTP Stock Preparation

Each dNTP was in a 100 mmol/L stock of dATP, dGTP, dTTP and dCTP. 10 µL of each stock was put into a microcentrifuge tube and was dissolved in 460 µl of nuclease free water

(GIBCO). The dNTPs (2 mmol/L) were aliquoted into microcentrifuge tubes at a volume of 25 µl were stored at -20°C.

11. 1.5% Agarose gel

Reagents	**Volume (40 mL)**
Distilled Water	40 mL
Agarose	0.6 g

40 mL of distilled water was added with 0.6 g Agarose in a conical flask. The solution was heated in a microwave until all Agarose was dissolved. 10 µL of Ethidium working solution was added to the melted agarose solution (Appendix B.7), in a fume hood.

12. Tris-base EDTA (TBE) Buffer

10 × TBE Buffer

Reagents	**Volume (400 mL)**
Tris Base (Merck)	43.2 g
Boric Acid (Merck)	22 g
EDTA	3.72 g
Distilled Water	Up to a final volume of 400 mL

The reagents listed above were combined and mixed up to a final volume of 400 mL with distilled water. The pH of the solution was adjusted to a final pH of 8.3.

1 × TBE running Buffer

Reagents	**Volume (1000 mL)**
10 × TBE Buffer	100 mL
Distilled Water	900 mL

1 × TBE buffer: 100 mL of 10 × TBE Buffer was diluted in 900 mL of distilled water (1:10 dilution).

C. Western Blot Recipes

1. RIPA buffer with protease inhibitor cocktail

Reagents	Volume (220 µL)
RIPA buffer (Sigma®-Aldrich)	200 µL
Protease inhibitor cocktail (Sigma®-Aldrich)	20 µL

2. Reducing Sample Treatment Buffer

Reagents	Volume (10 mL)
4 × Stacking gel buffer	2.5 mL
10% SDS stock solution (Merck)	4 mL
Glycerol (Saarchem)	2 mL
2-mercapthoethanol (Sigma)	1 mL
Bromophenol blue (Sigma)	0.05 g
Deionised water	Made up to a final volume of 10 mL

*Concentrations of reagents required: 125 mmol/L Tris-HCl (Merck), 4% (m/v) SDS (Merck), 20% (v/v) glycerol (Saarchem), 10% (v/v) 2-mercapthoethanol (Sigma), pH 6.8

3. Preparation of BSA Standard Concentrations

Microcentrifuge tube	Volume of Diluent (Nuclease free water) (µL)	Volume and Source of BSA (µL)	Final BSA Concentration (µg/mL)
A	0 µL	300 µL of Stock	2000 µg/mL
B	125 µL	375 µL of Stock	1500 µg/mL
C	325 µL	325 µL of Stock	1000 µg/mL
D	175 µL	175 µL of vial B dilution	750 µg/mL
E	325 µL	325 µL of vial C dilution	500 µg/mL
F	325 µL	325 µL of vial E dilution	250 µg/mL

G	325 µL	325 µL of vial F dilution	125 µg/mL
H	400 µL	100 µL of vial G dilution	25 µg/mL
I	400 µL	0 µL	0 = Blank

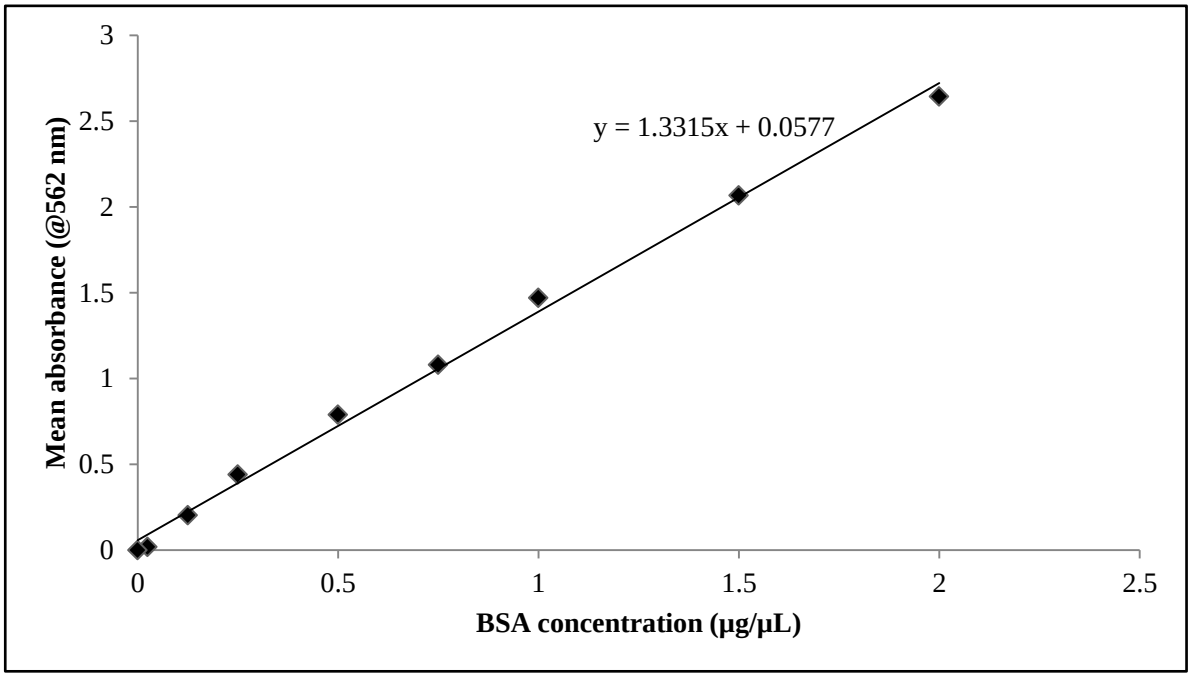

Figure 7.13. Example of a standard curve generated from the known dilutions and concentrations of BSA standards versus the mean absorbance reading at 562 nm. Unknown protein concentrations were determined based on the standard curve, using the straight line equation.

4. SDS-PAGE Gel solutions

SDS PAGE gel

Solutions	**Resolving gel (12.5%)**	**Resolving gel (13.5%)**	**Stacking gel (4%)**
Bis-acrylamide solution (30%/0.8% w/v) (Bio-Rad)	3.125 mL	3.375 mL	0.47 mL
4 × Running gel buffer (see below)	1.875 mL	1.875 mL	--
4 × Stacking gel buffer (see below)	--	--	0.875 mL
Deionised water (d.H_2O)	2.375 mL	2.099 mL	2.15 mL

10% SDS	75 µL	75 µL	35 µL
20% APS initiator	37.5 µL	37.5 µL	17.5 µL
TEMED	3.75 µL	3.75 µL	7.5 µL

*SDS – Sodium lauryl sulfate (Merck)

*APS – Ammonium persulfate initiator solution

*20% APS is made up by dissolving 0.05 g APS in 250 µl d.H_2O.

4 × Running gel buffer

Reagents	**Volume (50 mL)**
Tris-HCL (Merck)	9.09 g
Deionised Water	Up to a final volume of 50 mL

*****pH titrated to 8.8

4 × Stacking gel buffer

Reagents	**Volume (50 mL)**
Tris-HCL (Merck)	3.0 g
Deionised Water	Up to a final volume of 50 mL

*pH titrated to 6.8

10% SDS Stock Solution

Reagents	**Volume (50 mL)**
SDS (Merck)	5.0 g
Deionised Water	Up to a final volume of 50 mL

5. 1 × Electrode (Tank) Buffer

Reagents	**Volume (1L)**
250 mmol/L Tris-HCL (Merck)	3.94 g
192 mmol/L Glycine (Merck)	14.4 g
0.1% SDS (Merck)	1 g
Deionised Water	Up to a final volume of 1 L

*pH adjusted to 8.3

6. Protein transfer buffer

Reagents	**Volume (1L)**
2 mmol/L Tris-base (Merck)	3.03 g
192 mmol/L Glycine (Merck)	14.4 g
20% Methanol (Merck)	200 mL
0.1% SDS (Merck)	1 g
Deionised Water	Up to a final volume of 1 L

*pH adjusted to 8.3

* Stored in -20°C for an hour before use

7. TBS-T (Tris-Buffered Saline with Tween)

Reagents	**Volume (1L)**
NaCL (Merck)	8 g
KCl (Merck)	0.2 g
Tris-base (Merck)	3 g
Tween – 20	1 mL
Deionised Water	Up to a final volume of 1 L

*pH adjusted to 7.5

8. 6% Skim milk-blocking buffer solution

Reagents	**Volume (1L)**
Skim Milk Powder (Sigma®-Aldrich)	3.0 g
TBS-T (B.19.)	50 mL

9. Antibody Information and Antibody dilutions for Western Blots

Antibody (Ab)	**Primary Ab name**	**Primary Ab dilution (µL)**	**Secondary Ab name**	**Secondary Ab dilution (µL)**
Human GR (BD Biosciences)	Mouse Anti-GRα Monoclonal (611227)	1:24000	Goat Anti-mouse (554002)	1:2000
Human GAPDH **(**Cell Signalling)	Rabbit Anti-GAPDH (14C10)	1:3000	Anti-Rabbit (7074)	1:4000

*All of the antibodies were diluted in TBS-T, except for Mouse Anti-GR, which was diluted in a 6% skim milk blocking buffer solution.

10. Ponceau S Stain

1 × Ponceau S Stain

Reagents	**Volume (500 mL)**
Ponceau S (0.1%) (Sigma-Aldrich®)	0.5 g
Acetic acid (1%) (Merck)	5 mL
Deionised Water	Up to a final volume of 500 mL

Ponceau Destain

Reagents	**Volume (500 mL)**
Acetic acid (1%) (Merck)	5 mL
Deionised Water	Up to a final volume of 500 mL

D. Optimisation of DNA sonication

Sonication was performed to shear the chromatin into ~200-1000 bp fragment which was verified by agarose gel electrophoresis. Sonication was performed using the Misonix ultrasonic liquid processor XL 2000 on power setting 6. The 500 µL aliquots of cells in SDS lysis buffer were sonicated on wet ice with ten 15 second pulses with 50 second rests (on wet ice) in between pulses. It is important to keep the samples on wet ice to prevent chromatin denaturation. Once the DNA was sheared, it was centrifuged at 13,000 × *g* for 10 minutes to remove insoluble material. The supernatant was then aliquoted into a fresh 1.5 mL microcentrifuge tube.

The sonicated chromatin was resolved on a gel with unsheared chromatin to assess that the chromatin was sheared between ~200-1000 bp fragments. This was done by removing 20 µL of the sonicated or unsonicated lysate and diluting it up to 50 µL with ChIP dilution buffer. To each tube, 1 µL of RNase A was added and the tubes were incubated for 30 minutes at 37°C. 1 µL of Proteinase K was added and the samples were incubated for 2 h at 62°C. 10-15 µL of sheared or unsheared chromatin was loaded on a 1.5% agarose gel with a MWM. A smear of DNA between 200-1000 bp was observed with successful sonication as shown in Fig. 7.14.

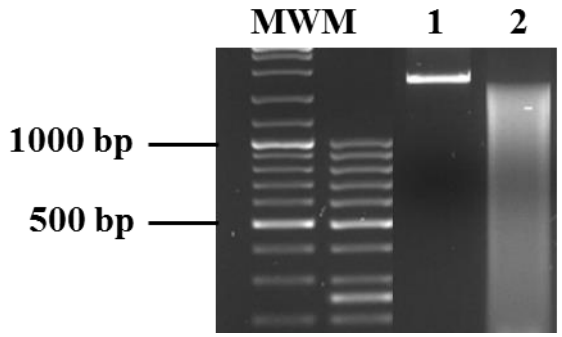

Figure 7.14. Agarose gel image of **MWM** – Molecular weight marker; **1** - Unsheared and **2** - sheared chromatin (~1000-200 bp) after DNA sonication.